

A study of the behaviour of multi-storey coupled shear walls.

TWIGG, David R.

Available from the Sheffield Hallam University Research Archive (SHURA) at:

<http://shura.shu.ac.uk/20463/>

A Sheffield Hallam University thesis

This thesis is protected by copyright which belongs to the author.

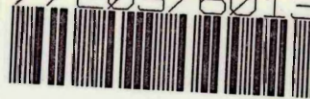
The content must not be changed in any way or sold commercially in any format or medium without the formal permission of the author.

When referring to this work, full bibliographic details including the author, title, awarding institution and date of the thesis must be given.

Please visit <http://shura.shu.ac.uk/20463/> and <http://shura.shu.ac.uk/information.html> for further details about copyright and re-use permissions.

POLYTECHNIC LIBRARY
POND STREET
SHEFFIELD S1 1WB

7720376013



LIBRARY SERVICE

MAIN LIBRARY

Sheffield City Polytechnic Library

REFERENCE ONLY

ProQuest Number: 10701110

All rights reserved

INFORMATION TO ALL USERS

The quality of this reproduction is dependent upon the quality of the copy submitted.

In the unlikely event that the author did not send a complete manuscript and there are missing pages, these will be noted. Also, if material had to be removed, a note will indicate the deletion.



ProQuest 10701110

Published by ProQuest LLC (2017). Copyright of the Dissertation is held by the Author.

All rights reserved.

This work is protected against unauthorized copying under Title 17, United States Code
Microform Edition © ProQuest LLC.

ProQuest LLC.
789 East Eisenhower Parkway
P.O. Box 1346
Ann Arbor, MI 48106 – 1346

A STUDY OF THE BEHAVIOUR
OF
MULTI-STOREY COUPLED SHEAR WALLS

A Thesis presented for the CNAA Degree of
MASTER OF PHILOSOPHY
for research conducted in the
Department of Civil Engineering
at
Sheffield City Polytechnic

by

DAVID RONALD TWIGG

December 1976



77-20376 01 3

ABSTRACT

This thesis deals with the elastic analysis of non-uniform coupled shear wall structures.

The main methods of analysis available for coupled shear walls, namely the wide column frame method, the continuous connection method and the finite element method, are discussed. Particular attention is given to non-uniform walls, non-rigid foundations, the importance of beam-wall flexibility and the importance of coupling action.

The direct solution of the governing differential equation, derived using the continuous connection approach, is briefly outlined for a uniform structure, but since the equations involved very soon became unmanageable when the method is extended to cater for non-uniform walls, a numerical solution in the form of the Matrix Progression Method is studied with a view to using it for complicated structures. The method is first applied to a uniform coupled shear wall containing one band of openings and subjected to both a uniformly distributed lateral load and a point load. The analysis is then extended to deal with structures having abrupt changes in geometry and containing more than one band of openings. A brief description of the computational methods involved in the solution is given.

Matrix Progression solutions are presented for a variety of non-uniform coupled shear walls, including walls of varying degrees of coupling action supported on both central and offset columns, and the results are compared with wide column frame solutions. In addition, for both symmetrical and non-symmetrical walls with one abrupt change in cross-section, the solutions are compared with experimental results obtained from tests on Araldite models.

ACKNOWLEDGEMENTS

The author is greatly indebted to Professor A Coull of Strathclyde University for his supervision, guidance and encouragement during the later stages of the work, to Dr R D Puri for suggesting the work and his supervision during the initial stages, and to Mr P Ahm and his colleagues at Ove Arup and Partners for interesting discussions on the practical problems of shear wall design.

Sincere thanks are due to all members of the Civil Engineering Department at Sheffield City Polytechnic who have given help during the period of the work.

The author also wishes to thank Miss J Bradley for her careful typing of the thesis.

CONTENTS

	<u>Page</u>
CHAPTER 1 INTRODUCTION	1
1.1 Introduction	1
1.2 Past Work	2
1.3 Scope of Present Work	15
CHAPTER 2 ANALYTICAL SOLUTION	17
2.1 Introduction	17
2.2 Notation	17
2.3 Assumptions	18
2.4 Uniform Coupled Shear Wall Containing One Band of Openings	19
2.5 Complex Shear Wall Systems	25
CHAPTER 3 MATRIX PROGRESSION SOLUTIONS	27
3.1 Introduction	27
3.2 Notation	29
3.3 Assumptions	30
3.4 Uniform Coupled Shear Walls Containing One Band of Openings	30
3.5 Coupled Shear Walls Containing One Band of Openings and with One Abrupt Variation in Cross-Section	43
3.6 Uniform Coupled Shear Walls Containing Two Bands of Openings	49
3.7 Coupled Shear Walls Containing Two Bands of Openings and with One Abrupt Variation in Cross-Section	56
3.8 Coupled Shear Walls Containing n Bands of Openings and with m Abrupt Variations in Cross-Section	59
CHAPTER 4 COMPUTER PROGRAMS	
4.1 Introduction	61
4.2 Analytical Solution	61
4.3 Matrix Progression Solutions	64

	<u>Page</u>
CHAPTER 5 EXPERIMENTAL WORK	69
5.1 Introduction	69
5.2 Material	69
5.3 The Models	70
5.4 Method of Test	70
CHAPTER 6 RESULTS	78
6.1 Introduction	78
6.2 Theoretical Results	78
6.3 Results for Walls Containing One Band of Openings and with One Abrupt Variation in Cross-Section	81
6.4 Results for Uniform Walls Supported on Columns	109
6.5 Results for Walls Containing Two Bands of Staggered Openings	136
CHAPTER 7 DISCUSSION OF RESULTS	140
7.1 Introduction	140
7.2 Walls Containing One Band of Openings and with One Abrupt Variation in Cross-Section	142
7.3 Uniform Walls Supported on Columns	144
7.4 Walls Containing Two Bands of Staggered Openings	147
7.5 Conclusions and Suggestions for Future Work	148
REFERENCES	150

CHAPTER 1

INTRODUCTION

1.1 Introduction

With low rise buildings the primary concern of a design is to provide an adequate structure to support the applied vertical loads. In tall buildings, however, the effect of lateral loads is very significant, from both the strength and serviceability points of view, and it is important to ensure adequate stiffness to resist these lateral loads which may be due to wind, blasts or earthquake action.

The required stiffness may be achieved in various ways. In framed structures it is obtained from the rigidity of the member connections but when the frame system alone is insufficient, additional bracing members may be added or, as is more usual, reinforced concrete 'shear walls' are introduced. The term 'shear wall' can cover stair wells, lift shafts and central service cores but in the present work it is used to denote plane walls in which the high in-plane stiffness is used to resist the lateral forces.

In its simplest form the shear wall consists of a single cantilevered wall which behaves according to simple bending theory. Internal walls, however, may not only

contain openings for doors and corridors but may also have an abrupt change in cross-section at a certain height or may even be supported on columns. In such cases the behaviour of the walls is much more complicated.

The structures considered in the present work are those comprising shear walls connected by beams which form part of the wall, or floor slabs, or a combination of both.

1.2 Past Work

Prior to 1960 little attention was paid to the development of analytical techniques for shear walls. In recent years, however, much research has been carried out and comprehensive reviews of the methods of analysis, and sources of information on the subject have been presented by Coull and Stafford Smith (1 and 2) and Fintel et al (3).

The only work which will be mentioned here is that which is relevant to the work considered in this thesis.

The analysis of walls pierced by sets of openings (coupled shear walls) has received much attention but as with any complicated structural system the accuracy of the analysis is dependent upon the form of idealization given to the actual structure together with the assumptions that the idealization involves. Since methods of analysis involving the solution of the governing plane stress elasticity equations are difficult to implement in connection

with coupled shear walls, all the methods of analysis which have been used previously have involved the idealization of the structure as an interconnection of elements of which the properties are known or can be estimated. The main methods which have been used are:

- (i) frame analogies
- (ii) finite element method
- (iii) continuous connection method.

Frame Analogies

The first of the frame analogies is the 'equivalent frame method'. In this method the walls are replaced by line members along their centroidal axes and the lengths of the connecting beams are taken to be the distances between the resulting line members, thus making the structure a vertical vierendeel girder (see Figure 1.1(b)). Because in most cases the width of the walls is not negligible compared with their centre line distances, this approach is unrealistic and will generally overestimate the deflections.

Green (4) adopted this procedure and used the 'portal frame' method of analysis, assuming points of contraflexure at the mid-points of all members. Although he used modified stiffnesses to take account of shear as well as bending, he neglected axial deformations of the walls and these may be of major importance in tall slender structures.

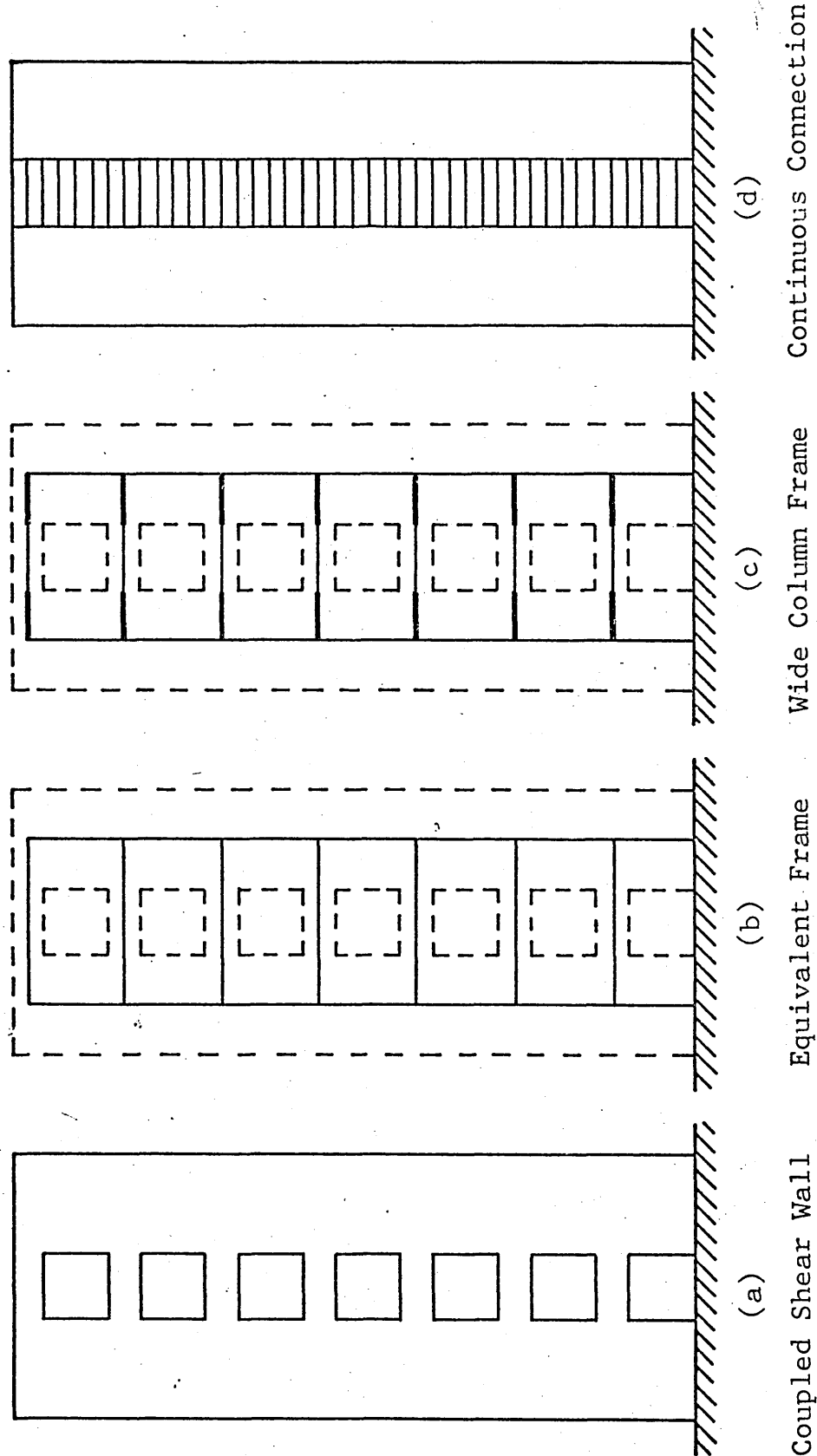


Figure 1.1 Coupled Shear Wall and Idealized Structures

An improvement on the 'equivalent frame method' is the so-called 'wide column frame'. In this method the length of the beam connecting elements is taken as the clear distance between adjacent walls and account is taken of the effect of the vertical deflections at the ends of the beams, which are due to rotation of the walls, by assuming that the member joining the beam end to the wall centre-line is infinitely rigid (see Figure 1.1(c)).

Once the analogous system has been set up, the analysis is best preformed by using matrix stiffness or matrix flexibility methods of analysis. Both methods are well established and documented (e.g. 5 and 6) and standard computer programs are available, usually adopting the stiffness approach (e.g. 7 and 8).

Frischmann, Prabhu and Topler (9) used the flexibility method for the solution of a wide column frame, but as with Green axial deformations of the walls were ignored.

MacLeod (10) used the stiffness method to obtain a solution by incorporating stiffness matrices for elements which have infinitely stiff end sections.

A variation of the above method, allowing standard computer programs to be used, was presented by Schwaighofer and Microys (11). They considered the rigid arms as additional members with high but finite values of cross-

sectional area and moment of inertia. A disadvantage of this method, however, is that the number of nodes in the structure is doubled, thus making much heavier demands on computer capacity and time.

A further variation for symmetrical structures only was presented by Stafford Smith (12) who replaced the rigid-armed beam by an analogous uniform beam with the same rotational end stiffness. This allowed a standard computer program to be used without any increase in the number of nodes.

Finite Element Method

The basis of the finite element method is that any structure can be considered as an assemblage of individual elements, of which the properties are known, connected to each other only at discrete nodes. This is in fact what has been done in the frame analogies but finite element analysis usually refers to systems where the elements are two or three dimensional rather than line elements. The method is well documented and typical works are by Zienkiewicz (13) and Rockey et al (14).

Although elements of any shape can be used it is general, in shear wall analysis, to use either rectangular or triangular elements with the triangular elements being used in transitional areas between coarse meshes in regions

of nearly uniform stress and fine meshes in regions of high stress gradients. One very big disadvantage of the technique is the large amount of computer storage required for a solution and because of this the value of the method lies in the analysis of local stress distributions rather than an overall analysis of a structure.

Choudhury (15) used the method to make comparisons with the solutions obtained from other forms of analysis and MacLeod (10) used the method for the analysis of coupled shear walls with relatively stiff beams. His work showed that rectangular elements gave satisfactory results provided the mesh was not too coarse.

MacLeod (16) also derived a special element having a rotational degree of freedom at each node and was thus able to combine line elements in bending, which are needed for slender connecting beams, with the plane stress elements of the walls.

Continuous Connection Method

In the 'continuous connection method' the discrete set of connecting beams, which are usually evenly spaced, is replaced by an equivalent continuous medium which is assumed to be rigidly attached to the walls but which is only capable of transmitting actions of the same type as the discrete system (see Figure 1.1(d)). By assuming that

the connecting beams have a point of contraflexure at mid-span and that they do not deform axially, the method leads to a definition of the behaviour of the system as a second order differential equation which can be solved for particular load cases.

Although the replacement of a series of members had been used before for tall frame buildings by Chitty (17), Beck (18) appears to have been the first to apply this method to coupled shear walls when he considered the single case of two uniform coupled shear walls on a rigid foundation, subjected to a uniformly distributed lateral load. In the analysis he used the shear forces in the connecting medium as the statically indeterminate function.

Using the integral of the shear force in the connecting medium as the indeterminate function, Rosman (19) derived solutions for a wall system with one or two symmetric bands of openings, with various support conditions at the base of the walls, and for both a uniformly distributed load and a single point load at the top.

Coull and Puri (20) considered the same problem as Beck but in their analysis they took account of the shear deformations in the walls, in addition to the axial and bending deformations in the walls, and the bending and shear deformations in the connecting medium. These effects

of shear had been ignored by previous researchers and were shown not to have a significant effect on the results of the analysis.

In the design procedure for shear walls put forward by Pearce and Mathews (21), the basic equations of the continuous connection method were re-written to include the wind loading shape of CP3 (22). However, it was concluded that for practical purposes, satisfactory results could be obtained by using the formulae for a uniform loading.

The simplicity of the general technique has enabled Coull and Choudhury to put forward design curves (23 and 24) and Rosman to put forward design tables (25) which enable a rapid and accurate analysis of the structure for standard load cases.

Importance of Beam-Wall Flexibility

In all the analyses outlined it has been assumed that the beam-wall connection is fully rigid, but due to high stress intensities at these connections local deformations will occur which effectively increase the flexibility of the connecting beams.

Michael (26) analysed these local deformations by considering the wall as a semi-infinite elastic plane and the effects of these deformations were calculated as reduction factors for the beam stiffnesses. The variations

of the reduction factors with the geometric proportions of the beam were presented as graphs. He suggested that for most span to depth ratios likely to occur in practice it is possible to take this extra flexibility into account by assuming an increase in the clear span of the beam of half its depth on each side.

Further work was done by Bhatt (27) who conducted an investigation of the local deformations using the finite element procedure. He concluded that the effect of junction deformations was only important when the ratio of beam length to depth was less than 5, and that for ratios between 5 and 3 the correction suggested by Michael could be used. For the analysis of walls with stiffer connecting beams he presented further modifications in graphical and tabular form which could be applied to both the continuous connection and wide column frame methods of analysis.

Importance of Coupling Action

When the openings in a coupled shear wall system are very small their effect on the overall state of stress is minor. Larger openings have a more pronounced effect and, if large enough, result in a system in which typical frame action predominates. The degree of coupling between the two walls connected by beams has been conveniently expressed in terms of the non-dimensional geometric parameter αH , which

gives a measure of the relative stiffness of the connecting beams with respect to that of the walls. The parameter appears in the basic differential equation of the continuous connection method.

A study by Marshall (28) indicated that when αH exceeds 13 the walls may be analysed as a single solid cantilever, and when αH is less than 0.8 the walls may be treated as two separate cantilevers. For intermediate values, the stiffness of the connecting beams should be considered.

The question of when coupling action is important was also considered by Pearce and Mathews (21) and they decided that the upper limit for αH should be 16 and that the lower limit should be 4.

However, despite the difference in the sets of figures given, it would appear that for most wall systems likely to occur in practice the coupling action should be considered.

Non-Uniform Coupled Shear Walls

Because the coupled shear wall system is replaced by a large number of individual elements in the wide column frame method, any number of variations in cross-section or any number of connected walls can easily be accommodated, subject to computer capacity not being exceeded.

However, with the continuous connection method the algebraic expressions involved only allow a limited number of discontinuities to be incorporated.

Traum (29) used the continuous connection method to analyse a system of symmetrical coupled shear walls pierced by one band of openings and with a single stepped variation in cross-section and intensity of uniformly distributed loading. The upper zone of the wall was solved as being elastically supported on the lower one and that was then analysed by subjecting it to axial forces, bending moment and shearing force at its top together with the external horizontal loading.

Using the same approach, but applying all the loads simultaneously, Coull and Puri (30) presented a simpler analysis of the problem considered by Traum but which also included the effects of shearing deformations in the walls. Pisanty and Traum (31) presented their own simplified analysis but there seemed to be disagreement between the two sets of authors as to the conditions to be adopted at the change in wall section.

Another type of discontinuity was presented by Coull and Puri (32) who considered a stepped variation in the thickness of the walls.

To overcome the complexity of analysing shear wall

systems with more than one abrupt change in cross-section and/or more than one band of openings by the analytical procedures (i.e. by direct solution of the governing differential equations) a numerical approach to the problem in the form of a matrix progression solution was presented by Puri (33).

The essential features of the 'matrix progression method' are given by Tottenham (34). When applied to coupled shear wall analysis the basis of the method is that the structure is divided into uniform zones and differential equations governing the behaviour of each zone can be determined. An overall solution is then obtained by applying boundary and continuity conditions. The only limitation of the method, when applied to shear walls, is that the centre line of each band of openings must be continuous throughout the total height of the wall.

The method was extended by Coull, Puri and Tottenham (35) to the solution of coupled shear wall systems containing any number of stepped variations in cross-section and any number of bands of openings. At the same time the number of differential equations governing the behaviour of each zone was reduced, thus lessening the work load required in an analysis.

The method was also adopted by Tso and Chan (36) who

only considered walls containing one band of openings but included the effects of flexible foundations in their analysis.

Non-Rigid Foundations

Many shear wall systems are rigidly built in at foundation level but in practice other base conditions can occur. On one hand the walls may be built on independent foundations which yield vertically and rotationally relative to each other. On the other hand, the walls may be supported at first floor level on a column system to allow large open spaces at ground floor level. If either of these two conditions occur, the behaviour of the lower parts of the wall system can be significantly altered.

The analysis of walls on flexible foundations using the wide column frame method presents no problems as most standard computer programs allow prescribed displacements to be applied at any node.

MacLeod and Green (37) used the wide column frame method to analyse a wall with one band of openings supported on a beam and column system. They considered symmetrical and non-symmetrical walls with both stiff and flexible connecting beams and they showed that the results obtained agree satisfactorily with finite element analysis.

The use of the continuous connection method for the

analysis of walls supported on columns was first put forward by Rosman (19).

Further work using this method has been done by Coull and Chantoksinopas (38) who presented design curves for any pair of walls or a set of three symmetrical walls supported on any elastic foundation or any beam column system. Three loading cases, namely a uniformly distributed load, a point load at the top and a triangular load were considered and a complete solution for any load form and any base condition can be obtained using only three design charts. A comprehensive series of formulae, rather than charts, for the analysis of similar structures have also been presented by Coull and Mukherjee (39).

Arvidsson (40) also considered the problem and presented a method for analysing shear walls with two bands of openings supported on an elastic foundation.

1.3 Scope of Present Work

Although the continuous connection method is well accepted for the analysis of uniform coupled shear wall systems, it has frequently been criticised as not having the flexibility of the wide column frame method to cover non-uniform structures. Although this criticism is justified when the analytical solution is employed, it has been shown, in theory, that the method has much greater

potential for the analysis of complex wall systems if a numerical solution is adopted.

The object of the present work is to check the accuracy of the matrix progression solution of the continuous connection method against both experimental results and the wide column frame method for a variety of non-uniform coupled shear walls, including walls supported on columns.

ANALYTICAL SOLUTION

2.1 Introduction

In this chapter, the differential equations governing the behaviour of a uniform coupled shear wall structure with a rigid foundation are derived using the continuous connection, and an analytical solution is obtained.

Although the method itself has appeared frequently before, it was thought necessary to include it here to show the procedure adopted in the solution, and also as an introduction to the numerical method presented in Chapter 3.

To achieve consistency with the numerical solution, the equations have been derived using the base of the wall as the origin for the x co-ordinate, and in this respect they differ from previously published equations.

The only loading case considered is that of a uniform lateral load.

2.2 Notation

The following symbols are used in this chapter.

A_A, A_B	Cross-sectional area of walls A and B respectively
b	Length of connecting beams
d	Depth of connecting beams
E	Young's modulus

G	Shear modulus
H	Total height of wall
h	Storey height
I_A, I_B	Moment of inertia of walls A and B respectively
I_b	Moment of inertia of connecting beams
I_v	Reduced moment of inertia of connecting beams
l	Distance between centroidal axes of walls
M_A, M_B	Bending moment in walls A and B respectively at a height x
M_q	Applied bending moment at a height x
N_A, N_B	Axial force in walls A and B respectively at a height x
q	Applied lateral distributed load
V_A, V_B	Shear force in walls A and B respectively at a height x
v	Distributed shear force in the substitute connecting medium at a height x
x	Height above foundation
y	Lateral deflection of walls at a height x

Any other symbols used are defined as they are introduced.

2.3 Assumptions

- (a) The walls have a rigid foundation
- (b) The moments of inertia and cross-sectional areas of both the walls and the connecting beams, and the storey height are constant throughout the height of the structure.

- (c) The points of contraflexure of the connecting beams are at their midspan
- (d) The connecting beams do not deform axially and hence the lateral deflection of individual walls is the same at any level
- (e) In each zone the discrete set of uniform connecting beams may be replaced by a uniform equivalent connecting medium of the same stiffness. The stiffness of the connecting medium for half a storey height above the foundation is considered as taken from the rigid connection at the foundation
- (f) Plane sections of the wall before bending remain plane after bending. This allows the moment-curvature relations based on the engineers theory of bending to be used for individual walls
- (g) The beam-wall connection is fully rigid.

2.4 Uniform Coupled Shear Wall Containing One Band of Openings

The structure considered is shown in Figure 2.1, where the individual connecting beams of stiffness EI_b are replaced by an equivalent continuous medium or lamellae of stiffness EI_b/h per unit height.

Governing Differential Equation

Consider a 'cut' along the centre line of the medium connecting the two walls. There will be movement of the two parts of the medium due to both rotation and vertical movement of the walls.

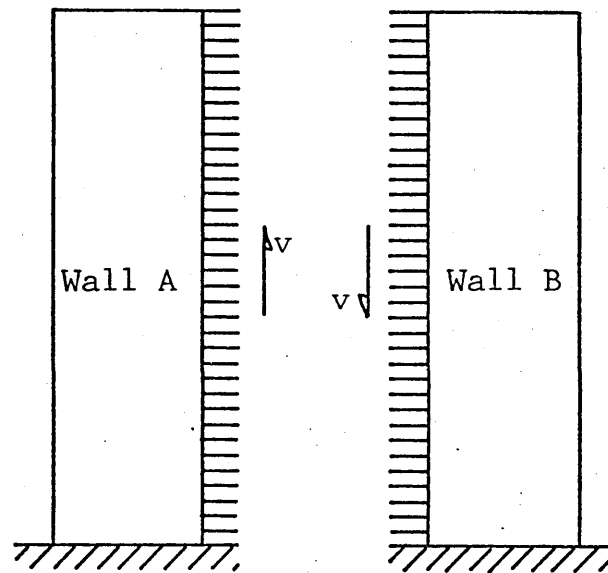
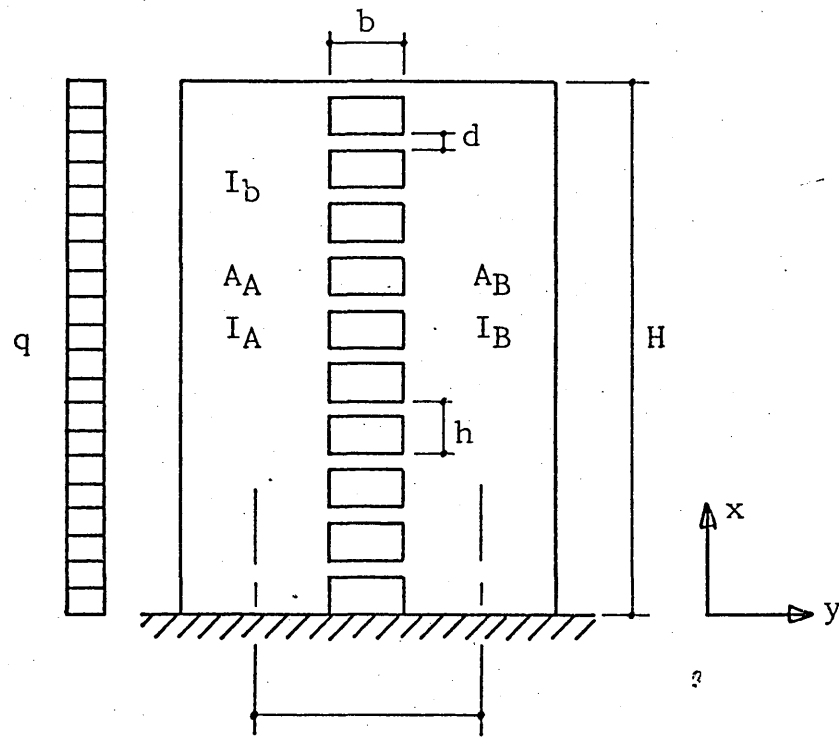


Figure 2.1 Coupled Shear Wall and Substitute System

The axial force in wall A at any height x is given by:

$$N_A = \int_x^H v dx$$

and thus the vertical movement of wall A at a height x is given by:

$$\frac{1}{EA_A} \int_0^x \int_{\gamma}^H v d\gamma dx$$

where γ is a dummy variable which is used to signify the variation of N_A within the region 0 to x .

For vertical equilibrium of the wall system

$$N_B = -N_A$$

and thus the vertical movement of wall B at a height x is given by:

$$- \frac{1}{EA_B} \int_0^x \int_{\gamma}^H v d\gamma dx$$

Thus the total relative displacement at the cut is given by:

$$\delta = \ell \frac{dy}{dx} - \frac{1}{E} \left(\frac{1}{A_A} + \frac{1}{A_B} \right) \int_0^x \int_{\gamma}^H v d\gamma dx$$

To restore continuity in the connecting medium, a shearing force v must be applied across the cut so that

$$v = \frac{12EI_v}{hb^3} \delta$$

where I_v is a reduced moment of inertia to take account of shear and is given by:

$$I_v = \frac{I_b}{1 + 1.2 \frac{E}{G} \left(\frac{d}{b} \right)^2}$$

Thus the compatibility equation is:

$$\frac{dy}{dx} - \frac{hb^3}{12EI_v} v - \frac{1}{E} \left(\frac{1}{A_A} + \frac{1}{A_B} \right) \int_0^x \int_y^H v dy dx = 0 \quad (2.1)$$

The moment curvature relationship for the walls is:

$$\frac{d^2y}{dx^2} = \frac{-M}{EI}$$

where $M = M_A + M_B$

and $I = I_A + I_B$

and thus:

$$EI \frac{d^2y}{dx^2} = \frac{q}{2} (H - x)^2 - q \int_x^H v dx \quad (2.2)$$

A differential equation governing the distributed shear force can now be obtained by differentiating Equation 2.1 w.r.t.x, substituting Equation 2.2 and differentiating again.

Thus:

$$\frac{d^2v}{dx^2} - \alpha^2 v = -2\beta (H - x) \quad (2.3)$$

where $\alpha^2 = \frac{12I_v}{hb^3} \left(\frac{q^2}{I} + \frac{A}{A_A A_B} \right)$

and $\beta = \frac{q q}{2} \cdot \frac{12I_v}{hb^3} \cdot \frac{1}{I}$

and where $A = A_A + A_B$

Solution for Distributed Shear Force

The general solution of Equation 2.3 is:

$$v = Pe^{\alpha x} + Qe^{-\alpha x} + \frac{2\beta}{\alpha^2} (H - x) \quad (2.4)$$

where P and Q are constants of integration which depend on

the boundary conditions.

At the base, the rotation is zero and thus, from Equation 2.1, we obtain:

$$v = 0 \text{ when } x = 0$$

At the top of the wall, the moment, and thus the curvature are zero and once again from Equation 2.1 we obtain:

$$\frac{dv}{dx} = 0 \text{ when } x = H$$

Using the above conditions, Equation 2.4 becomes:

$$v = \frac{qH}{\mu l} F_1 \quad (2.5)$$

where

$$F_1 = \frac{1 + \alpha H \sinh \alpha H}{\alpha H \cosh \alpha H} \sinh \left(\alpha H \frac{x}{H} \right) - \cosh \left(\alpha H \frac{x}{H} \right) + \left(1 - \frac{x}{H} \right) \quad (2.6)$$

and

$$\mu = 1 + \frac{A}{A_A A_B} \frac{I}{l^2}$$

Height of Maximum Distributed Shear Force

From Equation 2.5 it is seen that the maximum value of the distributed shear force v occurs when F_1 is a maximum.

Thus, differentiating Equation 2.6 w.r.t. x and equating to zero, the only valid solution for x is

$$\frac{x}{H} = 1 - \frac{1}{\alpha H} \log_e \left(\frac{\cosh \alpha H + \sinh \alpha H - \alpha H}{\cosh \alpha H - \sinh \alpha H + \alpha H} \right) \quad (2.7)$$

Thus, the value of v_{\max} is obtained by substituting

Equation 2.7 into Equation 2.6 to give $F_{1\max}$ and then substituting this value into Equation 2.5.

Axial Force and Bending Moment

The axial force in each wall is given by:

$$N = \int_x^H v dx$$

Substituting Equation 2.5 and re-arranging the terms we obtain:

$$N = \frac{Mq}{\mu l} F_2 \quad (2.8)$$

where

$$Mq = \frac{q(H-x)^2}{2}$$

and

$$F_2 = \frac{2}{(\alpha H)^2 \left(1 - \frac{x}{H}\right)^2} \left\{ 1 - \frac{1 + \alpha H \sinh \alpha H}{\cosh \alpha H} \cosh \left(\alpha H \frac{x}{H} \right) + \alpha H \sinh \left(\alpha H \frac{x}{H} \right) + \frac{(\alpha H)^2}{2} \left(1 - \frac{x}{H}\right)^2 \right\}$$

The moment resisted by the axial forces N is Nl , which from Equation 2.8 is equal to $\frac{MqF_2}{\mu}$

Thus the moment resisted by bending of both walls is given by:

$$M = Mq \left(1 - \frac{F_2}{\mu} \right) \quad (2.9)$$

Deflections

The deflection y at any height can be obtained by substituting Equation 2.5 into Equation 2.2, integrating twice w.r.t. x and applying the appropriate boundary conditions,

i.e. $\frac{dy}{dx} = 0$ and $y = 0$ at $x = 0$

Thus

$$y = \frac{qH^4}{EI} F_3 \quad (2.10)$$

where

$$F_3 = \left\{ \frac{1}{24} \left(1 - \frac{x}{H} \right)^4 + \frac{1}{6} \frac{x}{H} - \frac{1}{24} \right\} \left\{ 1 - \frac{1}{\mu} \right\} \\ + \frac{1}{\mu} \left\{ \frac{x/H}{(\alpha H)^2} \left(1 - \frac{1}{2} \frac{x}{H} \right) + \frac{(1 + \alpha H \sinh \alpha H)}{(\alpha H)^4 \cosh \alpha H} \left(\cosh \left(\alpha H \frac{x}{H} \right) - 1 \right) \right. \\ \left. - \frac{1}{(\alpha H)^3} \sinh \left(\alpha H \frac{x}{H} \right) \right\}$$

For the maximum deflection y_{\max} the condition $x = H$ can be substituted into the equation for F_3 and thus

$$y_{\max} = \frac{qH^4}{EI} F_4 \quad (2.11)$$

where

$$F_4 = \left(\frac{\mu - 1}{\mu} \right) + \frac{8}{\mu} \left\{ \frac{1}{2(\alpha H)^2} + \frac{\cosh \alpha H - \alpha H \sinh \alpha H - 1}{(\alpha H)^4 \cosh \alpha H} \right\}$$

2.5 Complex Shear Wall Systems

The method of analysis presented in Section 2.4 can obviously be extended to cater for any number of bands of openings and any number of abrupt changes in cross-section.

However, each band of openings produces a differential equation of second order, and each change in cross-section requires the solutions of the equations below and above the discontinuity to be matched. Thus only two, or possibly three, such effects can be dealt with before the algebraic expressions involved become unmanageable and it is for

this reason that alternative methods of analysis have been developed.

MATRIX PROGRESSION SOLUTIONS

3.1 Introduction

The Matrix Progression Method, as outlined by Tottenham (34), is a technique of structural analysis especially designed for application to complex structures composed of several shell or plate elements. The analysis of these structures involves a considerable amount of numerical computation whatever method is used and the purpose of the matrix progression method is to make the analysis as simple as possible, because by using matrix algebra the calculations are readily planned.

The basis of the method is a special form of solution of the basic differential equations governing the stress and displacement conditions in a structure. The solution is in two parts, corresponding to the complementary function and the particular integral, the first part of which depends only on the boundary conditions at one end of the structure and the second part of which depends only on the loading system. By using the solution in this form we can write the solution for an element of the structure in general terms and add in the effects of applied loads, or changes in structural properties, as and when they occur.

The essential requirements of the method are that the sum of the order of the basic differential equations must be even, and one half of the boundary conditions must be known at each end.

In this chapter, a uniform coupled shear wall containing one band of openings and subjected to both a uniformly distributed load and a point load is considered first. The analysis is then extended to deal with systems in which an abrupt change in geometry of the structure takes place at a particular height. This is done by splitting the structure into two zones such that the geometric properties and applied loading intensity remain constant in any one zone. The only restriction to the variation of the geometric properties and loading from one zone to the other is that the line of the centres of the connecting beams is continuous through the two zones. Sets of differential equations governing the behaviour of each zone are determined and a solution is obtained by applying appropriate continuity and boundary conditions.

The solution is then extended to deal with structures containing two bands of openings and having an abrupt change in cross-section, and finally the analysis is generalised for coupled shear walls with any number of bands of openings and any number of abrupt variations in cross-section.

3.2 Notation

The following symbols are used in this chapter:

A_A, A_B	Cross-sectional area of walls A and B respectively
$a_{N,A}, a_{N,B}$	Axial displacement of walls A and B respectively at a height x
B_A, B_B	Width of walls A and B respectively
b	Length of connecting beams
d	Depth of connecting beams
E	Young's modulus
F	Applied point load
G	Shear modulus
H	Total height of wall or zone
h	Storey height
I_A, I_B	Moment of inertia of walls A and B respectively
I_b	Moment of inertia of connecting beams
I_v	Reduced moment of inertia of connecting beams
ℓ	Distance between centroidal axes of walls
M_A, M_B	Bending moment in walls A and B respectively at a height x
N_A, N_B	Axial force in walls A and B respectively at a height x
q	Applied distributed load
V_A, V_B	Shear force in walls A and B respectively at a height x
v	Distributed shear force in the substitute connecting medium at a height x

- x Height above foundation or discontinuity
- y Deflection of walls at a height x
- θ Rotation of walls at a height x

The additional suffices 1 and 2 after any symbol refer to zones 1 and 2 respectively.

Matrices are denoted by underlining the symbol e.g. A.

Any other symbols used are defined as they first appear.

3.3 Assumptions

The assumptions made are the same as in Section 2.3 except that (a) need not apply.

3.4 Uniform Coupled Shear Walls Containing One Band of Openings

The coupled shear wall system referred to in the following analysis is shown in Figure 3.1.

Displacement and Elasticity Relationships

At any distance x from the base, the lateral displacement y and the rotation θ are equal for both the walls and their relationship is given by:

$$\frac{dy}{dx} = \theta \quad (3.1)$$

Consider now a 'cut' along the centre line of the medium connecting the two walls. There will be a movement of the two parts of the medium due to both rotation and vertical movement of the walls (See Figure 3.2).

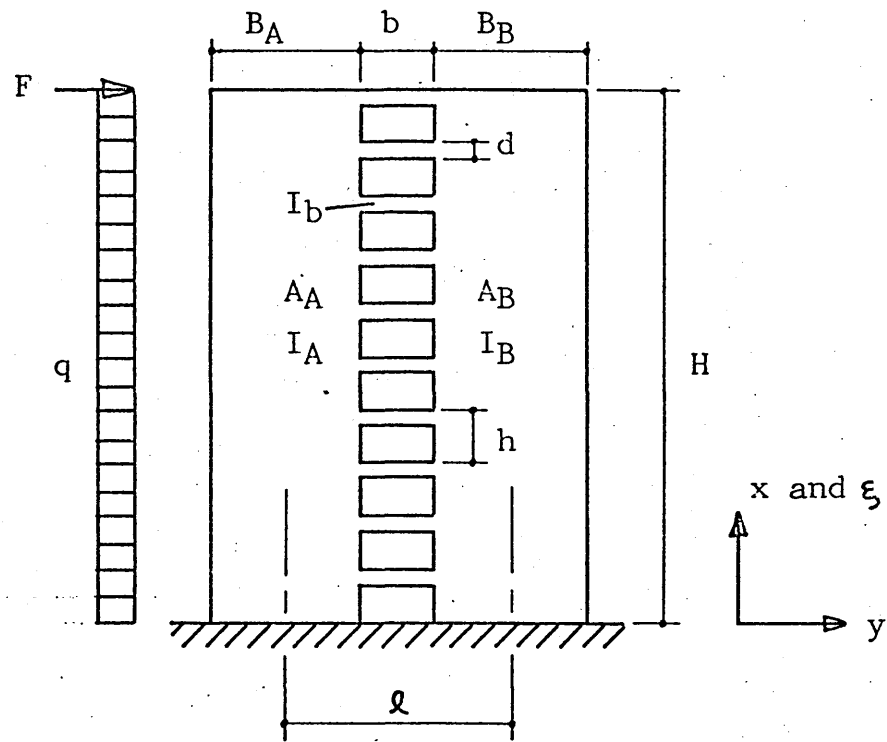


Figure 3.1 Coupled Shear Wall

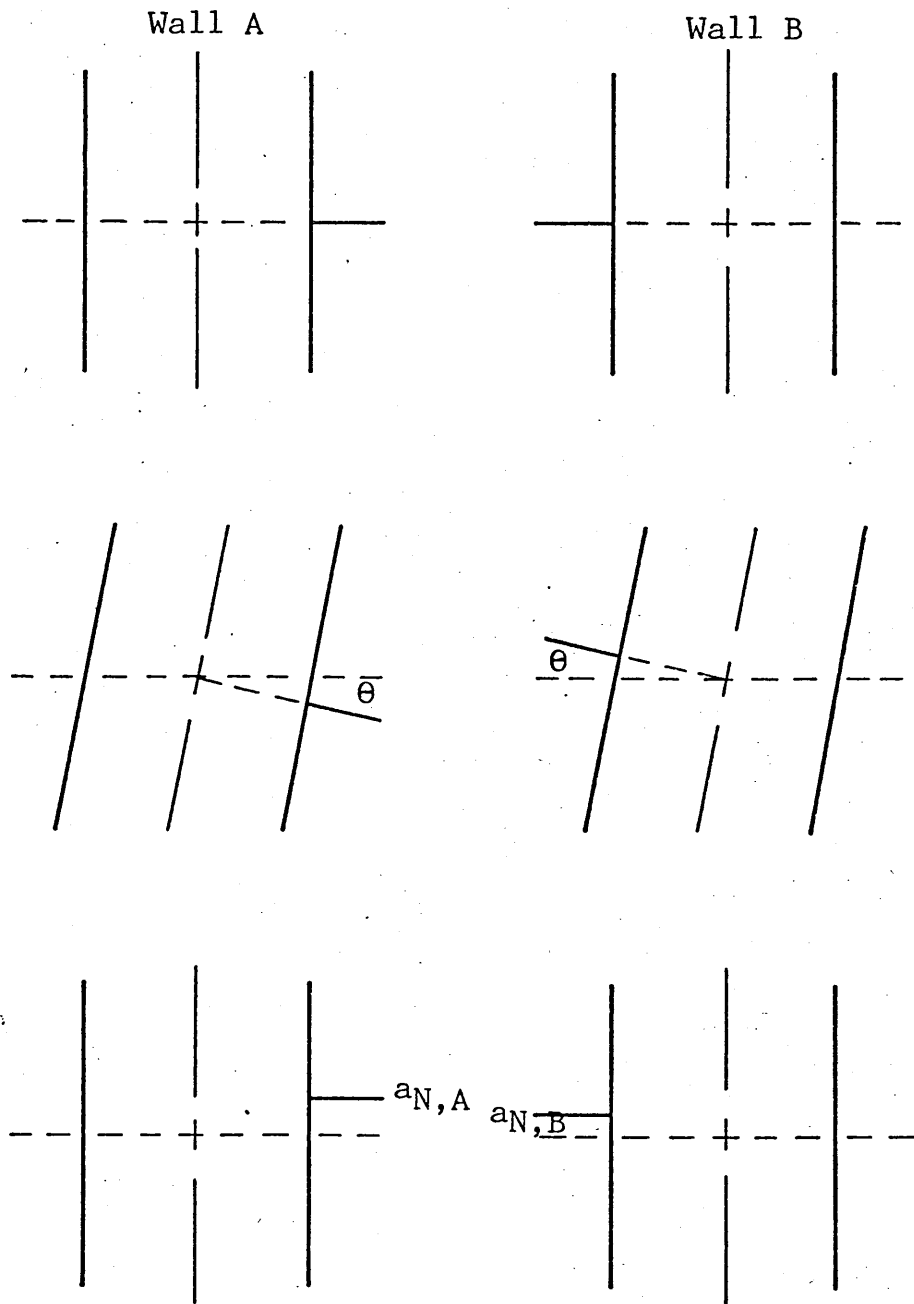


Figure 3.2 Displacement of the ends of the cut connecting medium

The end attached to wall A will approach the base by an amount

$$\left(\frac{b}{2} + \frac{B_A}{2}\right)\theta - a_{N,A}$$

while the end attached to wall B will move away from the base by an amount

$$\left(\frac{b}{2} + \frac{B_B}{2}\right)\theta + a_{N,B}$$

The relative displacement at the cut, δ , is thus given by

$$\delta = l\theta - a_{N,A} + a_{N,B}$$

To restore continuity in the connecting medium, a shearing force v must be applied across the cut.

The deflection of a unit cantilever due to bending and shear is given by

$$\delta = \frac{hb^3}{12EI_V} v$$

where I_V is a reduced moment of inertia to take account of shear force and is given by

$$I_V = \frac{I_b}{1 + 1.2E/G (d/b)^2}$$

Thus the value of the shear force is given by

$$v = \frac{12EI_V}{hb^3} (l\theta - a_{N,A} + a_{N,B}) \quad (3.2)$$

The moment-curvature relationship for the walls is

$$\frac{d\theta}{dx} = \frac{M}{EI} \quad (3.3)$$

where $M = M_A + M_B$ and $I = I_A + I_B$.

The vertical strain of the centre line of wall A is

$\frac{da_{N,A}}{dx}$ and is given by

$$\frac{da_{N,A}}{dx} = \frac{N_A}{EA_A} \quad (3.4)$$

Similarly

$$\frac{da_{N,B}}{dx} = \frac{N_B}{EA_B} \quad (3.5)$$

Diffentiating Equation 3.2, and substituting Equations 3.3, 3.4 and 3.5, we obtain

$$\frac{dv}{dx} = \frac{12I_v}{hb^3} \left(-\frac{M_0}{I} - \frac{N_A}{A_A} + \frac{N_B}{A_B} \right) \quad (3.6)$$

Equilibrium Conditions

Consider an elementary part of wall A of height dx as shown in Figure 3.3.

For vertical equilibrium

$$\frac{dN_A}{dx} = -v \quad (3.7)$$

For moment equilibrium, ignoring the second order derivatives

$$\frac{dM_A}{dx} = -v \left(\frac{B_A}{2} + \frac{b}{2} \right) + V_A \quad (3.8)$$

Consider now an elementary part of wall B of height dx as shown in Figure 3.4.

$$\frac{dN_B}{dx} = v \quad (3.9)$$

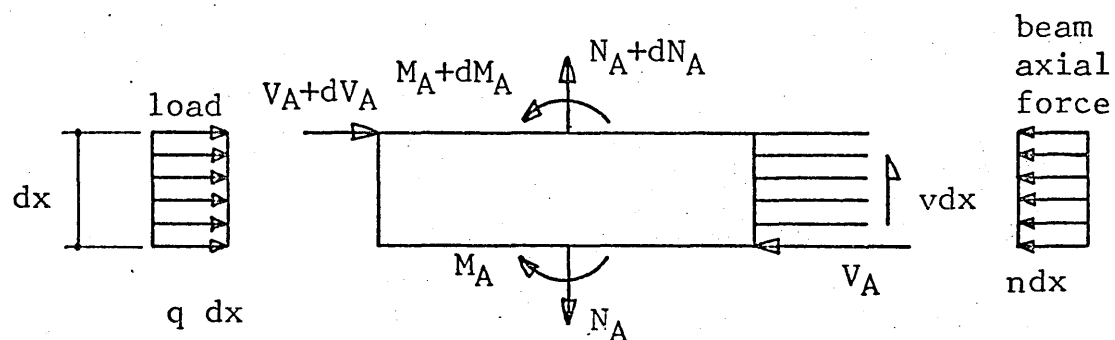


Figure 3.3 Elementary Part of Wall A

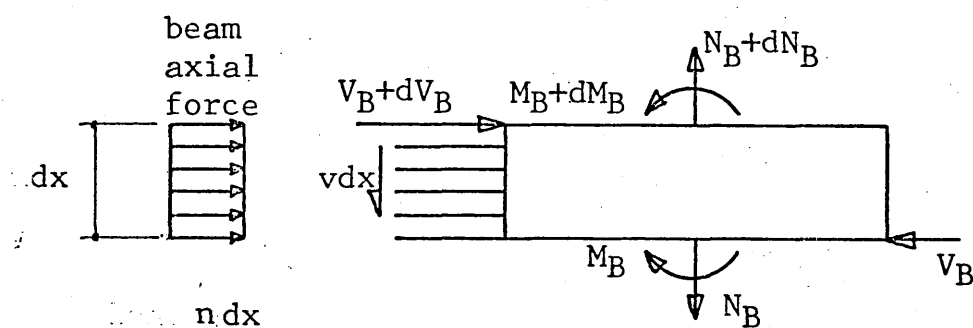


Figure 3.4 Elementary Part of Wall B

For moment equilibrium, once again ignoring the second order derivatives

$$\frac{dM_B}{dx} = -v \left(\frac{b}{2} + \frac{B_B}{2} \right) + V_B \quad (3.10)$$

Combining the moment equations 3.8 and 3.10 gives

$$\frac{dM}{dx} = -\ell v + V \quad (3.11)$$

where $V = V_A + V_B$

For vertical equilibrium of the wall system it is required that

$$N_B = -N_A \quad (3.12)$$

and substituting Equation 3.12 into Equation 3.6 gives

$$\frac{dv}{dx} = \frac{-12I_V \ell}{hb^3 I} M - \frac{12I_V}{hb^3} \left(\frac{1}{A_A} + \frac{1}{A_B} \right) N_A$$

or

$$\frac{dv}{dx} = \gamma M + \mu N_A \quad (3.13)$$

where

$$\gamma = \frac{-12I_V}{hb^3 I}$$

and

$$\mu = \frac{-12I_V}{hb^3} \left(\frac{1}{A_A} + \frac{1}{A_B} \right)$$

For horizontal equilibrium of the wall system

$$\frac{dV}{dx} = -q \quad (3.14)$$

System of Equations

In Equations 3.1, 3.3, 3.11, 3.14, 3.13 and 3.7 we have obtained a set of six first order differential equations containing the actions y , θ , M , V , v and N_A . If

we now express these equations in terms of a non-dimensional height co-ordinate ξ where

$$\xi = \frac{x}{H}$$

we obtain

$$\frac{dy}{d\xi} = H\theta$$

$$\frac{dO}{d\xi} = -H \frac{M}{EI}$$

$$\frac{dM}{d\xi} = -H \rho v + HV$$

$$\frac{dV}{d\xi} = -Hq$$

$$\frac{dv}{d\xi} = H\gamma M + H\mu N_A$$

$$\frac{dN_A}{d\xi} = -Hv$$

and these equations can be expressed in matrix form as

$$\frac{d}{d\xi} \begin{bmatrix} Ey \\ E\theta \\ M \\ V \\ v \\ N_A \end{bmatrix} = \begin{bmatrix} 0 & H & 0 & 0 & 0 & 0 \\ 0 & 0 & -H/I & 0 & 0 & 0 \\ 0 & 0 & 0 & H & -H\rho & 0 \\ 0 & 0 & 0 & 0 & 0 & 0 \\ 0 & 0 & H\gamma & 0 & 0 & H\mu \\ 0 & 0 & 0 & 0 & -H & 0 \end{bmatrix} \begin{bmatrix} Ey \\ E\theta \\ M \\ V \\ v \\ N_A \end{bmatrix} + \begin{bmatrix} 0 \\ 0 \\ 0 \\ -Hq \\ 0 \\ 0 \end{bmatrix}$$

which can be written as

$$\frac{d \underline{S}}{d \xi} = \underline{A} \underline{S} + \underline{B} \quad (3.15)$$

where

$$\underline{A} = H \begin{vmatrix} 0 & 1 & 0 & 0 & 0 & 0 \\ 0 & 0 & -1/I & 0 & 0 & 0 \\ 0 & 0 & 0 & 1 & -l & 0 \\ 0 & 0 & 0 & 0 & 0 & 0 \\ 0 & 0 & \gamma & 0 & 0 & \mu \\ 0 & 0 & 0 & 0 & 1 & 0 \end{vmatrix}$$

and $\underline{B} = \begin{vmatrix} 0 & 0 & 0 & -Hq & 0 & 0 \end{vmatrix}^T$

Solution of Equations

Equation 3.15 is a linear first order differential equation and the integrating factor required for its solution is

$$\left(\int \underline{A} d\xi \right)^{-1} = \left(\underline{e}^{\underline{A}\xi} \right)^{-1}$$

Multiplying the equation by this factor gives

$$\left(\underline{e}^{\underline{A}\xi} \right)^{-1} \frac{d \underline{S}(\xi)}{d\xi} - \left(\underline{e}^{\underline{A}\xi} \right)^{-1} \underline{A} \underline{S}(\xi) = \left(\underline{e}^{\underline{A}\xi} \right)^{-1} \underline{B}$$

which reduces to

$$\frac{d}{d\xi} \left\{ \left(\underline{e}^{\underline{A}\xi} \right)^{-1} \underline{S}(\xi) \right\} = \left(\underline{e}^{\underline{A}\xi} \right)^{-1} \underline{B}$$

Integrating, we obtain

$$\left(\underline{e}^{\underline{A}\xi} \right)^{-1} \underline{S}(\xi) = - \underline{A}^{-1} \left(\underline{e}^{\underline{A}\xi} \right)^{-1} \underline{B} + \underline{K} \quad (3.16)$$

where \underline{K} is a constant of integration.

Substituting the boundary condition of

$$\underline{S}(\xi) = \underline{S}(0) \text{ when } \xi = 0$$

gives

$$\underline{K} = \underline{S}(0) + \underline{A}^{-1} \underline{B}$$

Substituting this value of \underline{K} into Equation 3.16 gives

$$\underline{S}(\xi) = \underline{e}^{\underline{A}\xi} \underline{S}(0) - \left\{ \underline{I} - \underline{e}^{\underline{A}\xi} \right\} \underline{A}^{-1} \underline{B} \quad (3.17)$$

Now $\underline{e}^{\underline{A}\xi} = \underline{I} + \underline{A}\xi + \frac{\underline{A}^2 \xi^2}{2!} + \frac{\underline{A}^3 \xi^3}{3!} + \dots$

Thus $-\left\{ \underline{I} - \underline{e}^{\underline{A}\xi} \right\} = \underline{A}\xi + \frac{\underline{A}^2 \xi^2}{2!} + \frac{\underline{A}^3 \xi^3}{3!} + \dots$

and so

$$-\left\{ \underline{I} - \underline{e}^{\underline{A}\xi} \right\} \underline{A}^{-1} \underline{B} = \left\{ \underline{I}\xi + \frac{\underline{A}\xi^2}{2!} + \frac{\underline{A}^2 \xi^3}{3!} + \dots \right\} \underline{B}$$

Equation 3.17 can now be written as

$$\underline{S}(\xi) = \underline{G}(\xi) \underline{S}(0) + \underline{F}(\xi) \quad (3.18)$$

where

$$\underline{G}(\xi) = \underline{I} + \underline{A}\xi + \frac{\underline{A}^2 \xi^2}{2!} + \frac{\underline{A}^3 \xi^3}{3!} + \dots$$

and

$$\underline{F}(\xi) = \left\{ \underline{I}\xi + \frac{\underline{A}\xi^2}{2!} + \frac{\underline{A}^2 \xi^3}{3!} + \dots \right\} \underline{B}$$

Boundary Conditions

At the base of the wall, i.e. when $\xi = 0$, the displacements y , $a_{N,A}$ and $a_{N,B}$, and the rotation θ are all zero and by substituting the value of v as zero. Thus

$$y_0 = 0$$

$$\theta_0 = 0$$

$$v_0 = 0$$

These boundary conditions can be used to express the action matrix $\underline{S}(0)$ in terms of the matrix \underline{S}_0 which contains only the unknown conditions at the base i.e. M_0 , V_0 and N_0 .

Thus

$$\underline{S}(0) = \underline{K}_0 \underline{S}_0 \quad (3.19)$$

where

$$\underline{K}_o = \begin{vmatrix} 0 & 0 & 0 \\ 0 & 0 & 0 \\ 1 & 0 & 0 \\ 0 & 1 & 0 \\ 0 & 0 & 0 \\ 0 & 0 & 1 \end{vmatrix}$$

and

$$\underline{S}_o = \begin{vmatrix} M_o \\ V_o \\ N_o \end{vmatrix}$$

If the base is not fixed but is capable of rotation and vertical settlement then the forces and displacements at the base are related by

$$\begin{vmatrix} y_o \\ \theta_o \\ v_o \end{vmatrix} = \begin{vmatrix} 0 & 0 & 0 \\ C_1 & 0 & 0 \\ C_2 & 0 & C_3 \end{vmatrix} \begin{vmatrix} M_o \\ V_o \\ N_o \end{vmatrix}$$

where C_1 , C_2 and C_3 are constants dependent upon the rotational stiffness and the vertical displacement stiffness of the base and thus the value of \underline{K}_o in Equation 3.19 is given by

$$\underline{K}_o = \begin{vmatrix} 0 & 0 & 0 \\ C_1 & 0 & 0 \\ 1 & 0 & 0 \\ 0 & 1 & 0 \\ C_2 & 0 & C_3 \\ 0 & 0 & 1 \end{vmatrix}$$

By substituting Equation 3.19 into Equation 3.18 we can write the solution of Equation 3.15 as

$$\underline{S}(\xi) = \underline{G}(\xi) \underline{K}_0 \underline{S}_0 + \underline{F}(\xi) \quad (3.20)$$

Thus at the top of the wall, i.e. when $\xi = 1$

$$\underline{S}(1) = \underline{G}(1) \underline{K}_0 \underline{S}_0 + \underline{F}(1) \quad (3.21)$$

Now at the top of the wall, the bending moment and axial force are both zero and the horizontal shear force is equal to the applied point load. Thus

$$M_H = 0$$

$$V_H = F$$

$$N_H = 0$$

These boundary conditions can be used to write a second equation for the action matrix $\underline{S}(1)$.

Thus

$$\underline{K}_H \underline{S}(1) = \underline{F}_H \quad (3.22)$$

where

$$\underline{K}_H = \begin{vmatrix} 0 & 0 & 1 & 0 & 0 & 0 \\ 0 & 0 & 0 & 1 & 0 & 0 \\ 0 & 0 & 0 & 0 & 0 & 1 \end{vmatrix}$$

and

$$\underline{F}_H = \begin{vmatrix} 0 \\ F \\ 0 \end{vmatrix}$$

Substituting Equation 3.21 into Equation 3.22 gives

$$\underline{K}_H \underline{G}(1) \underline{K}_0 \underline{S}_0 + \underline{K}_H \underline{F}(1) = \underline{F}_H$$

and rearranging the terms we obtain

$$\underline{S}_0 = (\underline{K}_H \underline{G}(1) \underline{K}_0)^{-1} (\underline{F}_H - \underline{K}_H \underline{F}(1)) \quad (3.23)$$

Action Matrix Values

If the total height of the wall is divided into k sections each of height x_k then the value of \underline{S}_0 obtained from Equation 3.23 can be substituted into Equation 3.20 to obtain the values of the action matrix at a height of $x_k = \xi_k H$.

Thus

$$\underline{S}(\xi_k) = \underline{G}(\xi_k) \underline{K}_0 \underline{S}_0 + \underline{F}(\xi_k) \quad (3.24)$$

Similarly at a height of $2\xi_k H$, the values of the action matrix are given by

$$\underline{S}(2\xi_k) = \underline{G}(2\xi_k) \underline{K}_0 \underline{S}_0 + \underline{F}(2\xi_k) \quad (3.25)$$

Now from the definition of $\underline{G}(\xi)$ it follows that

$$\underline{G}(2\xi_k) = \underline{I} + 2\underline{A}\xi_k + \frac{4\underline{A}^2 \xi_k^2}{2!} + \frac{8\underline{A}^3 \xi_k^3}{3!} + \dots$$

and

$$\begin{aligned} \underline{G}^2(\xi_k) &= \underline{I}^2 + \underline{I} \underline{A}\xi_k + \frac{\underline{I} \underline{A}^2 \xi_k^2}{2!} + \frac{\underline{I} \underline{A}^3 \xi_k^3}{3!} + \dots \\ &\quad + \underline{I} \underline{A} \xi_k + \underline{A}^2 \xi_k^2 + \frac{\underline{A}^3 \xi_k^3}{2!} + \dots \\ &\quad + \frac{\underline{I} \underline{A}^2 \xi_k^2}{2!} + \frac{\underline{A}^3 \xi_k^3}{2!} + \dots + \frac{\underline{I} \underline{A}^3 \xi_k^3}{3!} + \dots \\ &= \underline{I} + 2\underline{A} \xi_k + \frac{4\underline{A}^2 \xi_k^2}{2!} + \frac{8\underline{A}^3 \xi_k^3}{3!} + \dots \end{aligned}$$

Thus

$$\underline{G}(2\xi_k) = \underline{G}^2(\xi_k) \quad (3.26)$$

From the definition of $\underline{F}(\xi)$ it follows that

$$\underline{F}(2\xi_k) = 2\underline{I}\xi_k + \frac{4\underline{A}\xi_k^2}{2!} + \frac{8\underline{A}^2 \xi_k^3}{3!} + \dots$$

but

$$\begin{aligned}
(\underline{G}(\xi_k) + \underline{I}) \underline{F}(\xi_k) &= 2\underline{I}^2 \xi_k + \frac{2\underline{I} \underline{A} \xi_k^2}{2!} + \frac{2\underline{I} \underline{A}^2 \xi_k^3}{3!} + \dots \\
&+ \underline{I} \underline{A} \xi_k^2 + \frac{\underline{A}^2 \xi_k^3}{2!} + \dots + \underline{I} \frac{\underline{A}^2 \xi_k^3}{2!} + \dots \\
&= 2\underline{I} \xi_k + \frac{4\underline{A} \xi_k^2}{2!} + \frac{8\underline{A}^2 \xi_k^3}{3!} + \dots
\end{aligned}$$

Thus

$$\underline{F}(2 \xi_k) = \underline{G}(\xi_k) \underline{F}(\xi_k) + \underline{F}(\xi_k) \quad (3.27)$$

Substituting Equations 3.26 and 3.27 into Equation 3.25

we obtain

$$\underline{S}(2 \xi_k) = \underline{G}(\xi_k) \underline{G}(\xi_k) \underline{K}_0 \underline{S}_0 + \underline{G}(\xi_k) \underline{F}(\xi_k) + \underline{F}(\xi_k)$$

or

$$\underline{S}(2 \xi_k) = \underline{G}(\xi_k) \underline{S}(\xi_k) + \underline{F}(\xi_k) \quad (3.28)$$

From Equation 3.28 it can be seen that the values of $\underline{S}(2 \xi_k)$ can be obtained by taking the values of $\underline{S}(\xi_k)$ as the initial boundary conditions for the region ξ_k to $2 \xi_k$.

Similarly for a height of $3 \xi_k$, the values of $\underline{S}(2 \xi_k)$ can be taken as the initial boundary conditions for the region $2 \xi_k$ to $3 \xi_k$, and thus

$$\underline{S}(3 \xi_k) = \underline{G}(\xi_k) \underline{S}(2 \xi_k) + \underline{F}(\xi_k) \quad (3.29)$$

Thus for any multiple of ξ_k , equations similar to 3.24, 3.28 and 3.29 can be written to obtain the values of the action matrix at any required height.

3.5 Coupled Shear Walls Containing One Band of Openings and with One Abrupt Variation in Cross Section

A typical structure covered by the analysis given in

this section is shown in Figure 3.5.

Zones 1 and 2 refer, respectively, to the wall systems below and above the change in cross-section.

Governing Equations

For the structure shown in Figure 3.5, the equations governing the actions in each of the two zones will be of a similar nature i.e.

$$\underline{S}_1(\xi_1) = \underline{G}_1(\xi_1) \underline{S}_1(0) + \underline{F}_1(\xi_1)$$

and

$$\underline{S}_2(\xi_2) = \underline{G}_2(\xi_2) \underline{S}_2(0) + \underline{F}_2(\xi_2)$$

Continuity Conditions

In this section the values of the individual actions at the top of zone 1 and at the base of zone 2 are referred to by using the suffices 1(1) and 2(0) respectively.

The action matrix $\underline{S}_2(0)$ is related to the action matrix $\underline{S}_1(1)$ by the equations of equilibrium and conditions of continuity at the change in cross-section.

For continuity of displacement

$$y_2(0) = y_1(1) \quad (3.30)$$

$$\theta_2(0) = \theta_1(1) \quad (3.31)$$

$$\delta_2(0) = \delta_1(1) \quad (3.32)$$

where δ denotes the relative displacement of the ends of the 'cut' lamellae.

From Equation 3.2, the distributed shearing force in each of the two zones is given by

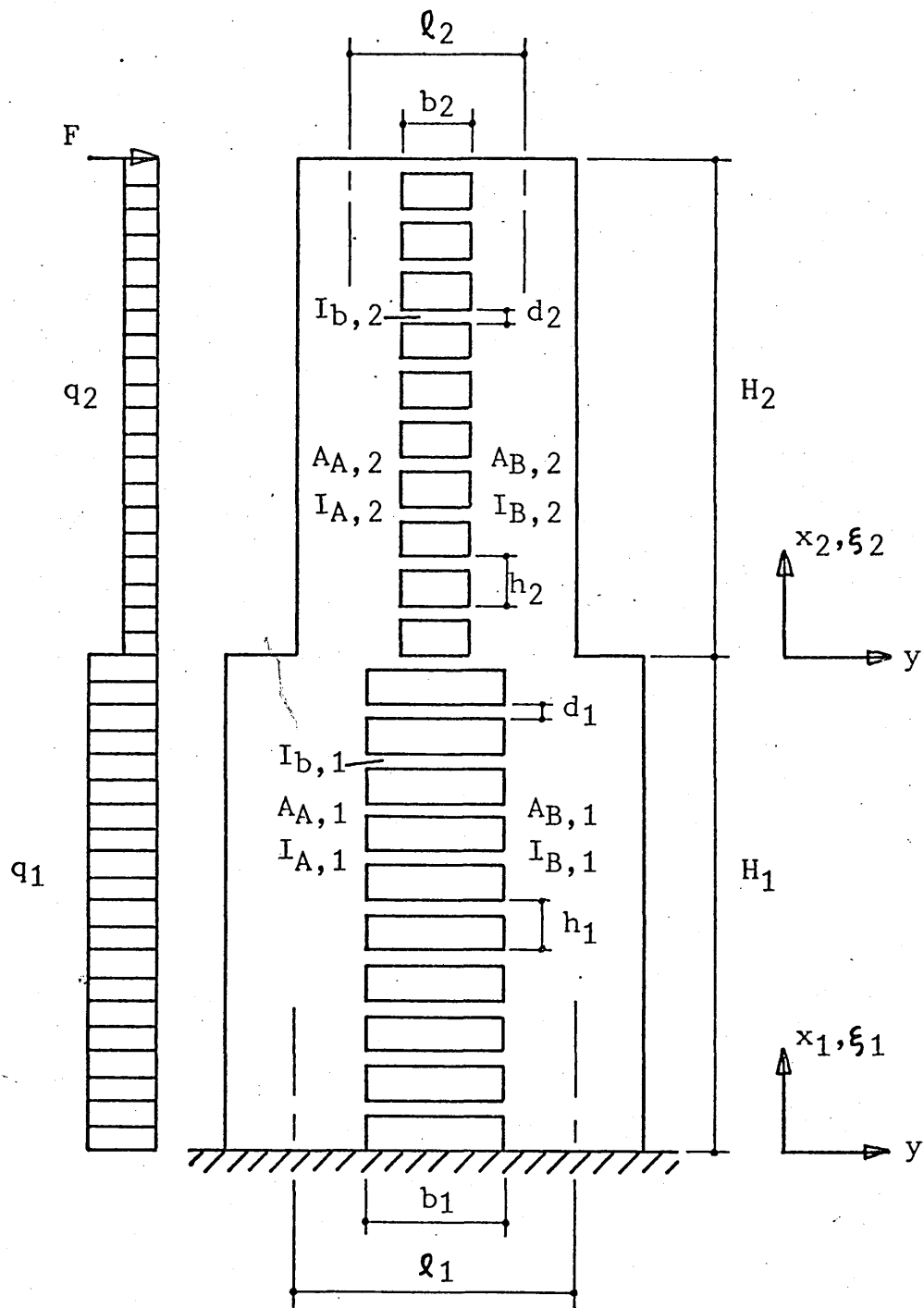


Figure 3.5 Coupled Shear Wall with One Abrupt Variation in Cross Section

$$v_2(0) = \frac{12EI_{v,2} \delta_2(0)}{h_2 b_2^3}$$

and

$$v_1(1) = \frac{12EI_{v,1} \delta_1(1)}{h_1 b_1^3}$$

and so, using Equation 3.32, we obtain

$$v_2(0) = \frac{h_1 b_1^3 I_{v,2}}{h_2 b_2^3 I_{v,1}} v_1(1) \quad (3.33)$$

The equilibrium conditions can be written with reference to Figure 3.6.

For equilibrium of axial forces in wall A

$$N_{A,2(0)} = N_{A,1(1)} \quad (3.34)$$

For shear force equilibrium of the wall system

$$V_{A,2(0)} + V_{B,2(0)} = V_{A,1(1)} + V_{B,1(1)}$$

or

$$V_2(0) = V_1(1) \quad (3.35)$$

For moment equilibrium of the wall system

$$\begin{aligned} M_{A,2(0)} + M_{B,2(0)} &= M_{A,1(1)} + M_{B,1(1)} - N_{A,1(1)}e_A \\ &\quad - N_{B,1(1)}e_B \end{aligned}$$

or

$$M_2(0) = M_1(1) - N_{A,1(1)}e_A - N_{B,1(1)}e_B$$

which can, using Equation 3.12, be written as

$$M_2(0) = M_1(1) - N_{A,1(1)}(e_A - e_B) \quad (3.36)$$

In Equation 3.36 the value of e for a particular wall is considered positive if the movement from the centre line of zone 1 of the wall to the centre line of zone 2 of the

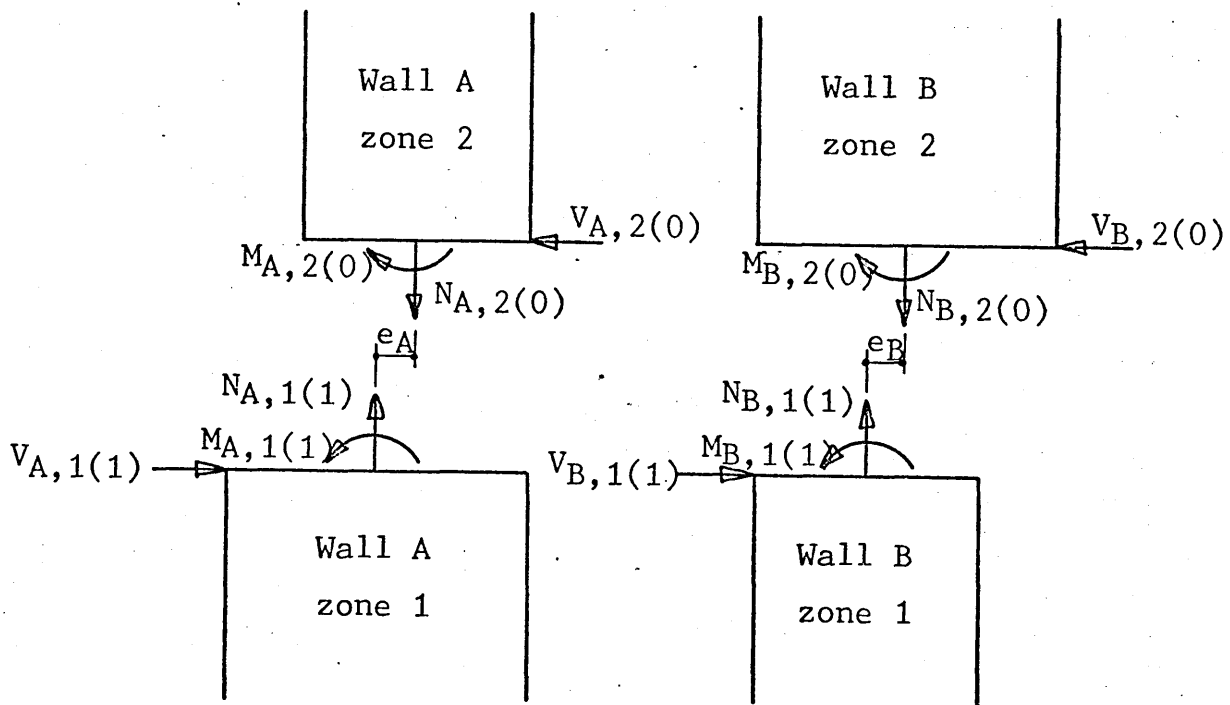


Figure 3.6 Interaction Forces at Discontinuity

wall is in the positive y direction.

We have now obtained six equations, namely 3.30, 3.31, 3.36, 3.35, 3.33 and 3.34, relating the actions at the base of zone 2 to the actions at the top of zone 1.

Thus the relationship between $\underline{S}_2(0)$ and $\underline{S}_1(1)$ can be expressed as

$$\underline{S}_2(0) = \underline{Q} \underline{S}_1(1) \quad (3.37)$$

where

$$\underline{Q} = \begin{vmatrix} 1 & 0 & 0 & 0 & 0 & 0 \\ 0 & 1 & 0 & 0 & 0 & 0 \\ 0 & 0 & 1 & 0 & 0 & -(e_A - e_B) \\ 0 & 0 & 0 & 1 & 0 & 0 \\ 0 & 0 & 0 & 0 & \rho & 0 \\ 0 & 0 & 0 & 0 & 0 & 1 \end{vmatrix}$$

and where

$$\rho = \frac{h_1 b_1^3 I_{v,2}}{h_2 b_2^3 I_{v,1}}$$

Values of Action Matrices

The matrix \underline{S}_0 can now be calculated by a process similar to the case of the uniform wall system.

Thus

$$\underline{S}_1(0) = \underline{K}_0 \underline{S}_0$$

$$\underline{S}_1(1) = \underline{G}_1(1) \underline{K}_0 \underline{S}_0 + \underline{F}_1(1)$$

and using Equation 3.37

$$\underline{S}_2(0) = \underline{Q} \underline{G}_1(1) \underline{K}_0 \underline{S}_0 + \underline{Q} \underline{F}_1(1) \quad (3.38)$$

$$\underline{S}_2(1) = \underline{G}_2(1) \underline{Q} \underline{G}_1(1) \underline{K}_0 \underline{S}_0 + \underline{G}_2(1) \underline{Q} \underline{F}_1(1) + \underline{F}_2(1)$$

Now

$$\underline{K}_H \underline{S}_2(1) = \underline{F}_H$$

and thus

$$\underline{S}_0 = (\underline{K}_H \underline{G}_2(1) \underline{Q} \underline{G}_1(1) \underline{K}_0)^{-1} (\underline{F}_H - \underline{K}_H \underline{G}_2(1) \underline{Q} \underline{F}_1(1) - \underline{K}_H \underline{F}_2(1)) \quad (3.39)$$

Thus knowing the value of \underline{S}_0 , the actions at any required height in zone 1 or zone 2 can be calculated using equations of the form

$$\underline{S}_1(n\xi_{k,1}) = \underline{G}_1(\xi_{k,1}) \underline{S}_1((n-1)\xi_{k,1}) + \underline{F}_1(\xi_{k,1}) \quad (3.40)$$

and

$$\underline{S}_2(n\xi_{k,2}) = \underline{G}_2(\xi_{k,2}) \underline{S}_2((n-1)\xi_{k,2}) + \underline{F}_2(\xi_{k,2}) \quad (3.41)$$

for zones 1 and 2 respectively.

3.6 Uniform Coupled Shear Wall Containing Two Bands of Openings

The coupled shear wall system referred to in the following analysis is shown in Figure 3.7.

Displacement and Elasticity Relationship

The displacement-rotation relationship for the wall system is

$$\frac{dy}{dx} = \theta \quad (3.42)$$

By considering a cut along the centre line of each connecting medium, the distributed shearing forces may be shown to be

$$v_A = \frac{12EI_{V,A}}{h_A b_A^3} (l_A \theta - a_{N,A} + a_{N,B}) \quad (3.43)$$

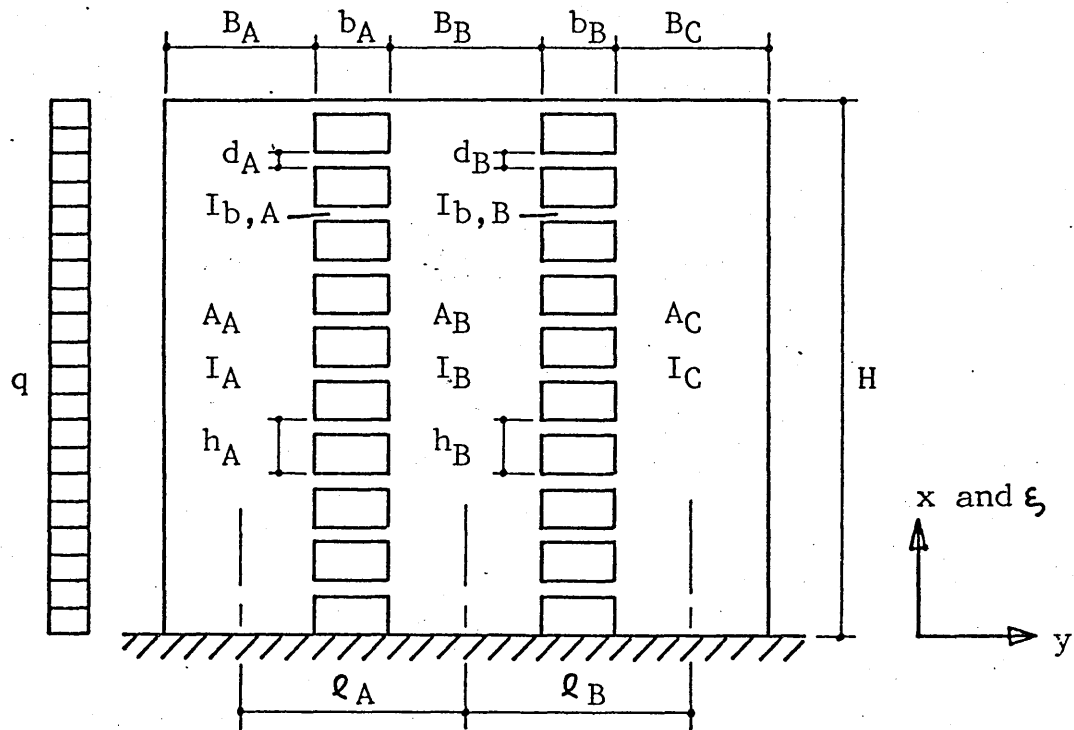


Figure 3.7 Coupled Shear Wall with Two Bands of Openings

$$\text{and } v_B = \frac{12EI_{v,B}}{h_B b_B^3} (\varrho_B \theta - a_{N,B} + a_{N,C}) \quad (3.44)$$

for connecting medium A and connecting medium B respectively.

The vertical strains of the centre lines of walls A, B and C are, respectively

$$\frac{da_{N,A}}{dx} = \frac{N_A}{EA_A} \quad (3.45)$$

$$\frac{da_{N,B}}{dx} = \frac{N_B}{EA_B} \quad (3.46)$$

$$\frac{da_{N,C}}{dx} = \frac{N_C}{EA_C} \quad (3.47)$$

The moment curvature relationship for the walls is

$$\frac{d\theta}{dx} = \frac{-M}{EI} \quad (3.48)$$

where

$$M = M_A + M_B + M_C$$

and

$$I = I_A + I_B + I_C$$

Now, differentiating Equations 3.43 and 3.44 and substituting Equations 3.45, 3.46, 3.47 and 3.48 we obtain

$$\frac{dv_A}{dx} = \frac{12I_{v,A}}{h_A b_A^3} \left(-\frac{M}{I} - \frac{N_A}{A_A} + \frac{N_B}{A_B} \right) \quad (3.49)$$

and

$$\frac{dv_B}{dx} = \frac{12I_{v,B}}{h_B b_B^3} \left(-\frac{M}{I} - \frac{N_B}{A_B} + \frac{N_C}{A_C} \right) \quad (3.50)$$

Equilibrium Conditions

The equilibrium conditions may be determined by considering elementary parts of each of the walls as shown in Figure 3.8.

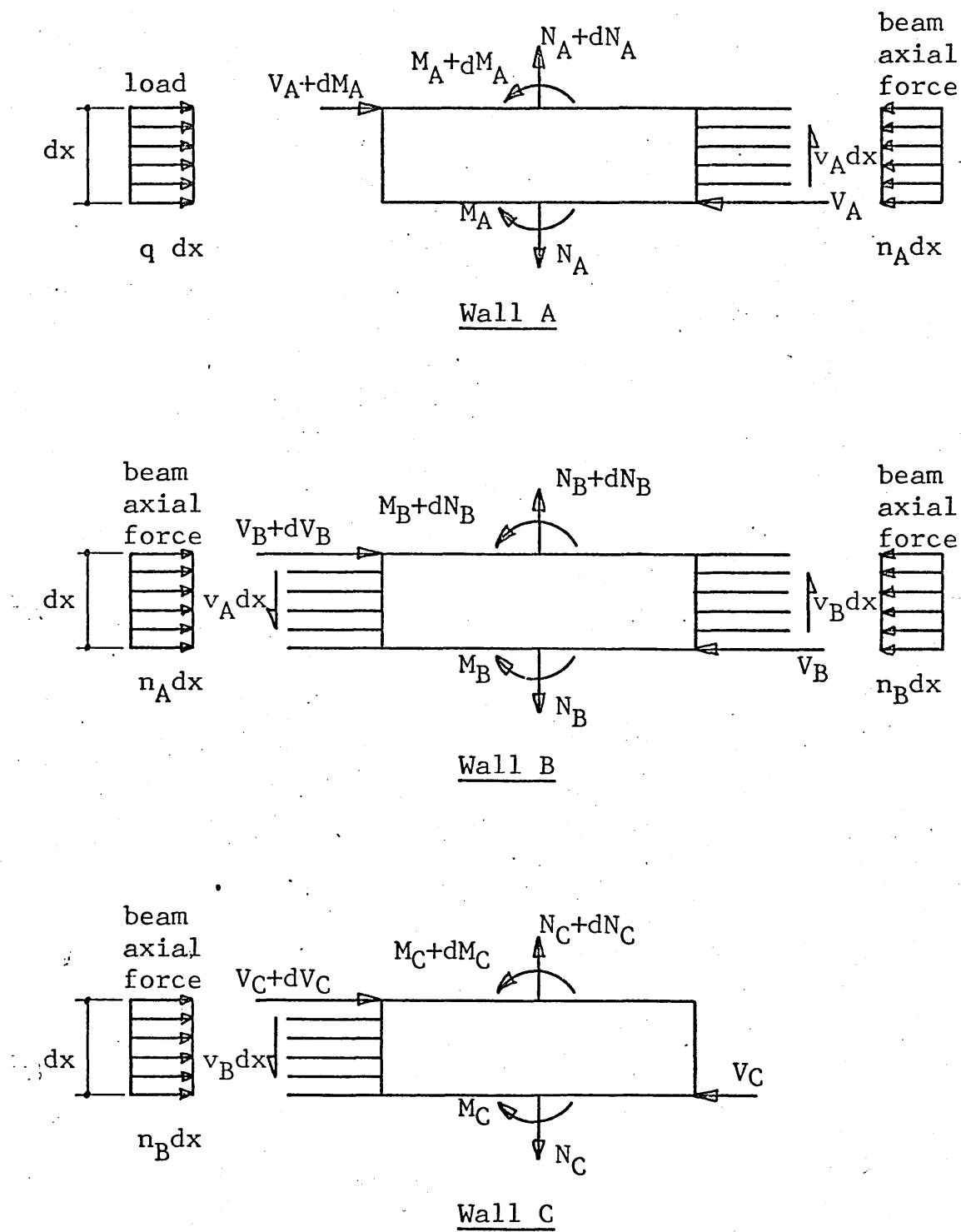


Figure 3.8 Elementary parts of Walls A, B and C

For horizontal equilibrium of the wall system

$$\frac{dV}{dx} = -q \quad (3.51)$$

where $V = V_A + V_B + V_C$

For moment equilibrium of each of the walls

$$\frac{dM_A}{dx} = -v_A \left(\frac{B_A}{2} + \frac{q_A}{2} \right) + V_A \quad (3.52)$$

$$\frac{dM_B}{dx} = -v_A \left(\frac{B_B}{2} + \frac{q_A}{2} \right) - v_B \left(\frac{B_B}{2} + \frac{q_B}{2} \right) + V_B \quad (3.53)$$

$$\frac{dM_C}{dx} = -v_B \left(\frac{B_C}{2} + \frac{q_B}{2} \right) + V_C \quad (3.54)$$

Combining the moment equations 3.52, 3.53 and 3.54

gives

$$\frac{dM}{dx} = -q_A v_A - q_B v_B + V \quad (3.55)$$

For vertical equilibrium of walls A and B

$$\frac{dN_A}{dx} = -v_A \quad (3.56)$$

and

$$\frac{dN_B}{dx} = v_A - v_B \quad (3.57)$$

Now for vertical equilibrium of the wall system it is required that

$$N_A + N_B + N_C = 0 \quad (3.58)$$

and substituting Equation 3.58 into Equation 3.50 gives

$$\frac{dv_B}{dx} = \frac{12I_{v,B}}{h_B b_B^3} \left\{ \frac{-M q_B}{I} - \frac{N_A}{A_C} - N_B \left(\frac{1}{A_B} + \frac{1}{A_C} \right) \right\}$$

or

$$\frac{dv_B}{dx} = \gamma_B^M + \mu_C^{N_A} + \mu_{BC}^{N_B} \quad (3.59)$$

where

$$\gamma_B = \frac{-12I_{V,B}l_B}{h_B b_B^3 I}$$

$$\mu_C = \frac{-12I_{V,B}}{h_B b_B^3 A_C}$$

$$\mu_{BC} = \frac{-12I_{V,B}}{h_B b_B^3} \left(\frac{1}{A_B} + \frac{1}{A_C} \right)$$

Now, Equation 3.49 can be re-written in a form similar to Equation 3.59.

Thus

$$\frac{dv_A}{dx} = \gamma_A^M + \mu_A^{N_A} + \mu_B^{N_B} \quad (3.60)$$

where

$$\gamma_A = \frac{-12I_{V,A}l_A}{h_A b_A^3 I}$$

$$\mu_A = \frac{-12I_{V,A}}{h_A b_A^3 A_A}$$

$$\mu_B = \frac{-12I_{V,A}}{h_A b_A^3 A_B}$$

System of Equations

In Equations 3.42, 3.48, 3.55, 3.51, 3.60, 3.59, 3.56 and 3.57 we have established a set of eight first order differential equations containing the actions y , θ , M , V , v_A , v_B , N_A and N_B . If we now express these equations in both matrix form and in terms of a non-dimensional height co-ordinate ξ we obtain

$$\frac{d}{d\xi} \begin{vmatrix} Ey \\ E\theta \\ M \\ V \\ v_A \\ v_B \\ N_A \\ N_B \end{vmatrix} = \begin{vmatrix} 0 & H & 0 & 0 & 0 & 0 & 0 & 0 \\ 0 & 0 & -H/I & 0 & 0 & 0 & 0 & 0 \\ 0 & 0 & 0 & H & -H\ell_A & -H\ell_B & 0 & 0 \\ 0 & 0 & 0 & 0 & 0 & 0 & 0 & 0 \\ 0 & 0 & H\gamma_A & 0 & 0 & 0 & H\mu_A & H\mu_B \\ 0 & 0 & H\gamma_B & 0 & 0 & 0 & H\mu_C & H\mu_{BC} \\ 0 & 0 & 0 & 0 & -H & 0 & 0 & 0 \\ 0 & 0 & 0 & 0 & H & -H & 0 & 0 \end{vmatrix} \begin{vmatrix} Ey \\ E\theta \\ M \\ V \\ v_A \\ v_B \\ N_A \\ N_B \end{vmatrix} + \begin{vmatrix} 0 \\ 0 \\ 0 \\ -Hq \\ 0 \\ 0 \\ 0 \\ 0 \end{vmatrix}$$

or

$$\frac{d\underline{S}}{d\xi} = \underline{A} \underline{S} + \underline{B} \quad (3.61)$$

Solution of Equations and Boundary Conditions

The method of solution of Equation 3.61 for values of the action matrix at any required height is exactly the same as in Section 3.4 except that the boundary matrices \underline{K}_0 , \underline{S}_0 , \underline{K}_H and \underline{F}_H must be re-defined.

At the base of the wall system, the following conditions exist

$$\begin{aligned} y_0 &= 0 \\ \theta_0 &= 0 \\ v_{0,A} &= 0 \\ v_{0,B} &= 0 \end{aligned}$$

Thus

$$\underline{K}_0 = \begin{vmatrix} 0 & 0 & 0 & 0 \\ 0 & 0 & 0 & 0 \\ 1 & 0 & 0 & 0 \\ 0 & 1 & 0 & 0 \\ 0 & 0 & 0 & 0 \\ 0 & 0 & 0 & 0 \\ 0 & 0 & 1 & 0 \\ 0 & 0 & 0 & 1 \end{vmatrix}$$

and

$$\underline{S}_O = \begin{matrix} M_O \\ V_O \\ N_{O,A} \\ N_{O,B} \end{matrix}$$

At the top of the wall system the following conditions exist

$$M_H = 0$$

$$V_H = 0$$

$$N_{H,A} = 0$$

$$N_{H,B} = 0$$

Thus

$$\underline{K}_H = \begin{vmatrix} 0 & 0 & 1 & 0 & 0 & 0 & 0 & 0 \\ 0 & 0 & 0 & 1 & 0 & 0 & 0 & 0 \\ 0 & 0 & 0 & 0 & 0 & 0 & 1 & 0 \\ 0 & 0 & 0 & 0 & 0 & 0 & 0 & 1 \end{vmatrix}$$

and

$$\underline{F}_H = \begin{vmatrix} 0 \\ 0 \\ 0 \\ 0 \end{vmatrix}$$

3.7 Coupled Shear Walls Containing Two Bands of Openings and with One Abrupt Variation in Cross Section

Once new continuity conditions have been determined, the approach used in Section 3.6 can also be used here. However, it should be remembered that the centre-line of each band of openings must be continuous throughout the height of the wall system.

The displacement and rotation continuity conditions are

$$y_2(0) = y_1(1)$$

and

$$\theta_2(0) = \theta_1(1)$$

By considering the vertical displacement continuity conditions, the distributed shearing forces above and below the discontinuity for each connecting band can be related by similar equations to Equation 3.33. Thus

$$v_{A,2}(0) = \frac{h_{A,1}b_{A,1}^3 I_{v,A,2}}{h_{A,2}b_{A,2}^3 I_{v,A,1}} v_{A,1}(1)$$

$$v_{B,2}(0) = \frac{h_{B,1}b_{B,1}^3 I_{v,B,2}}{h_{B,2}b_{B,2}^3 I_{v,B,1}} v_{B,1}(1)$$

The equilibrium equations can be written with reference to Figure 3.9.

For equilibrium of axial forces in walls A and B

$$N_{A,2}(0) = N_{A,1}(1)$$

$$N_{B,2}(0) = N_{B,1}(1)$$

For shear force equilibrium of the wall system

$$V_2(0) = V_1(1)$$

For moment equilibrium of the wall system

$$M_2(0) = M_1(1) - N_{A,1}(1)e_A - N_{B,1}(1)e_B - N_{C,1}(1)e_C$$

and using Equation 3.58

$$M_2(0) = M_1(1) - N_{A,1}(1)(e_A - e_C) - N_{B,1}(1)(e_B - e_C)$$

Thus the relationship between $\underline{S}_2(0)$ and $\underline{S}_1(1)$ is

$$\underline{S}_2(0) = \underline{Q} \underline{S}_1(1)$$

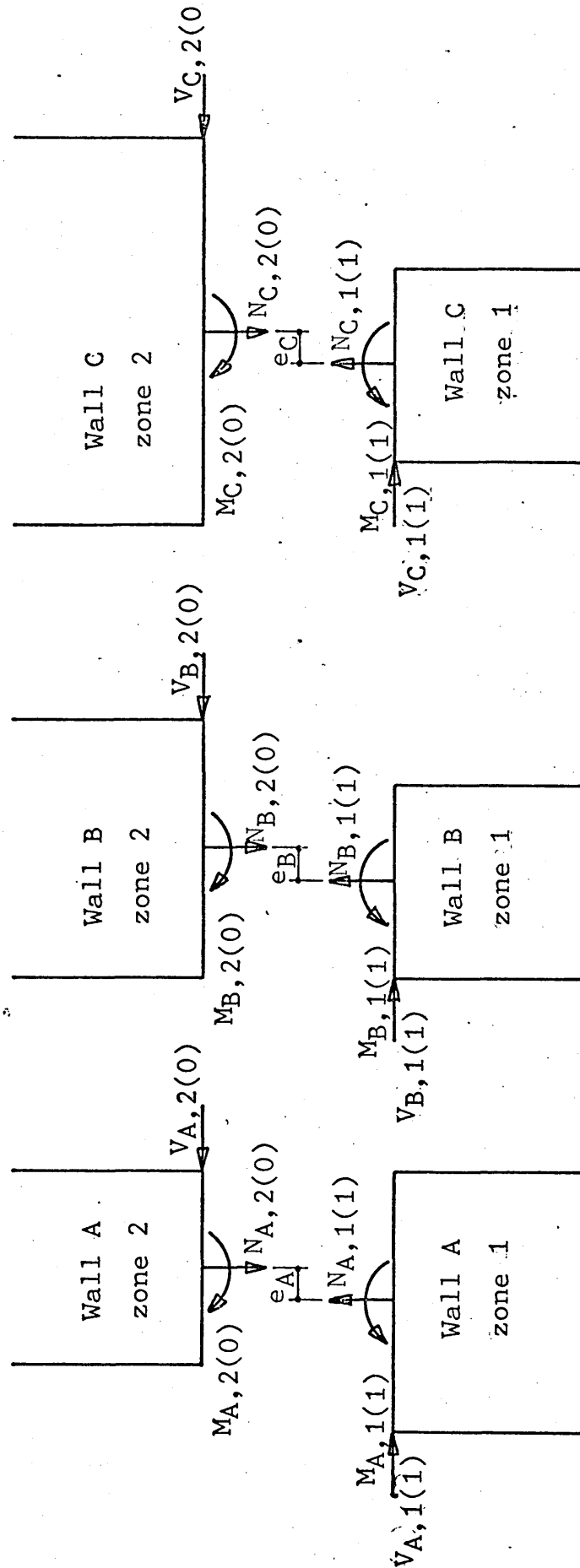


Figure 3.9 Interaction Forces at Discontinuity

where

$$Q = \begin{vmatrix} 1 & 0 & 0 & 0 & 0 & 0 & 0 & 0 \\ 0 & 1 & 0 & 0 & 0 & 0 & 0 & 0 \\ 0 & 0 & 1 & 0 & 0 & 0 & -(e_A - e_C) & -(e_B - e_C) \\ 0 & 0 & 0 & 1 & 0 & 0 & 0 & 0 \\ 0 & 0 & 0 & 0 & \rho_A & 0 & 0 & 0 \\ 0 & 0 & 0 & 0 & 0 & \rho_B & 0 & 0 \\ 0 & 0 & 0 & 0 & 0 & 0 & 1 & 0 \\ 0 & 0 & 0 & 0 & 0 & 0 & 0 & 1 \end{vmatrix}$$

where

$$\rho_A = \frac{h_{A,1} b_{A,1} {}^3I_{v,A,2}}{h_{A,2} b_{A,2} {}^3I_{v,A,1}}$$

and

$$\rho_B = \frac{h_{B,1} b_{B,1} {}^3I_{v,B,2}}{h_{B,2} b_{B,2} {}^3I_{v,B,1}}$$

3.8 Coupled Shear Walls Containing n Bands of Openings and with m Abrupt Variations in Cross Section

The methods presented can obviously be extended to cater for shear wall systems containing any number of bands of openings and having any number of abrupt variations in cross section.

System with n walls

The method of solution is similar to that presented in Sections 3.4 and 3.6 but the order of the various matrices will increase with the increase in the number of walls.

For a system with n walls the action matrix will consist of y, θ , M and V plus the (n-1) distributed shearing forces plus the axial forces in the first (n-1) walls.

System with m discontinuities

The method of solution is similar to that presented in Sections 3.5 and 3.7 but different continuity matrices Q_i must be set up for each of the m discontinuities.

COMPUTER PROGRAMS

4.1 Introduction

Computer programs have been written for both the analytical solution presented in Chapter 2 and the matrix progression solutions presented in Chapter 3. If the analytical equations are to be used only for the calculation of maximum values, then a computer is not strictly necessary as the equations can be simplified and use made of a scientific pocket calculator. The matrix progression method, however, is computer orientated and the use of a computer is essential.

All the programs have been written in both FORTRAN and BASIC and the computations were performed initially on an IBM 1130 and later on an IBM 370 computer. The latter machine offers both batch and remote terminal facilities.

4.2 Analytical Solution

A program has been written to calculate the variation in bending moment, axial force, distributed shear force and deflection throughout the height of the structure. The sequence of operations followed in the program is outlined in the flow diagram shown in Figure 4.1.

The input data required consists of the dimensions of

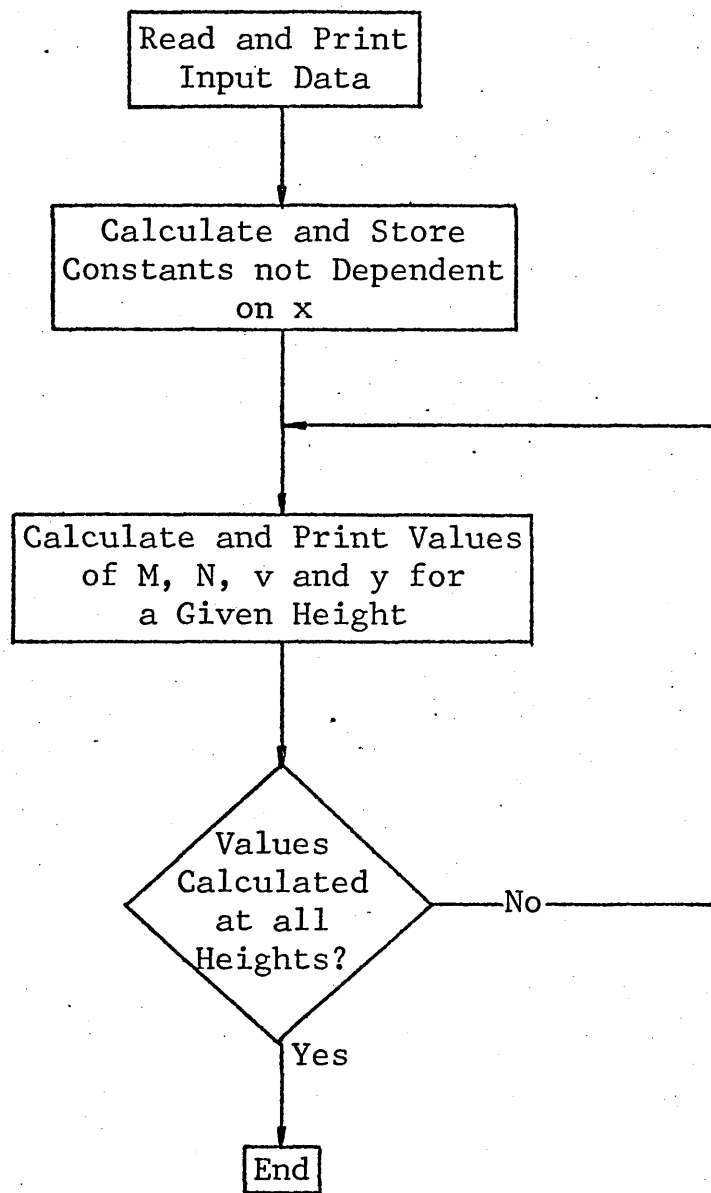


Figure 4.1 Flow Chart for Analytical Solution

the structure, load value, material properties and heights at which results are required. The latter is most easily catered for by specifying the number of results required, usually at each storey height.

The following equations are used to calculate the values required at each height.

Total bending moment	- M	Equation 2.9
Axial force in each wall	- N	Equation 2.8
Distributed shear force	- v	Equation 2.5
Deflection	- y	Equation 2.10

If only maximum values of each of the functions are required then a simpler program can be written consisting of the following steps.

(a) Read and print input data

(b) Calculate required values from the following equations:

M_{\max}	Equation 2.9 with $x = 0$
N_{\max}	Equation 2.8 with $x = 0$
v_{\max}	Equation 2.5 with x/H obtained from Equation 2.7
y_{\max}	Equation 2.11

(c) Print results.

The simplicity of the above procedure obviously lends itself to hand calculations.

4.3 Matrix Progression Solutions

Programs have been written for the solution of each of the four structures described in Sections 3.4 to 3.7. Because of the large number of matrix operations involved in the calculations, it has been found easier to use the BASIC language which offers simpler matrix subroutines. The sequence of operations followed in a general program for a structure containing any number of zones is given in Figure 4.2.

All the programs include subroutines for the following operations:

- (a) Reading and printing data for each zone and setting up A and B
- (b) Calculating G(ξ) and F(ξ)
- (c) Calculating and Printing S(ξ)

The common data consists of foundation conditions and material properties, and the zone data consists of the geometric properties of the zone, load value, and number of results required. The output gives values of total bending moment, axial force in each wall, horizontal shear force, distributed shear force, deflection and rotation at each required height.

All the calculations are performed using the equations set out in Chapter 3. Although matrix operations are

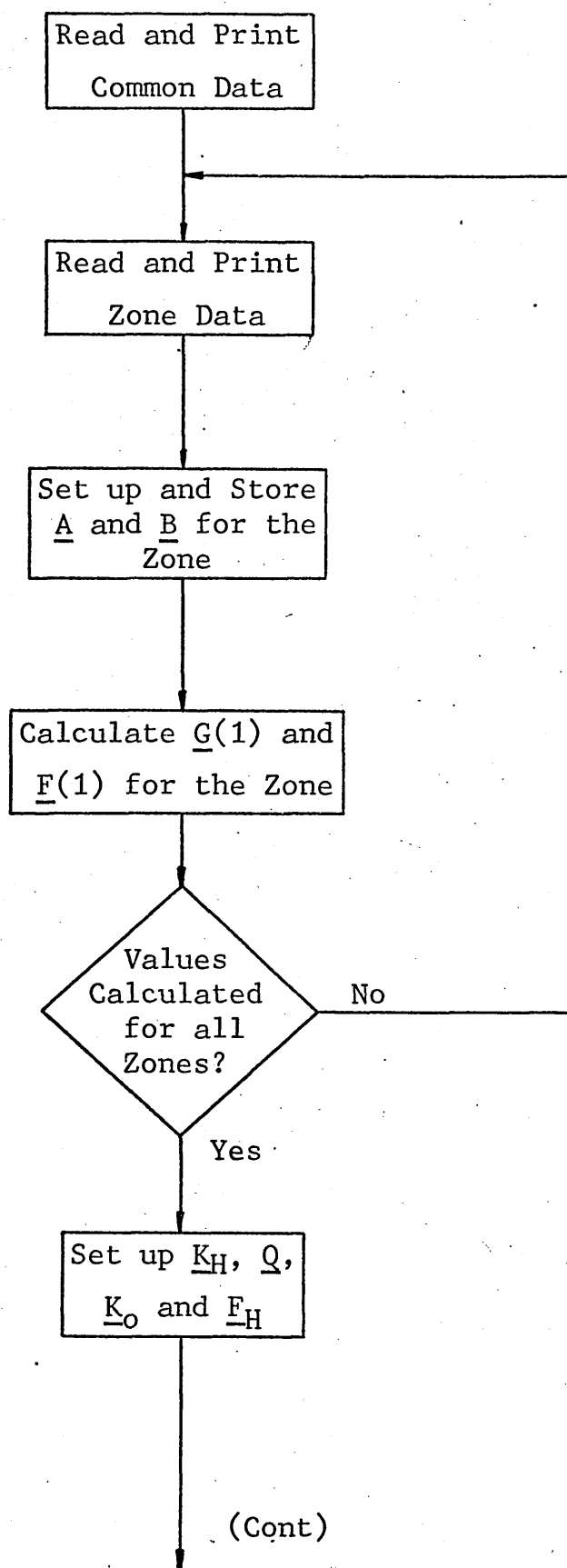


Figure 4.2 Flow Chart for Matrix Progression Solution

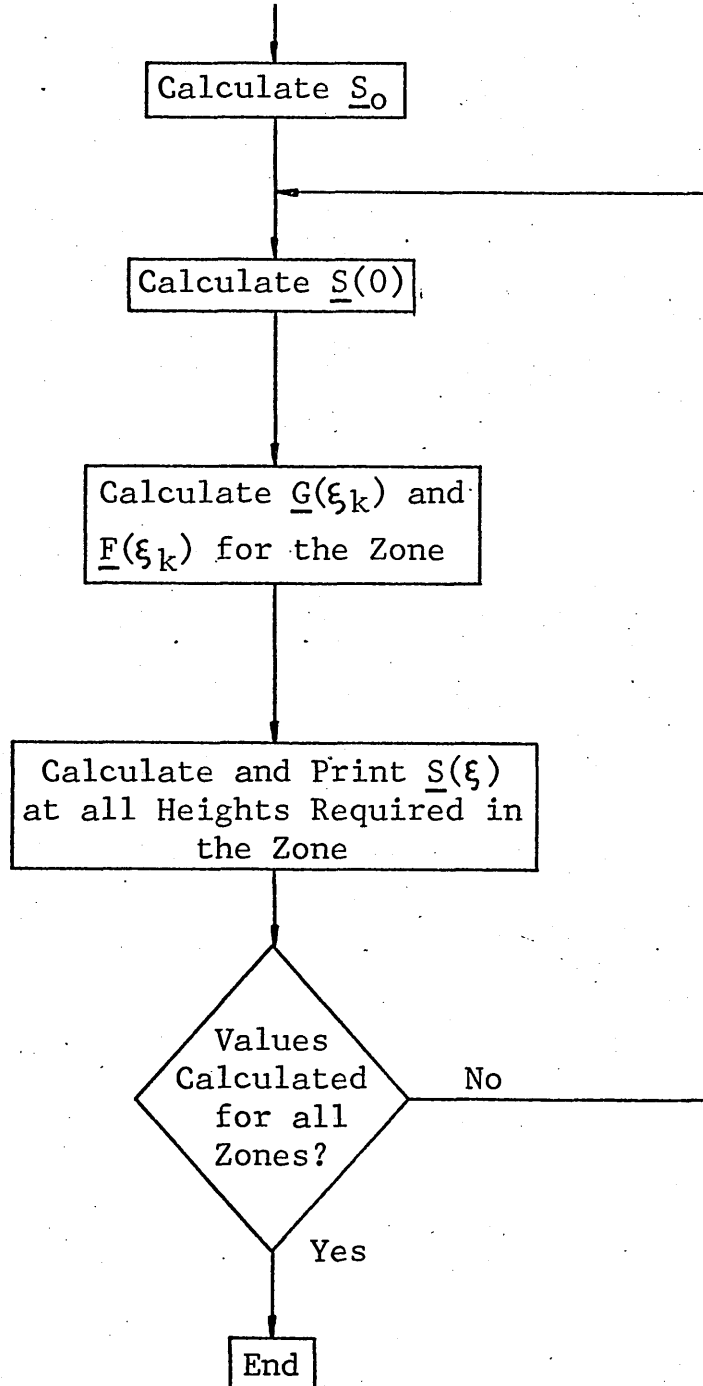


Figure 4.2 (Cont)

involved in these calculations the procedures used are quite straightforward, assuming a previous knowledge of programming, apart from the calculations of $\underline{G}(\xi)$ and $\underline{F}(\xi)$ and these are considered here in more detail.

The value of $\underline{G}(\xi)$ given in Equation 3.18 is

$$\underline{G}(\xi) = \underline{I} + \underline{A}\xi + \frac{\underline{A}^2\xi^2}{2!} + \frac{\underline{A}^3\xi^3}{3!} + \dots$$

Assuming, say, only five terms in the summations series it can be re-written as

$$\underline{G}(\xi) = \underline{I} + \underline{A}\xi \left(\underline{I} + \frac{\underline{A}\xi}{2} \left(\underline{I} + \frac{\underline{A}\xi}{3} \left(\underline{I} + \frac{\underline{A}\xi}{4} \right) \right) \right)$$

which is a very convenient form for programming, and this is the method which has been adopted.

For some structures that were analysed, only a few terms were needed in the series to ensure convergence, but for others a large number of terms were required and so to cover all possible analyses it was found necessary to program fifty terms of the series (see Section 6.2).

The value of $\underline{F}(\xi)$ given in Equation 3.18 is

$$\underline{F}(\xi) = \left(\underline{I} + \frac{\underline{A}^2}{2!} + \frac{\underline{A}^2}{3!} + \dots \right) \underline{B}$$

This can be re-written, as was done for $\underline{G}(\xi)$ but taking one less term in the summation, as

$$\underline{F}(\xi) = \left(\underline{I} + \frac{\underline{A}\xi}{2} \left(\underline{I} + \frac{\underline{A}\xi}{3} \left(\underline{I} + \frac{\underline{A}\xi}{4} \right) \right) \right) \underline{B}$$

Thus, to avoid a complete recalculation, the nest of brackets used in the calculation of $\underline{G}(\xi)$ can conveniently

be used in the determination of $\underline{F}(\xi)$.

It will be noticed that the method of calculation used in the present Chapter and in Chapter 3 is not the same as that presented by Coull, Puri and Tottenham(35).

In their solution the base matrix \underline{S}_0 was obtained from an equation of the form (assuming only one uniform zone for convenience),

$$\underline{S}_0 = (\underline{K}_H \underline{G}(\xi_k)^k \quad \underline{K}_0)^{-1} (\underline{F}_H - \underline{K}_H (\underline{G}(\xi_k)^{k-1} + \underline{G}(\xi_k)^{k-2} + \dots + \underline{G}(\xi_k) + \underline{I}) \quad \underline{F}(\xi_k))$$

and the action matrix $\underline{S}(n\xi_k)$ was evaluated from equation of the form

$$\underline{S}(n\xi_k) = \underline{G}(\xi_k)^n \quad \underline{K}_0 \underline{S}_0 + (\underline{G}(\xi_k)^{n-1} + \underline{G}(\xi_k)^{n-2} + \dots + \underline{G}(\xi_k) + \underline{I}) \quad \underline{F}(\xi_k)$$

where k is the total number of segments at which results are required in the zone.

Performing the operations in this manner involves a large amount of calculation and storage of the powers of $\underline{G}(\xi)$ which is unnecessary if the method of solution in this present work is adopted.

EXPERIMENTAL WORK

5.1 Introduction

Experimental work has been conducted on a series of Araldite models with the main aim of checking the validity of the matrix progression method of solution for symmetrical and non-symmetrical coupled shear walls with an abrupt change in cross-section at a particular height. Deflections and strains were measured on each of the models and compared with the theoretical values.

5.2 Material

The materials which have most commonly been used for shear wall models are the two plastics, perspex and araldite. Aluminium has been used, but to produce measurable deflections and strains either a very large load has to be applied or the model has to be made very thin, in which case lateral instability becomes a problem.

The low modulus of elasticity of both perspex and araldite make them suitable for use as a model material. Perspex has been used widely for structural models, but it has the disadvantage that its properties vary appreciably with change in temperature and humidity and it creeps under load even at low stress levels. A further disadvantage

is that its machineability is poor. Araldite has none of these shortcomings, although it is comparatively expensive.

The material used was Araldite CT 200 and it had a Poisson ratio of 0.36 and a Young's modulus, determined from tests on small beams, of 492000 lbf/in².

5.3 The Models

The first model tested was symmetrical and each new model was obtained by machining the previous one. From the material removed test beams were made for the determination of the modulus of elasticity of the material. The dimensions of the four models tested are shown in Figures 5.1 and 5.2. Although the linear dimensions of the models do not vary by a large amount, the maximum ratio of second moments of area of adjacent walls is about 2 to 1, and the maximum ratio of second moments of area below and above the abrupt change is about 5.4 to 1.

PL-10 electrical resistance strain gauges were attached to the first model as shown in Figure 5.3. During the machining operations, some gauges had to be removed but whenever this happened further gauges were glued to the edge of the new model.

5.4 Method of Test

Each of the models was tested under the action of a point load at the top and a uniformly distributed load

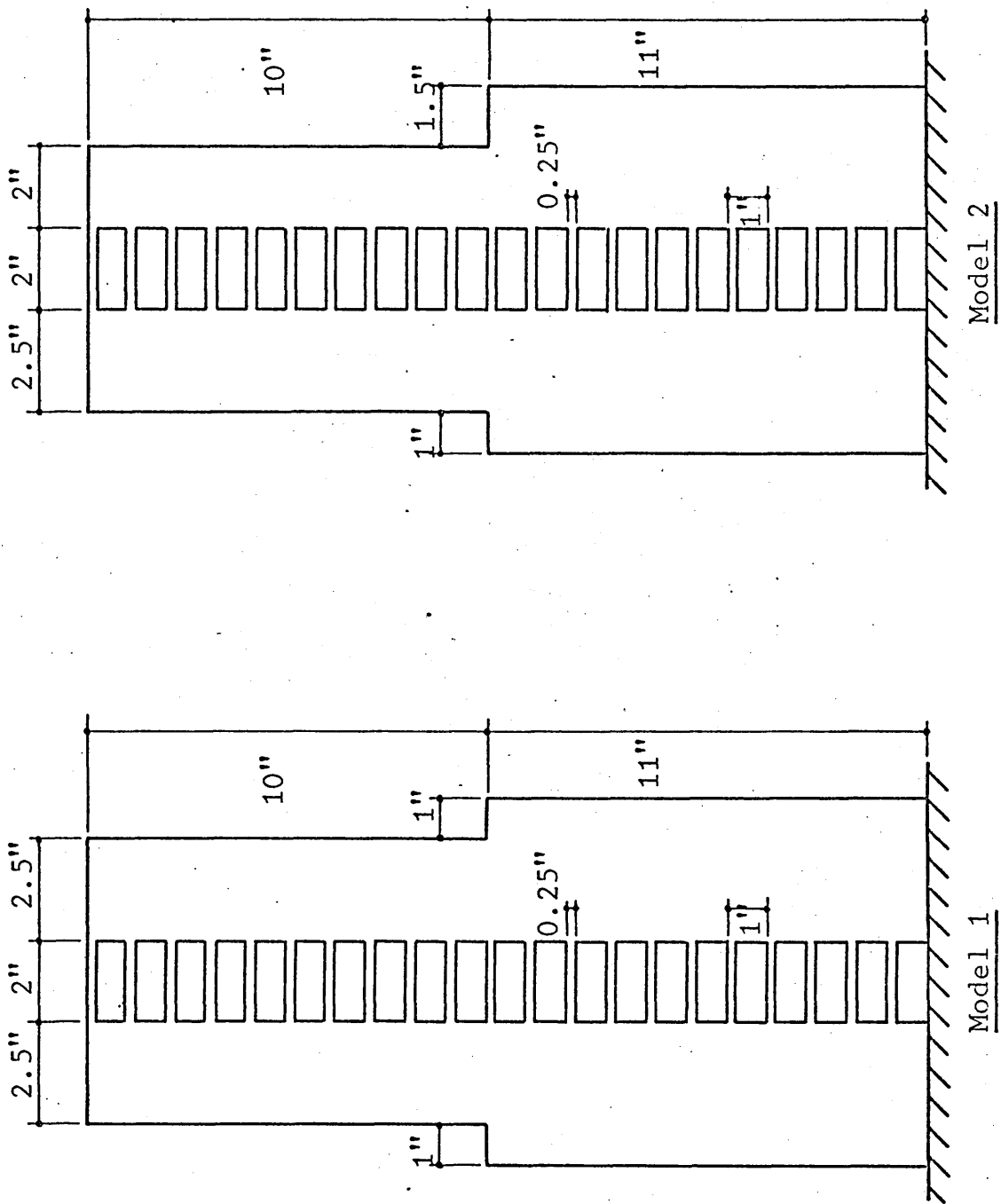


Figure 5.1 Dimensions of Models 1 and 2

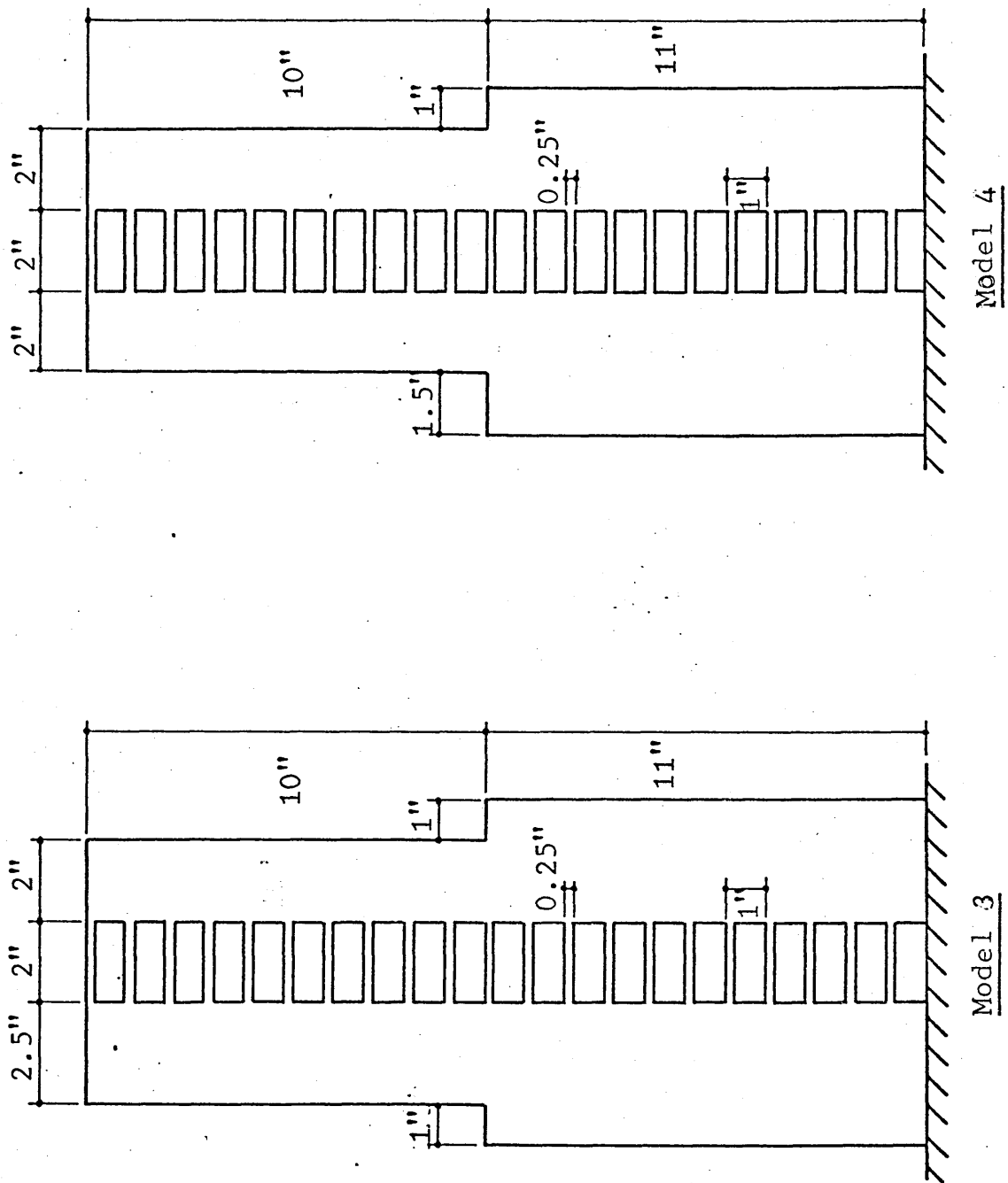
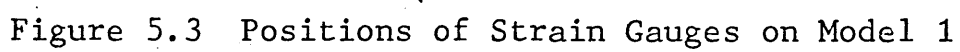


Figure 5.2 Dimensions of Models 3 and 4



along the length of the wall (but not both together).

The testing arrangement is shown in Figures 5.4 and 5.5.

The models were rigidly clamped at their base level by tightly compressing a 2in depth below the lowest opening between two hardened serrated steel bars. Point loads were applied to the top of the structure by means of a proving ring and were therefore 'exact'. For each test, loads were applied in increments of 10 lbf up to a maximum of 60 lbf. The uniform load condition was simulated by applying point loads at each storey level through hangers carrying dead weights, and increments of 1 lbf/in were used up to a maximum of 6 lbf/in.

Deflections were measured at alternate storey heights by means of dial gauges mounted on a supporting frame. The strain distribution across each wall was measured at two levels by means of the previously mentioned strain gauges which were connected to a Peekel automatic strain indicator. Separate dummy gauges, connected to a similar model to the one being tested, were used for each of the 'live' gauges to overcome heating effects.

For each test, the values of deflection per unit load for each dial gauge, and values of strain per unit load for each strain gauge were calculated using a linear regression procedure (using a Hewlett-Packard desk top

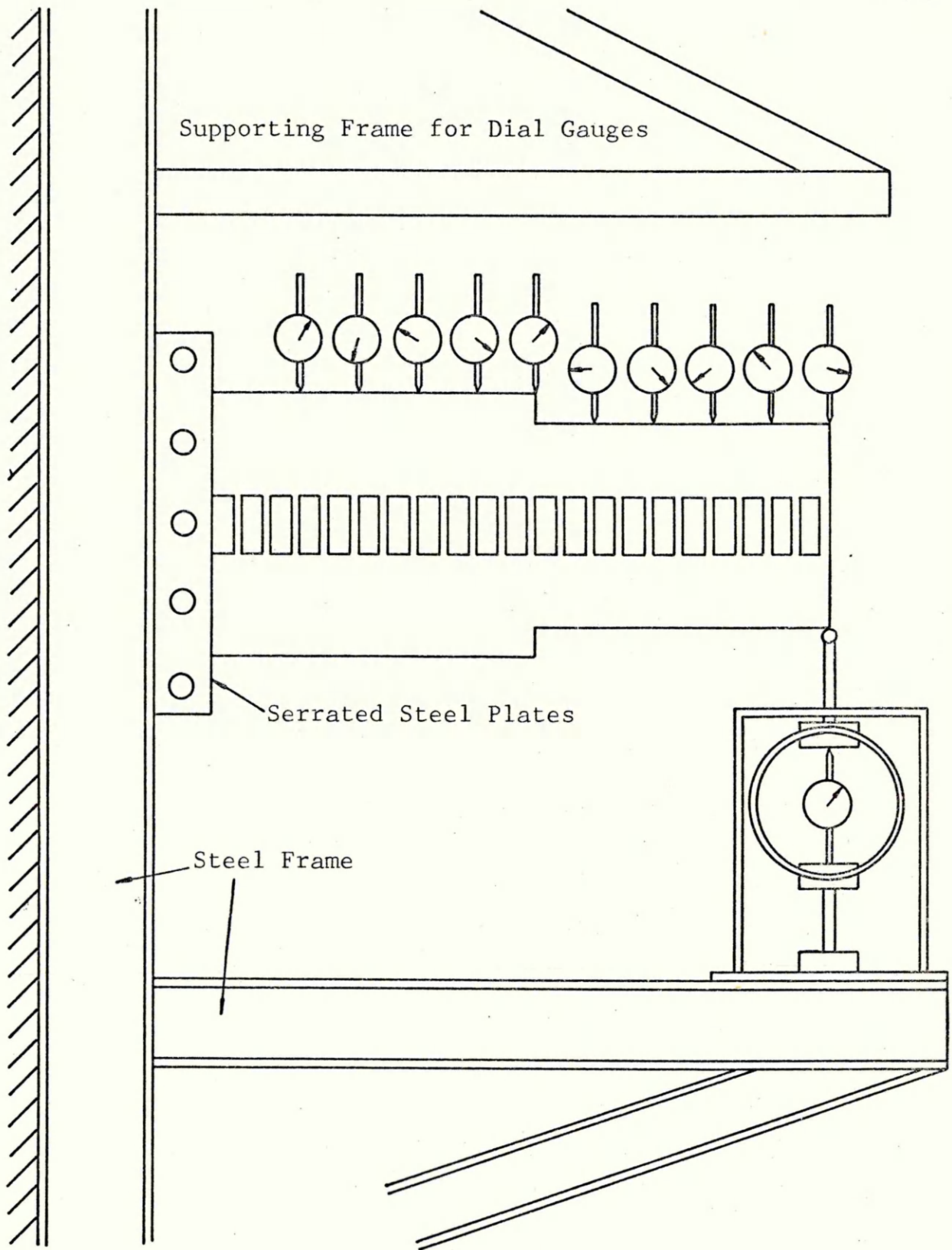


Figure 5.4 Testing Arrangement for Point Load .

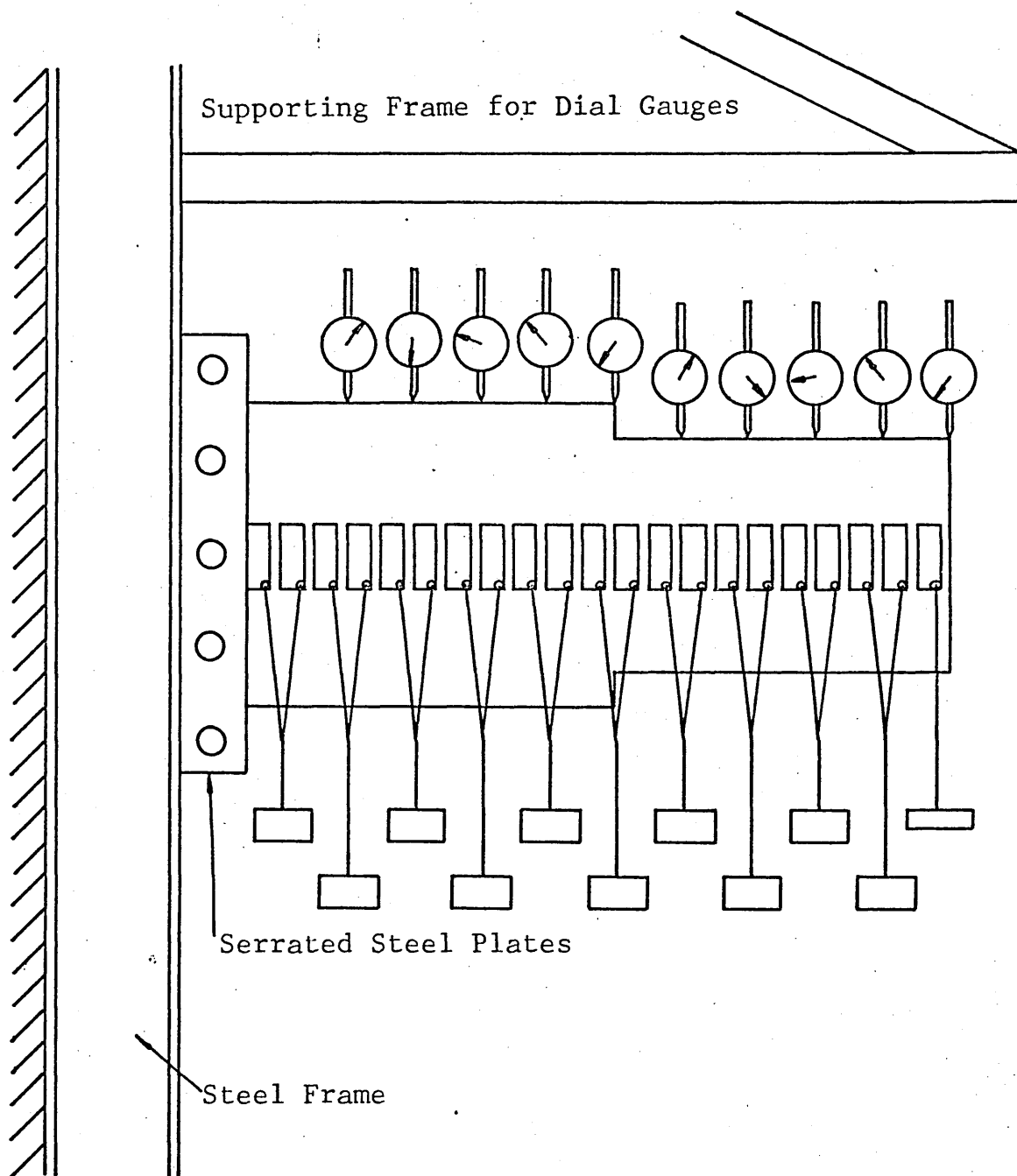


Figure 5.5 Testing Arrangement for UDL

computer). This was considered to be better than plotting all the values and drawing best fit lines by eye.

RESULTS

6.1 Introduction

In this chapter experimental and theoretical results for various shear wall systems are compiled in order to make comparisons between them. The systems considered are as follows:

- (i) walls with one band of openings and one abrupt variation in cross-section
- (ii) uniform walls supported on columns
- (iii) walls with two bands of staggered openings.

The following abbreviations are used on the graphs and tables which are presented:-

C.C. Result obtained using a matrix progression solution of the continuous connection method

W.C.F. Result obtained using a wide column frame

Expt. Experimental Result

6.2 Theoretical Results

The matrix progression solutions have been obtained using the methods outlined in Chapters 3 and 4. However, to achieve convergence of the solution, it was found that the number of terms required in the exponential series had to be increased proportionally to an increase in the value of αH . Ten terms were found satisfactory for $\alpha H = 4$,

whereas between forty and fifty terms were needed for $\alpha H = 16$. Beyond $\alpha H = 18$, convergence was found to be impossible no matter how many terms were included. To cover all the values of αH used in the analyses, fifty terms have been included in the solution.

The wide column frame solutions have been obtained using the IBM standard program, STRESS. This program does not have provisions for incorporating members which have infinitely stiff end sections, and therefore the recommendations put forward by Schwaighofer and Microy (11) and Stafford Smith (12) have been adopted for non-symmetrical and symmetrical structures respectively.

The equivalent frames suggested by the two authors are shown in Figure 6.1.

The constants K_1 and K_2 for Schwaighofer's frame were given in tabular form but from the given values, the following general equations can be developed

$$K_1 = 100 \frac{B}{b}$$

$$K_2 = 100 \left(\frac{B}{b} \right)^3 + 300 \left(\frac{B}{b} \right)^2 + 300 \left(\frac{B}{b} \right)$$

where B is the wall width

and b is the beam length.

The constant K for Stafford Smith's frame is given by

$$K = \left(1 + \frac{B}{b} \right)^3$$

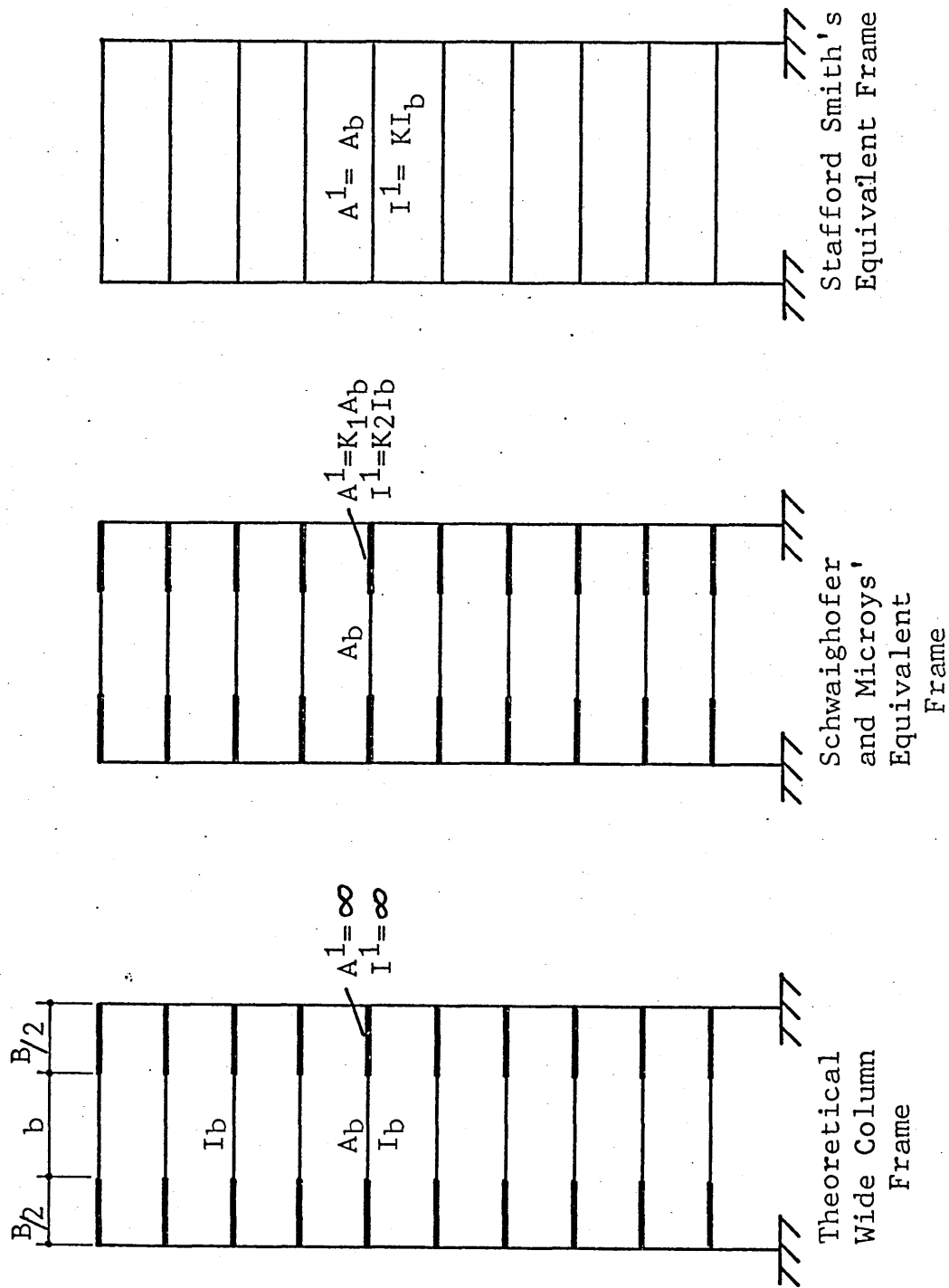


Figure 6.1 Equivalent Wide Column Frames

6.3 Results for Walls Containing One Band of Openings and with One Abrupt Variation in Cross-Section

The walls covered in this section are Models 1 to 4 described in Chapter 5.

All the models were subjected to two loading conditions, namely a point load at the top and a uniformly distributed lateral load. For each model and loading condition, experimental results are compared with a matrix progression solution and a wide column frame solution.

The deflection profiles for the models are shown in Figures 6.2 and 6.8.

Figures 6.9 and 6.10 show typical distributions of total wall bending moment M , the axial force in each wall N , and the distributed vertical shear force v . From such distributions, theoretical strain profiles have been calculated, for the matrix progression solution only, at the two heights where strain gauge readings were taken. These strain distributions are given in Figures 6.11 to 6.26.

Values of maximum deflection are compared in Table 6.1.

Using the experimental strain readings it is possible to calculate the magnitude of the internal moments and these can be compared with the known external moments, to provide an overall check on the accuracy of the measured strains. These moments are compared in Table 6.2.

Model		Load	in x 10 ⁻⁴					% from Expt.		% from W.C.F.
			Expt.	W.C.F.	C.C.			W.C.F.	C.C.	
1	P.L.	8.38	8.35	7.77	-0.4	-7.3	-6.9			
	U.D.L.	59.8	58.3	57.6	-2.5	-3.7	-1.2			
2	P.L.	8.52	8.65	8.19	+1.5	-3.9	-5.3			
	U.D.L.	61.3	59.0	58.5	-3.8	-4.6	-0.8			
3	P.L.	9.30	9.40	9.14	+1.1	-1.7	-2.8			
	U.D.L.	-	66.2	67.3	-	-	+1.7			
4	P.L.	10.0	9.83	9.79	-1.7	-2.1	-0.4			
	U.D.L.	68.9	66.2	68.5	-3.9	-0.6	+3.5			

Table 6.1 Comparison of the maximum deflections in Models 1 to 4

Model	Loading	Height in.	applied external moment lbf. in.	measured internal moment lbf. in.	% diff
1	P.L.	1.375	19.6	17.8	-9
		12.375	8.63	7.66	-11
	U.D.L.	1.375	196.0	153.0	-22
		12.375	38.5	30.8	-20
2	P.L.	1.375	19.6	17.36	-12
		12.375	8.63	7.77	-10
	U.D.L.	1.375	196.0	147.0	-25
		12.375	38.5	33.6	-13
3	P.L.	1.375	19.6	17.5	-11
		12.375	8.63	7.58	-12
	U.D.L.	1.375	196.0	122.0	-38
		12.375	38.5	-	-
4	P.L.	1.375	19.6	17.4	-11
		12.375	8.63	7.71	-11
	U.D.L.	1.375	196.0	168.0	-14
		12.375	38.5	31.3	-19

Table 6.2 Comparison of External and Internal Moments in Models 1 to 4

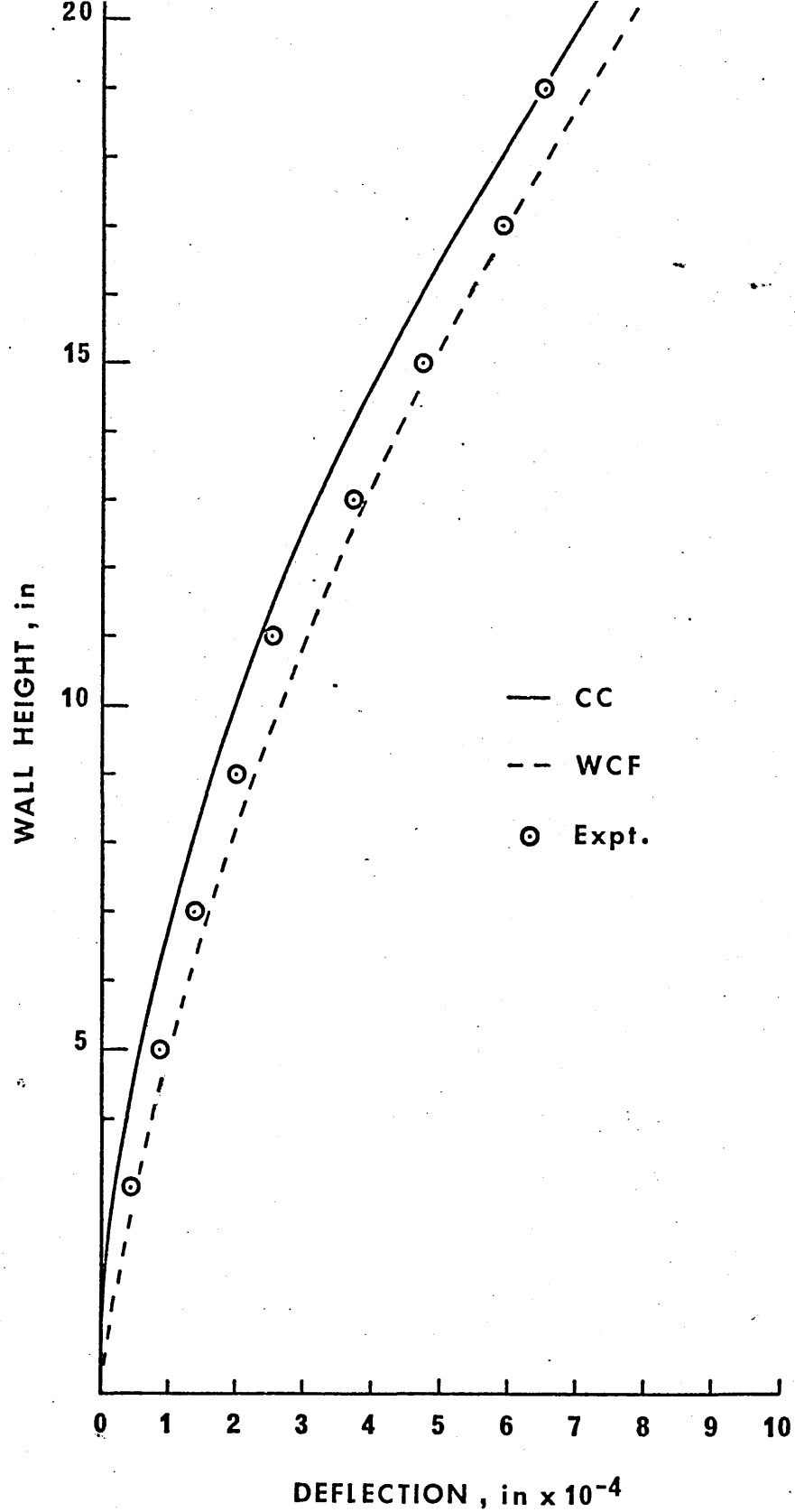


Figure 6.2 Deflection profile of Model 1 due to a Point Load of 1 lbf at the top

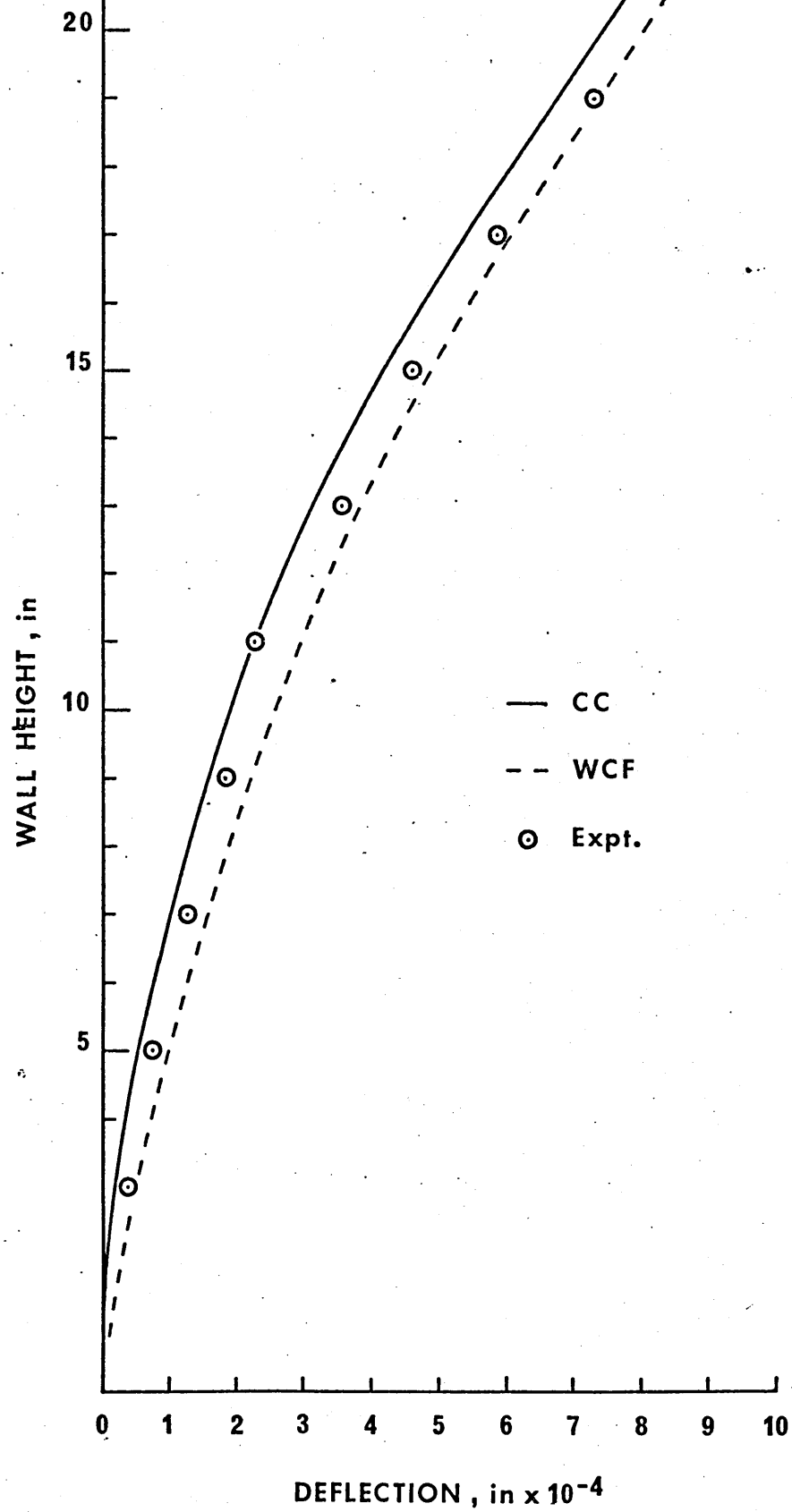


Figure 6.3 Deflection profile of Model 2 due to a Point Load of 1 lbf at the top

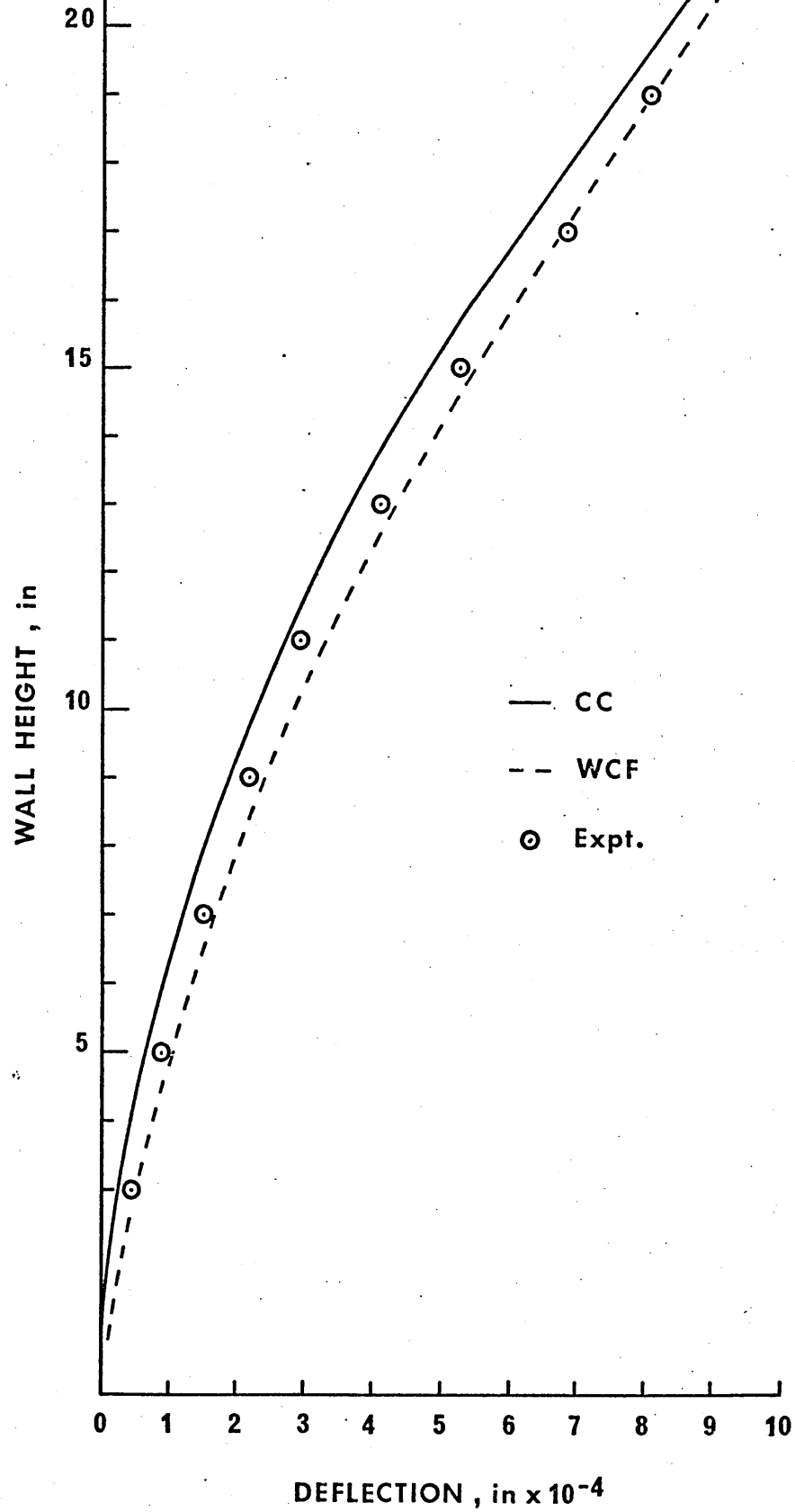


Figure 6.4 Deflection profile of Model 3 due to a Point Load of 1 lbf at the top

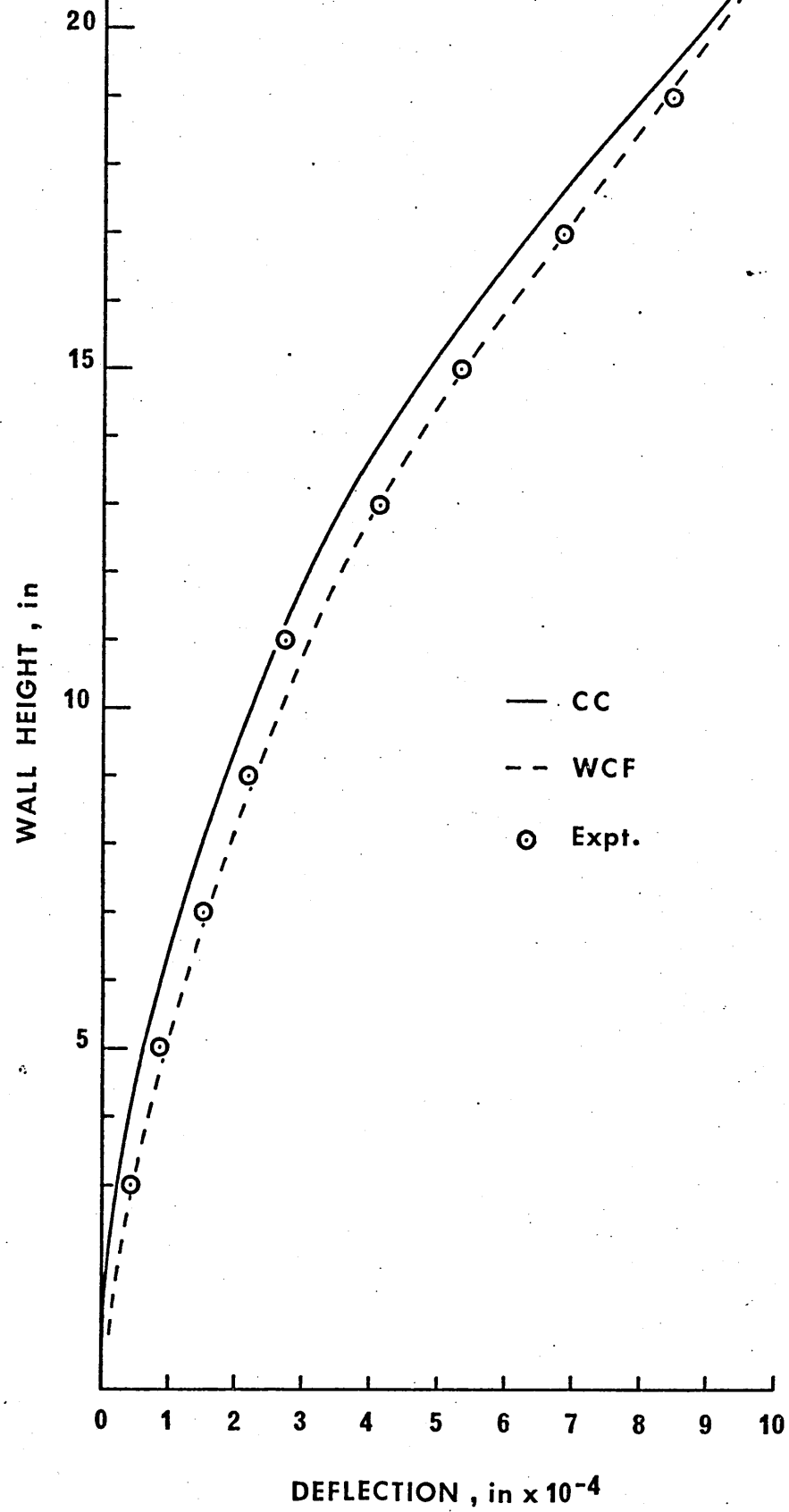


Figure 6.5 Deflection profile of Model 4 due to a Point Load of 1 lbf at the top

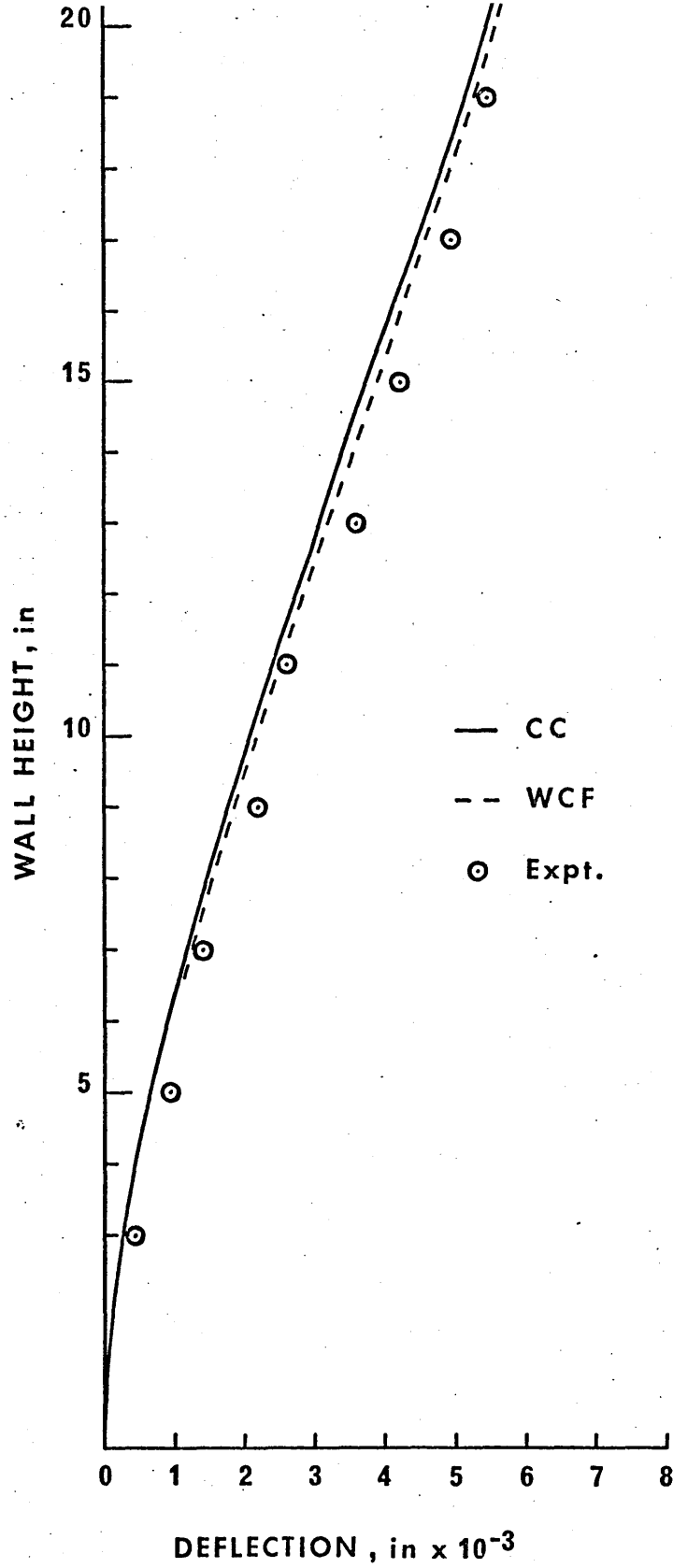


Figure 6.6 Deflection profile of Model 1 due to a U.D.L. of 1 lbf/in

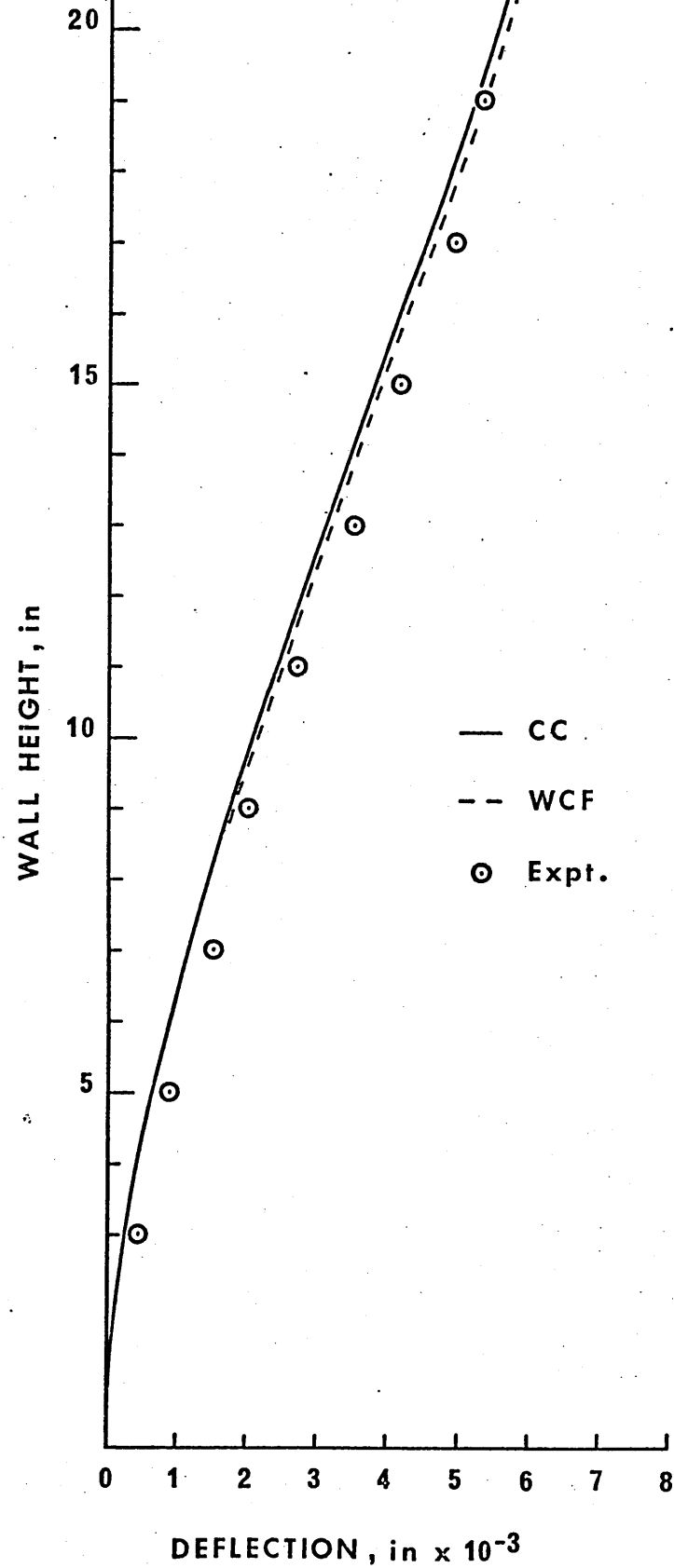


Figure 6.7 Deflection profile of Model 2 due to a U.D.L. of 1 lbf/in

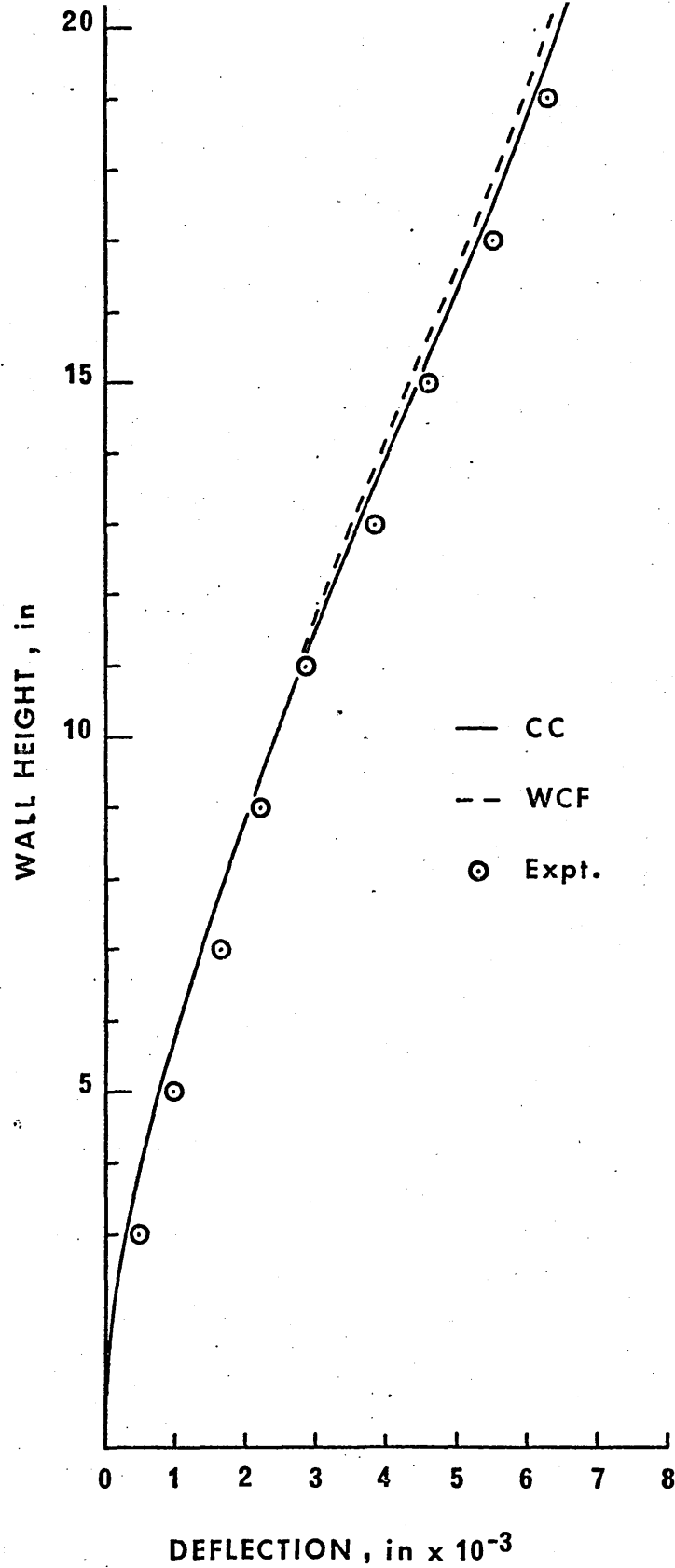


Figure 6.8 Deflection profile of Model 4 due to a U.D.L. of 1 lbf/in

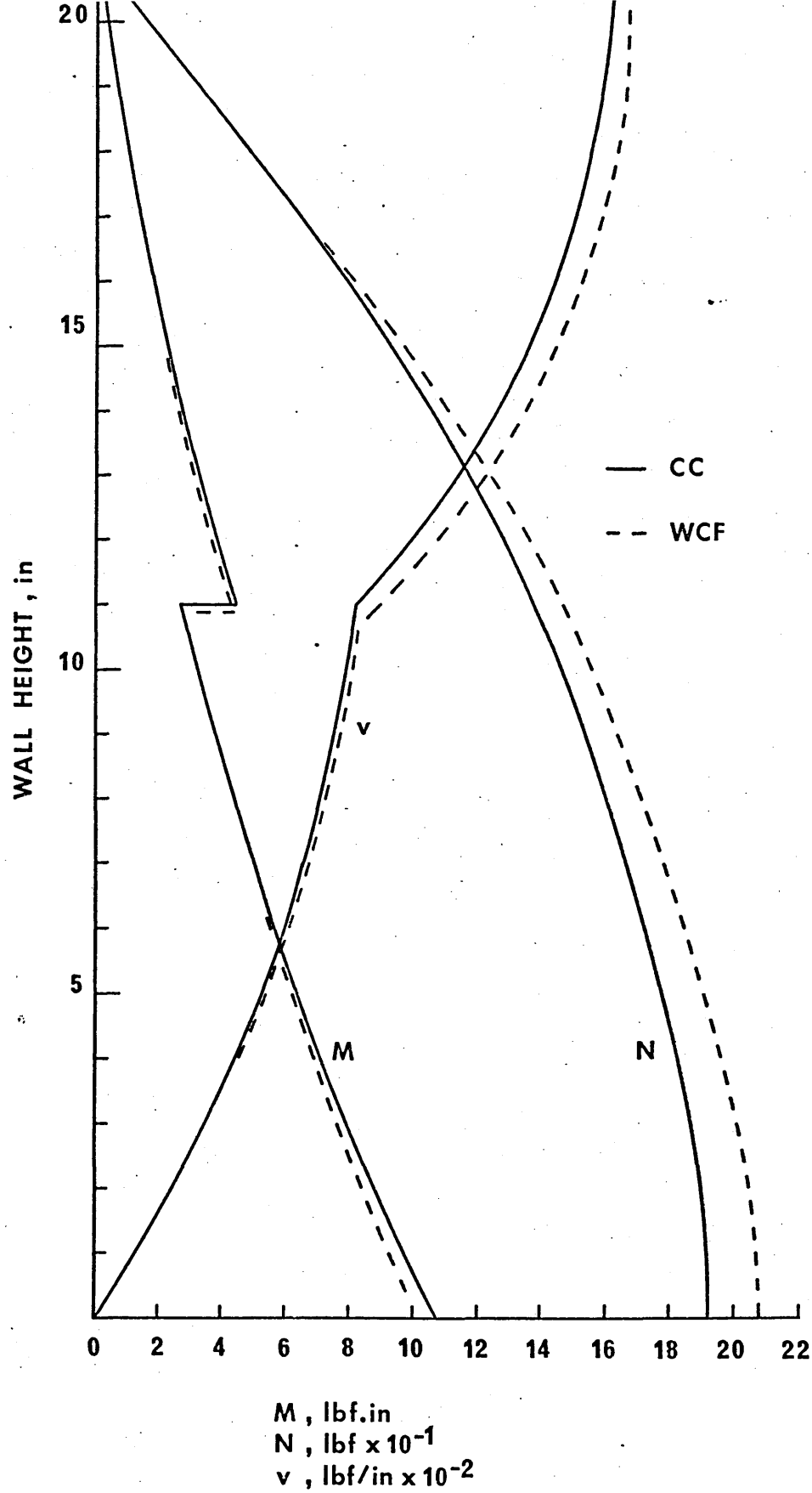


Figure 6.9 Distribution of M, N and v in Model 4 due to a Point Load of 1 lbf at the top

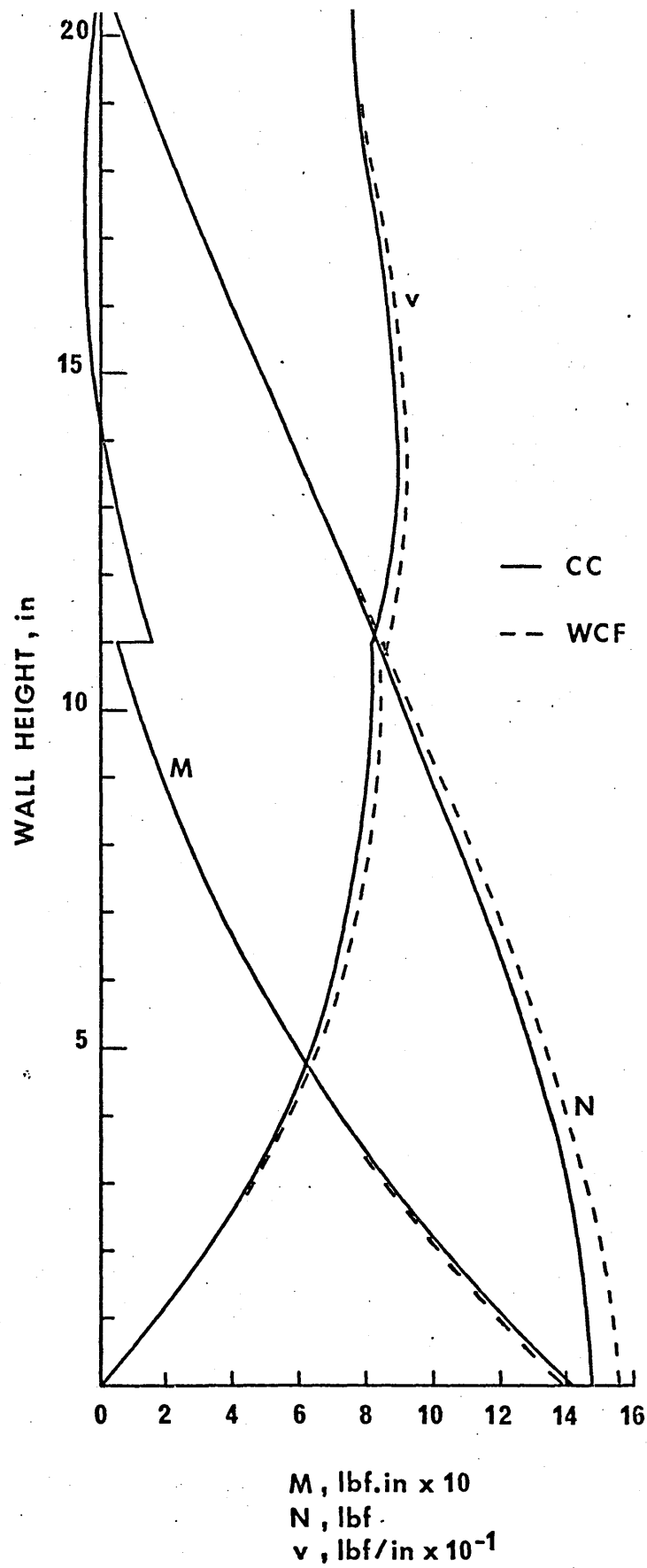


Figure 6.10 Distribution of M, N and v in Model 4 due to a U.D.L. of 1 lbf/in

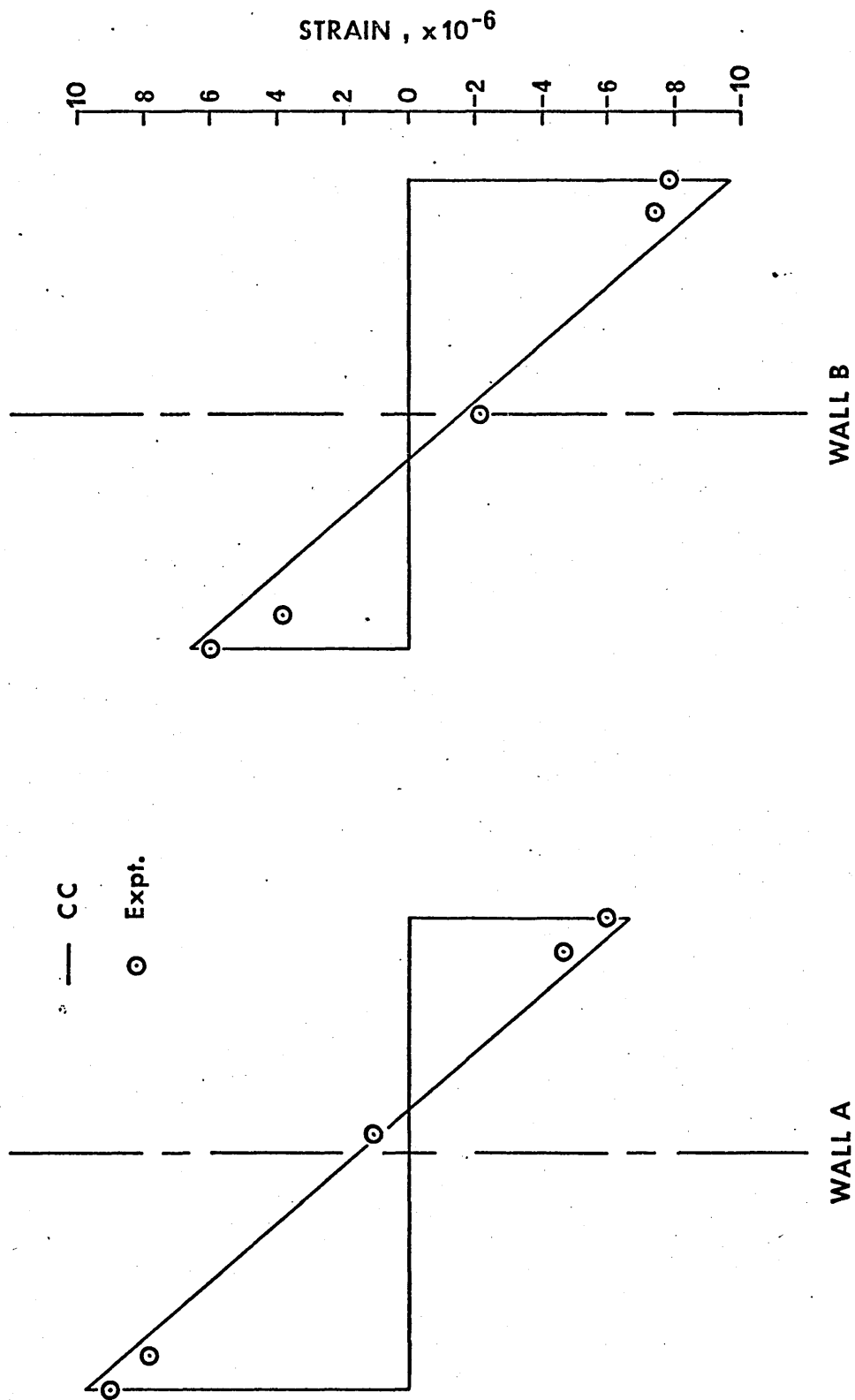


Figure 6.11 Strain distribution across Model 1 at a height of 1.375 in due to a Point Load of 1 lbf at the top

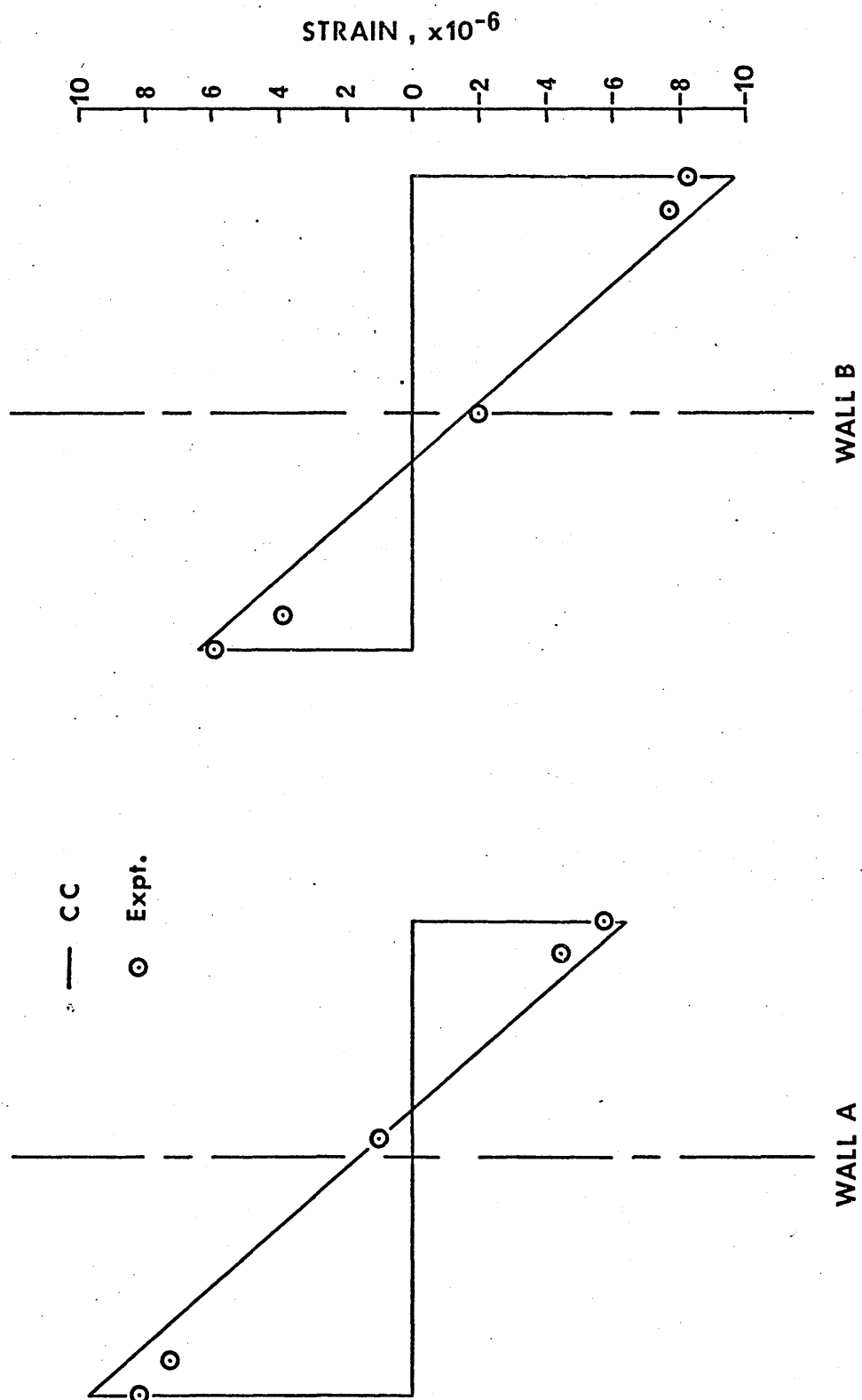


Figure 6.12 Strain distribution across Model 2 at a height of 1.375 in due to a Point Load of 1 lbf at the top

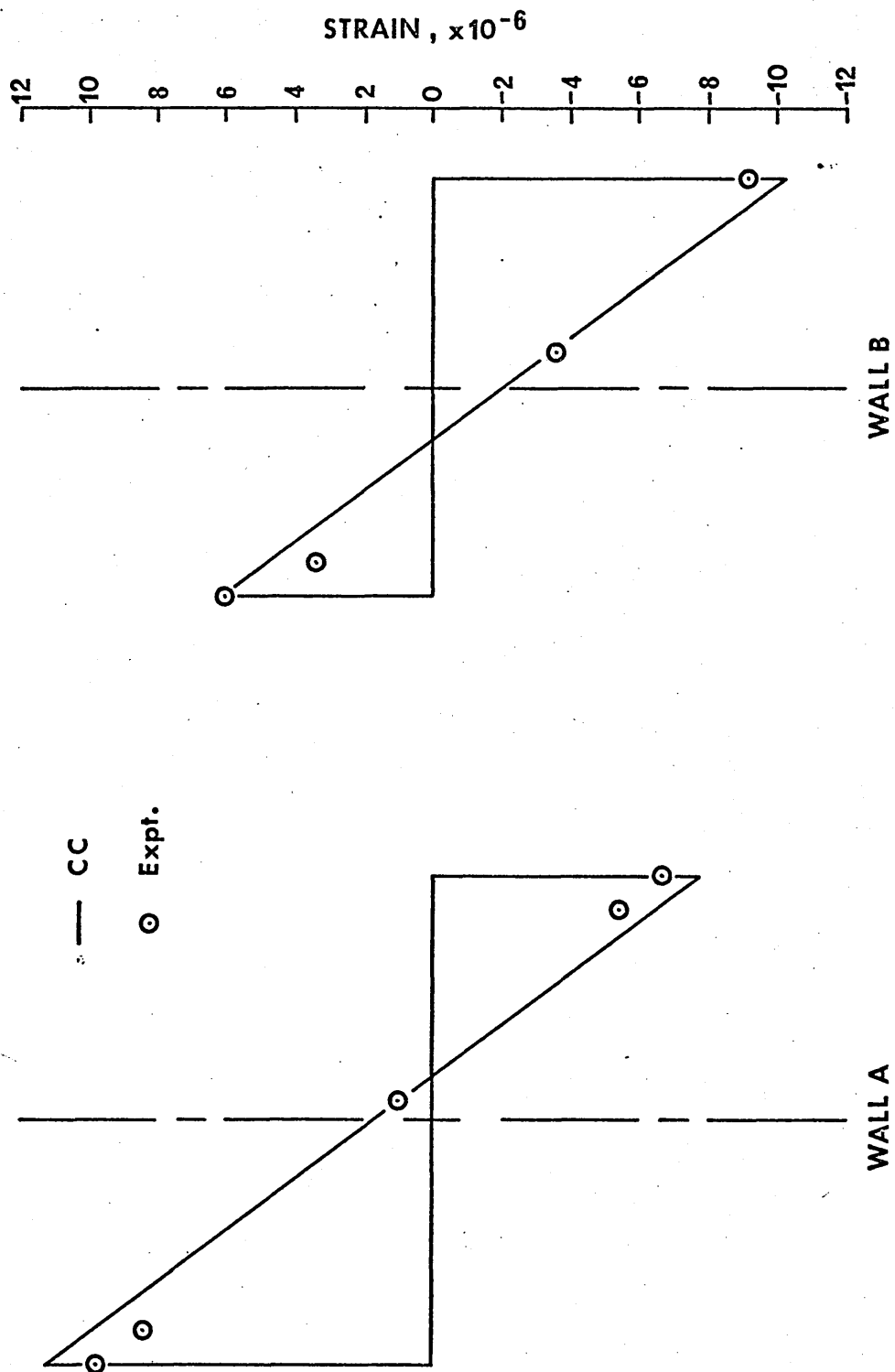


Figure 6.13 Strain distribution across Model 3 at a height of 1.375 in due to a Point Load of 1 lbf at the top

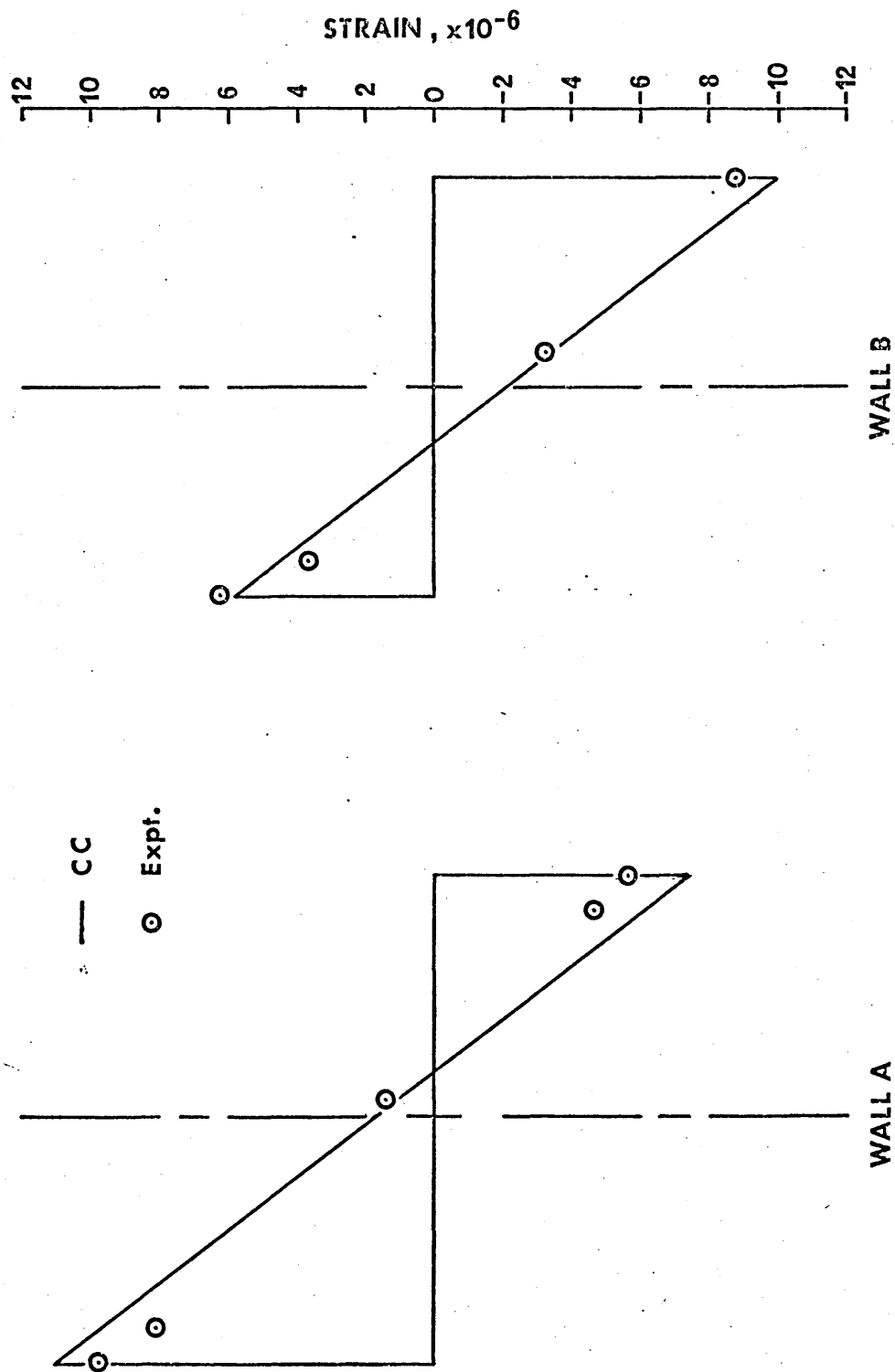


Figure 6.14 Strain distribution across Model 4 at a height of 1.375 in due to a Point Load of 1 lbf at the top

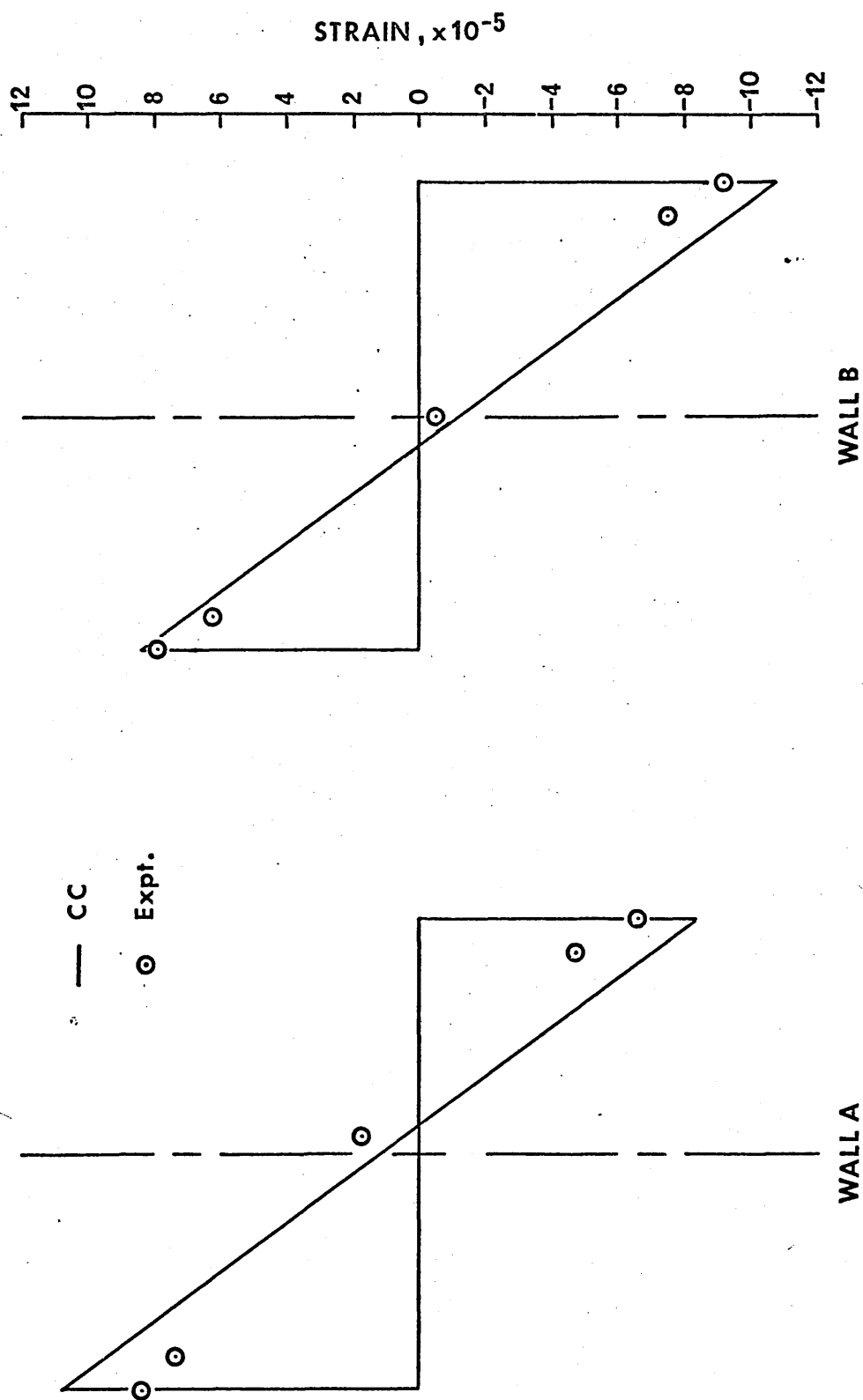


Figure 6.15 Strain distribution across Model 1 at a height of 1.375 in due to a U.D.L. of 1 lbf/in

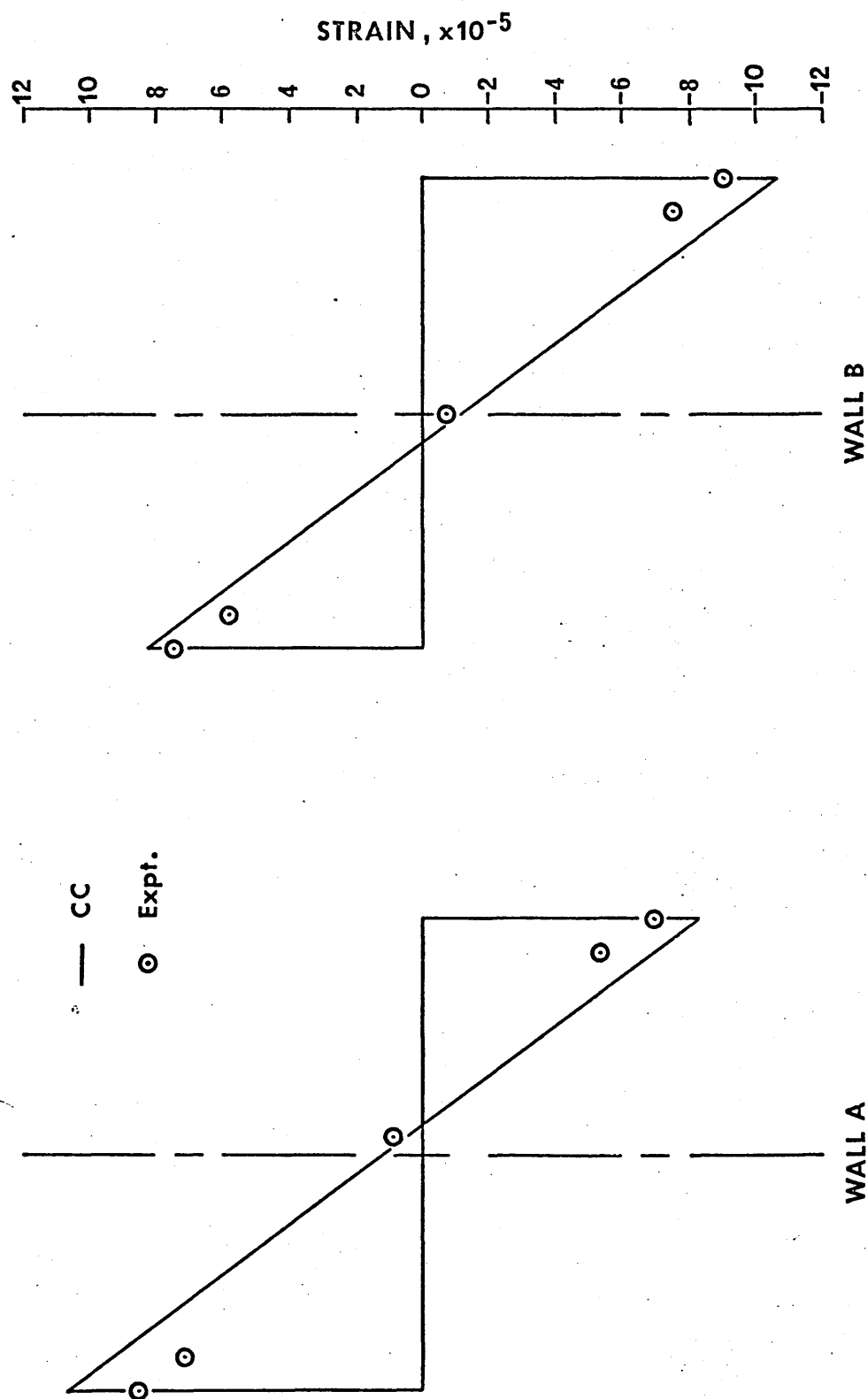


Figure 6.16 Strain distribution across Model 2 at a height of 1.375 due to a U.D.L. of 1 lbf/in

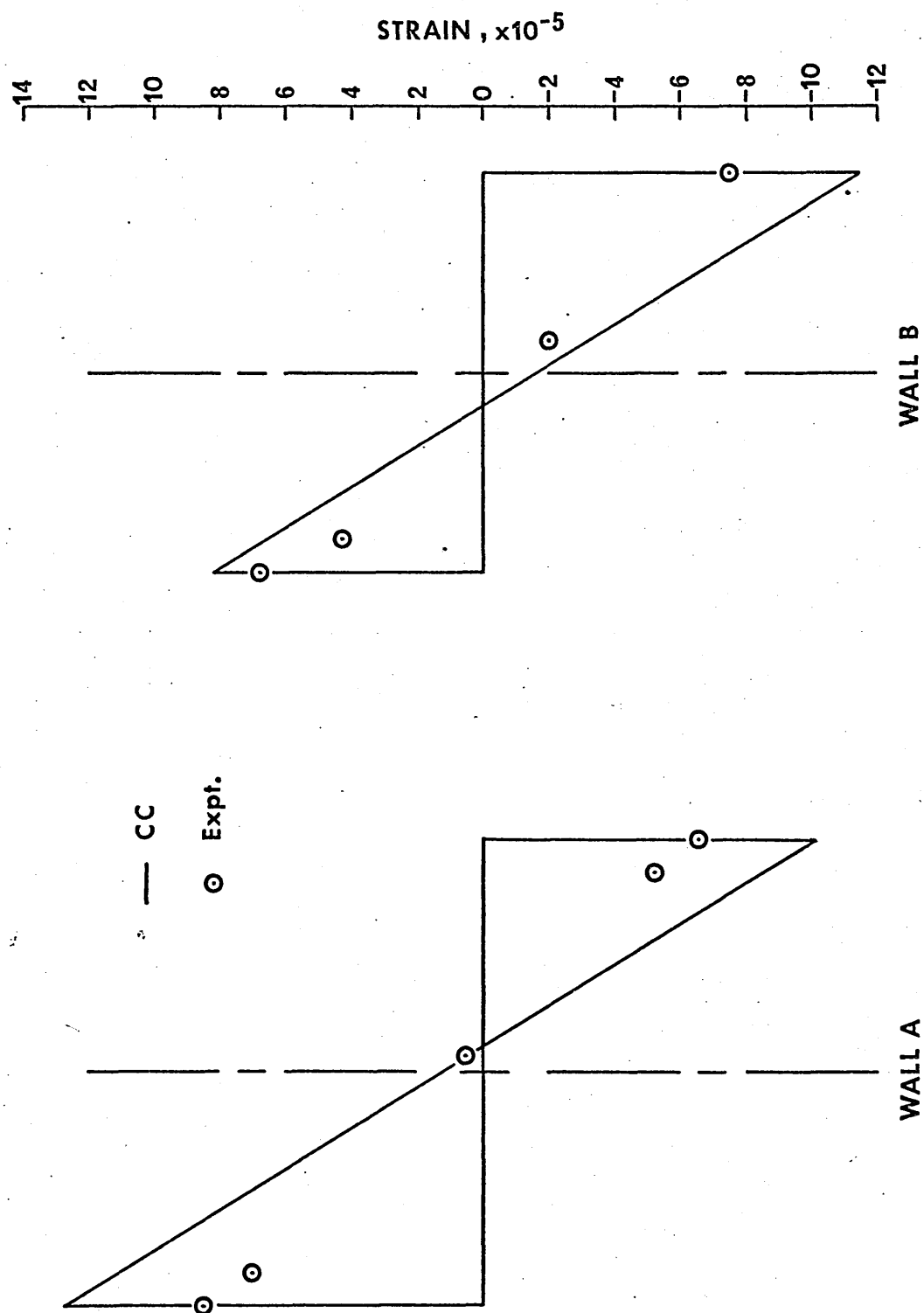


Figure 6.17 Strain distribution across Model 3 at a height of 1.375 in due to a U.D.L. of 1 lbf/in

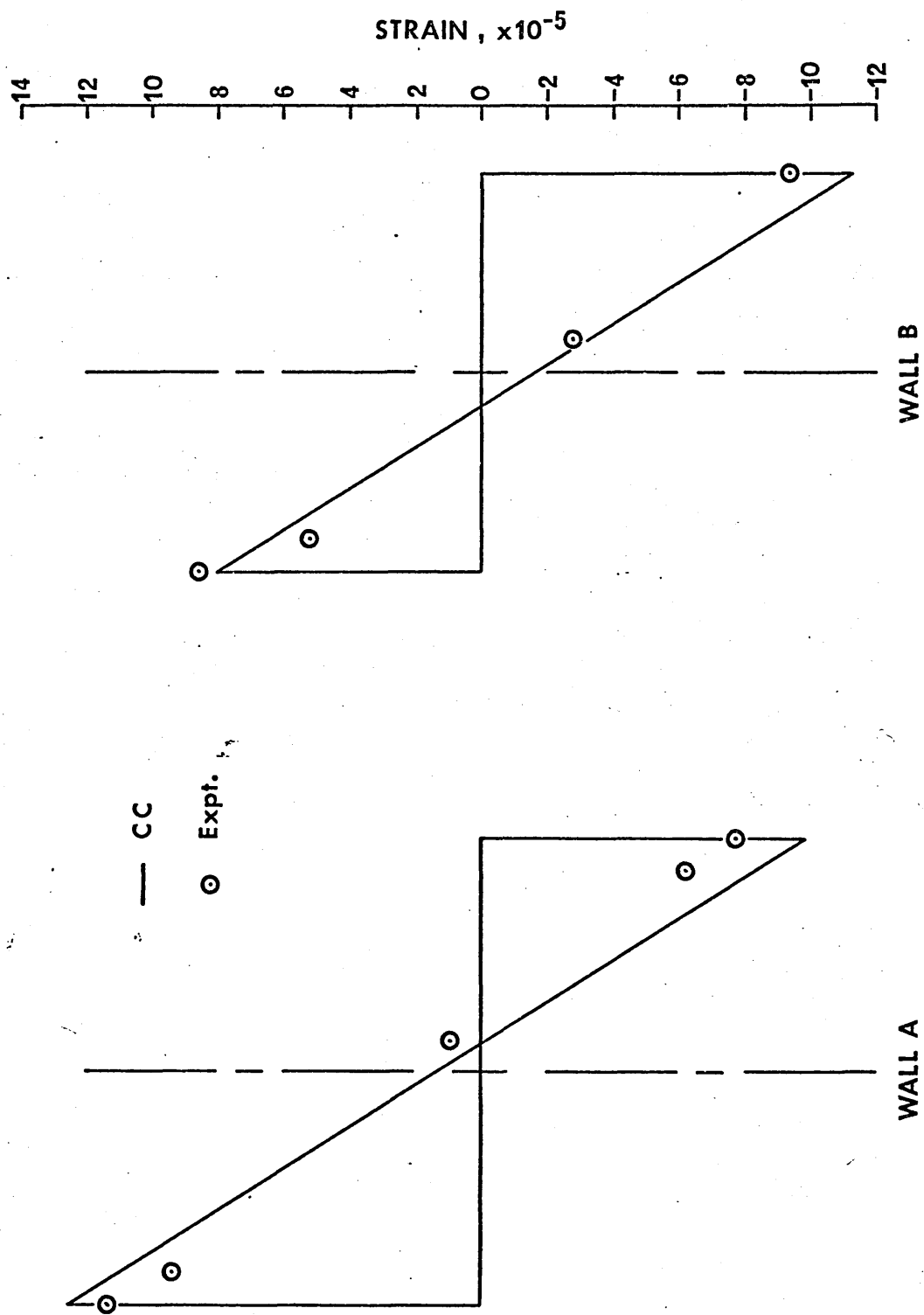


Figure 6.18 Strain distribution across Model 4 at a height of 1.375 in due to a U.D.L. of 1 lbf/in

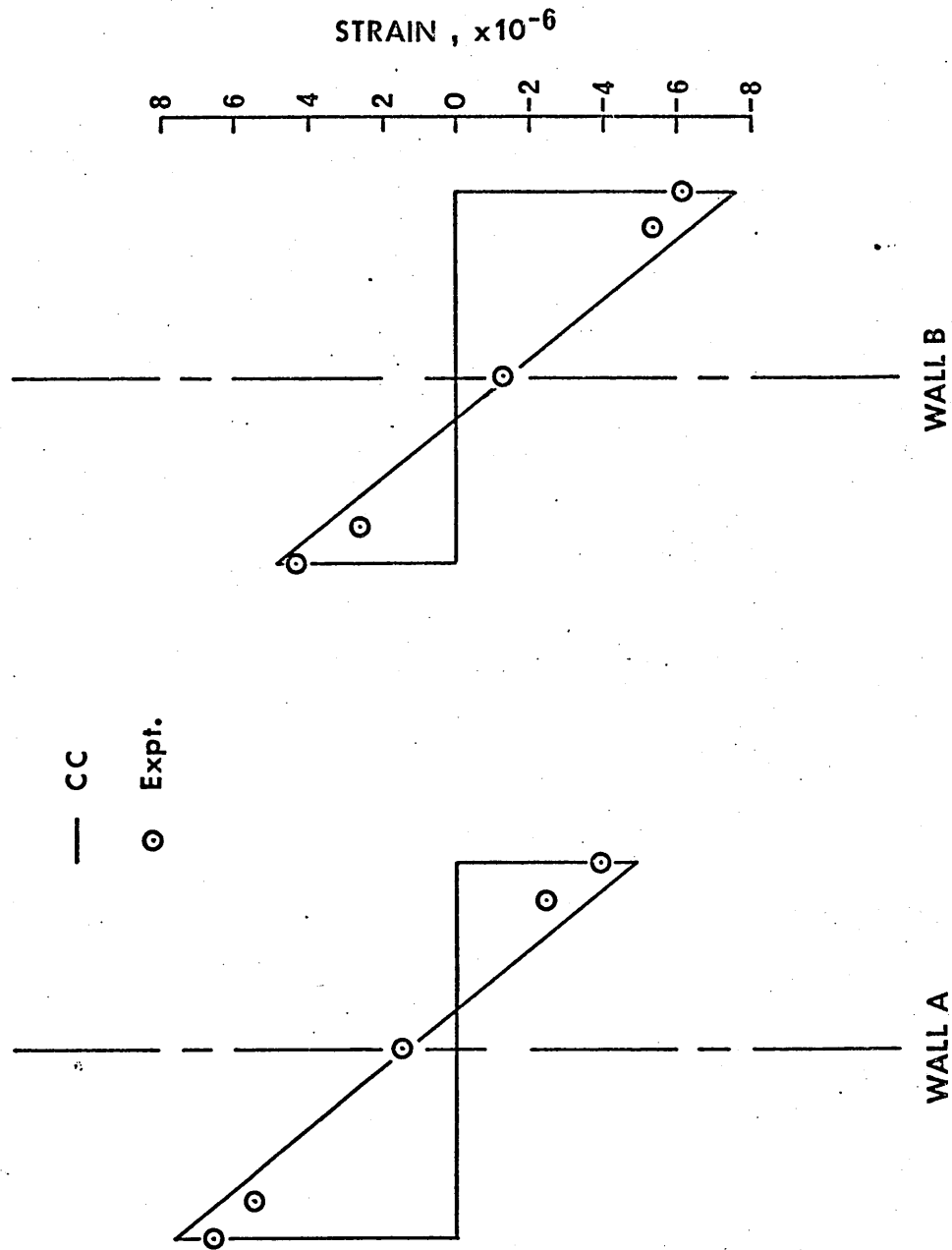


Figure 6.19 Strain distribution across Model 1 at a height of 12.375 in. due to a Point Load of 1 lbf at the top

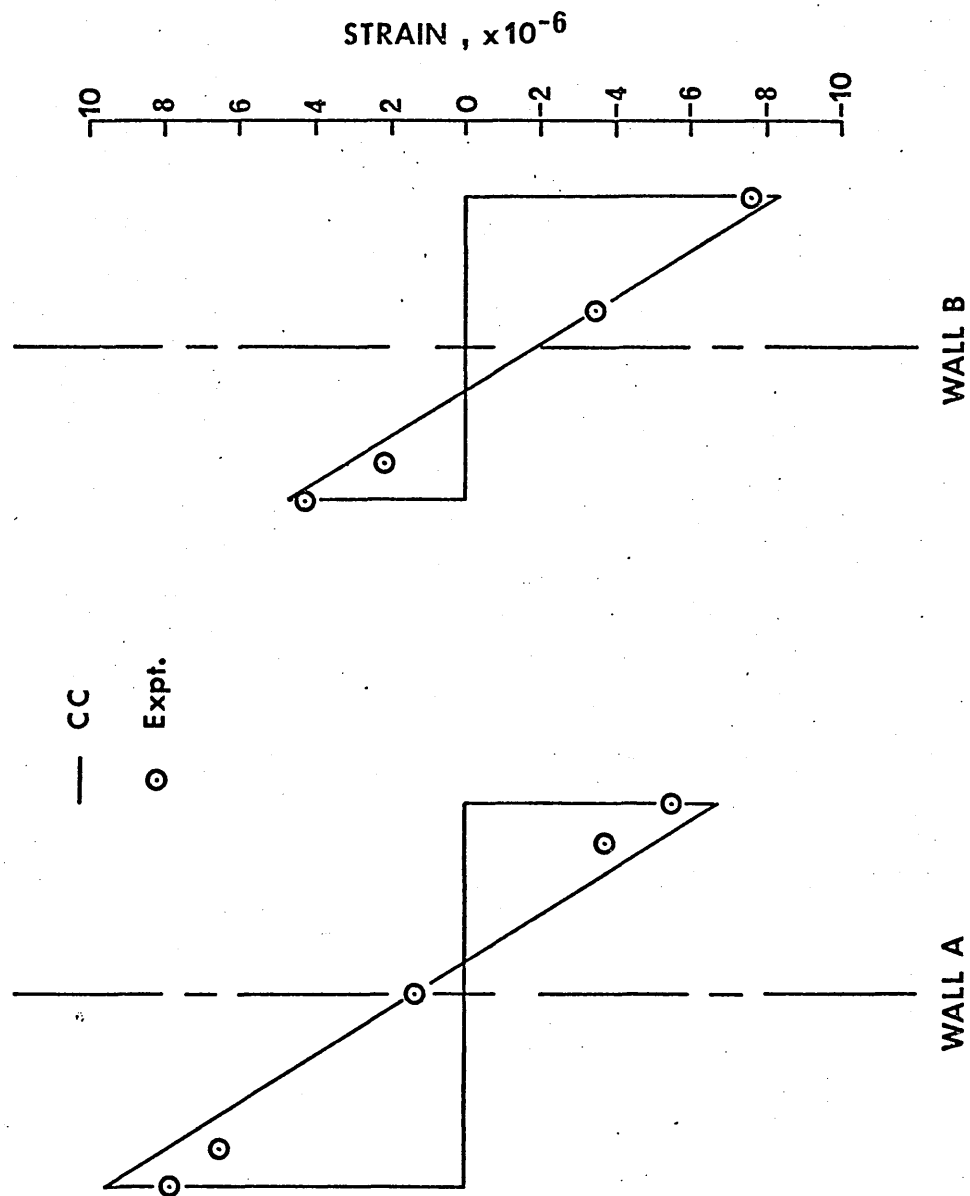


Figure 6.20 Strain distribution across Model 2. at a height of 12.375 in. due to a Point Load of 1 lbf at the top

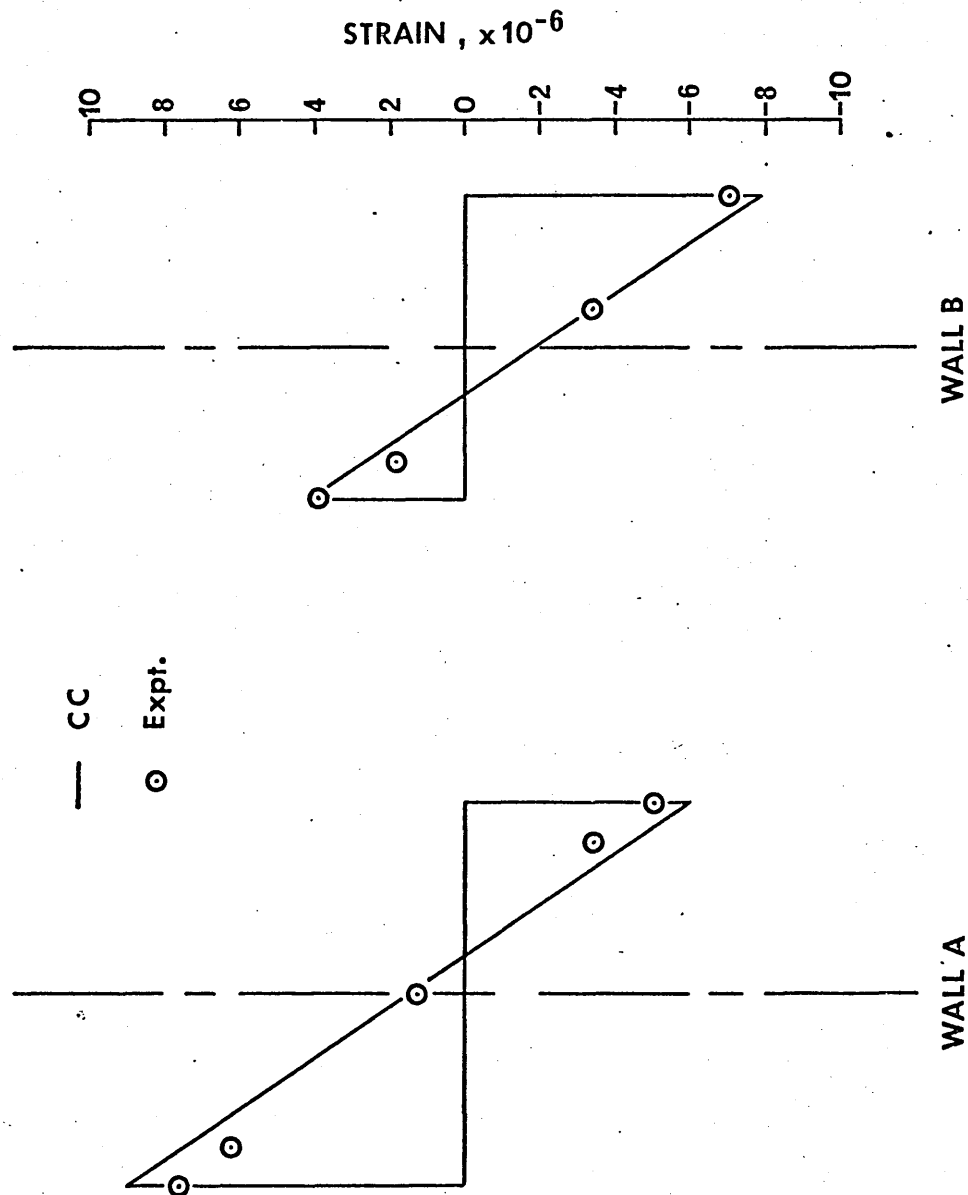


Figure 6.21 Strain distribution across Model 3 at a height of 12.375 in. due to a Point Load of 1 lbf at the top

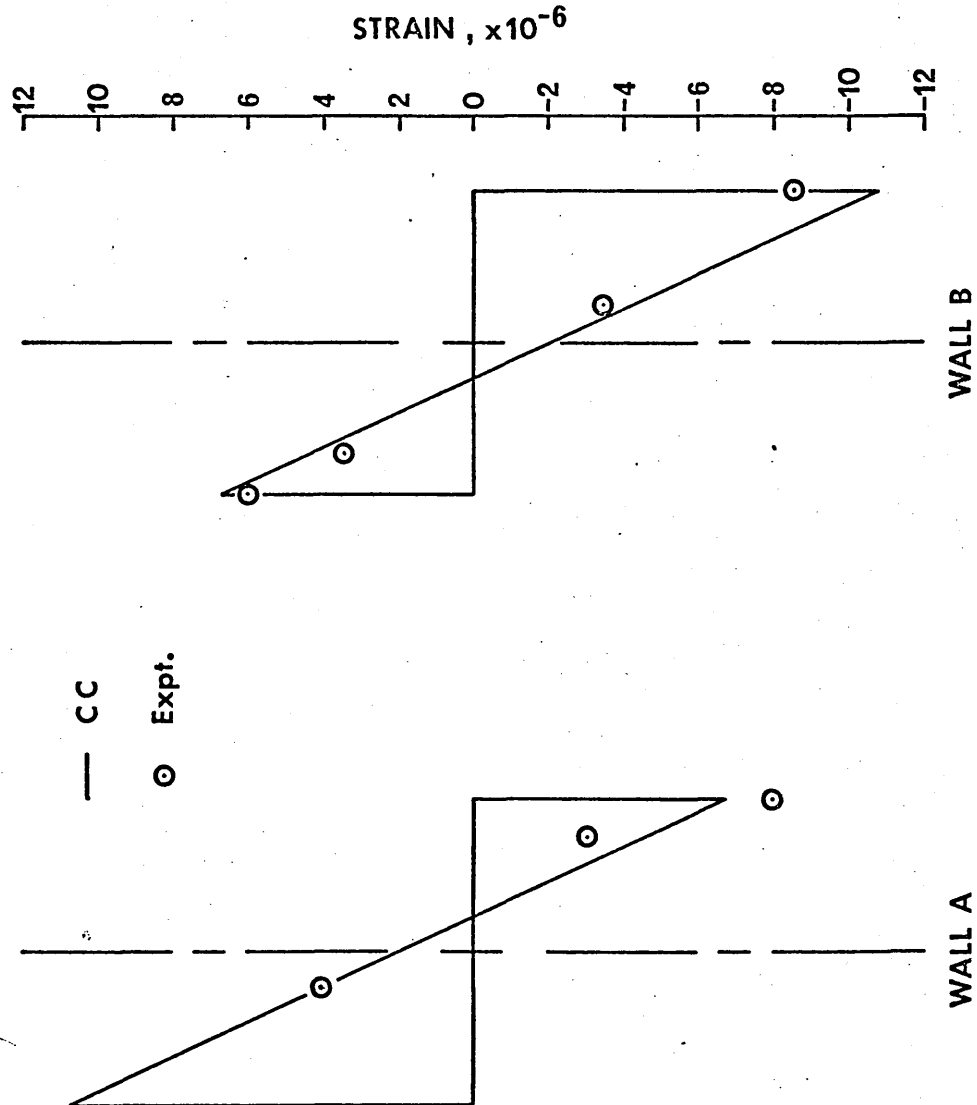


Figure 6.22 Strain distribution across Model 4 at a height of 12.375 in. due to a Point Load of 1 lb at the top

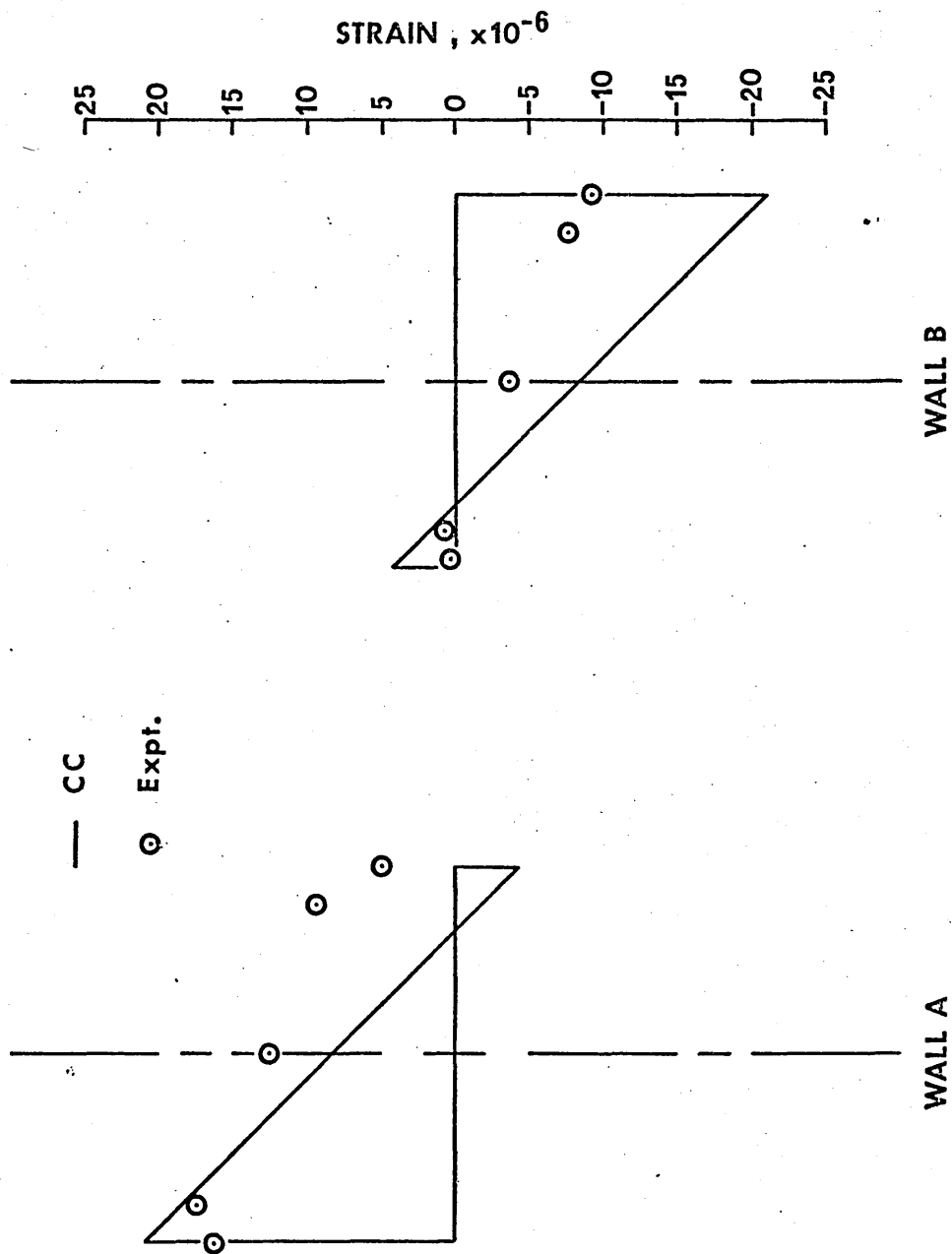


Figure 6.23 Strain distribution across Model 1 at a height of 12.375 in. due to a U.D.L. of 1 lbf/in.

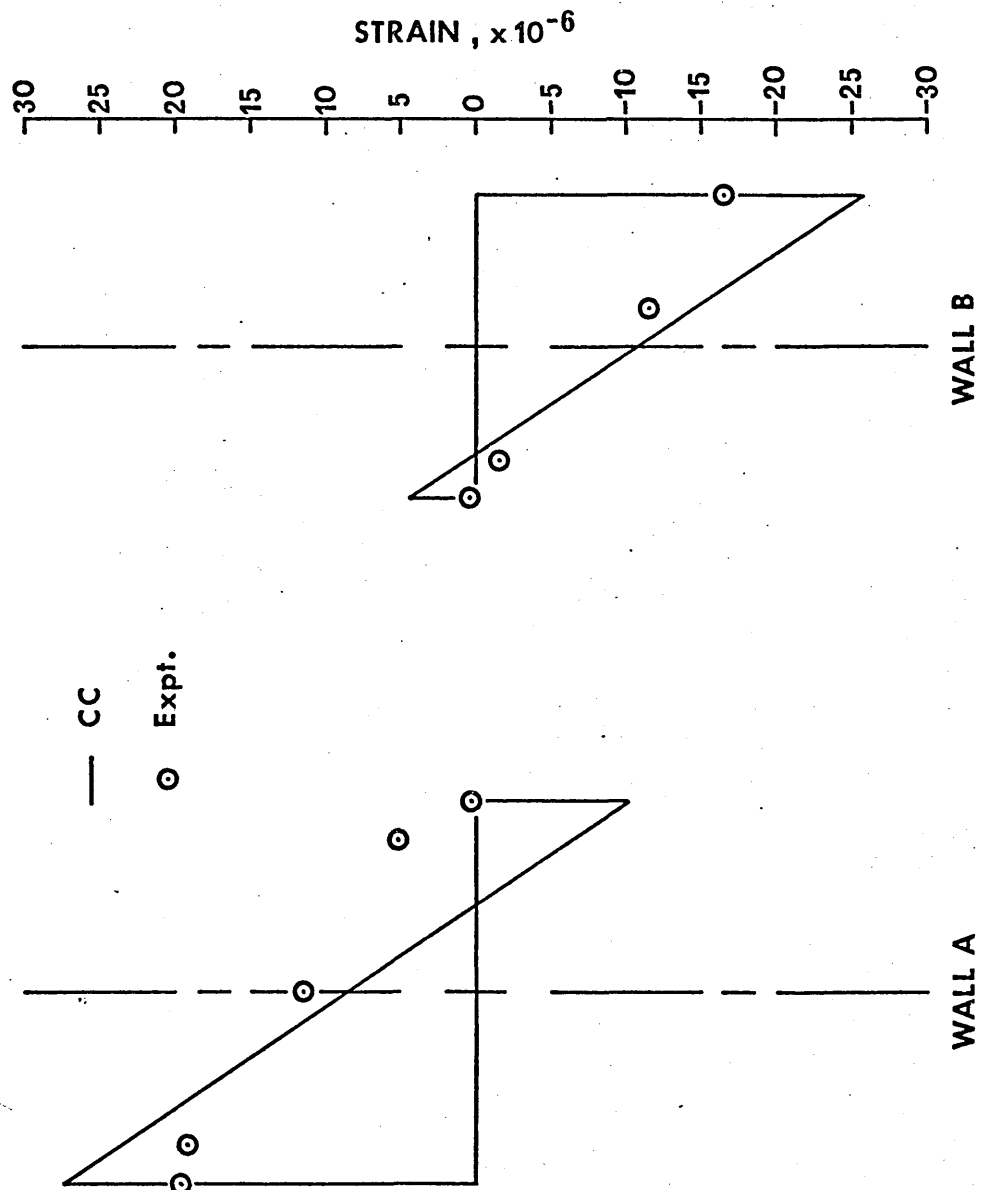


Figure 6.24 Strain distribution across Model 2 at a height of 12.375 in. due to a U.D.L. of 1 lbf/in.

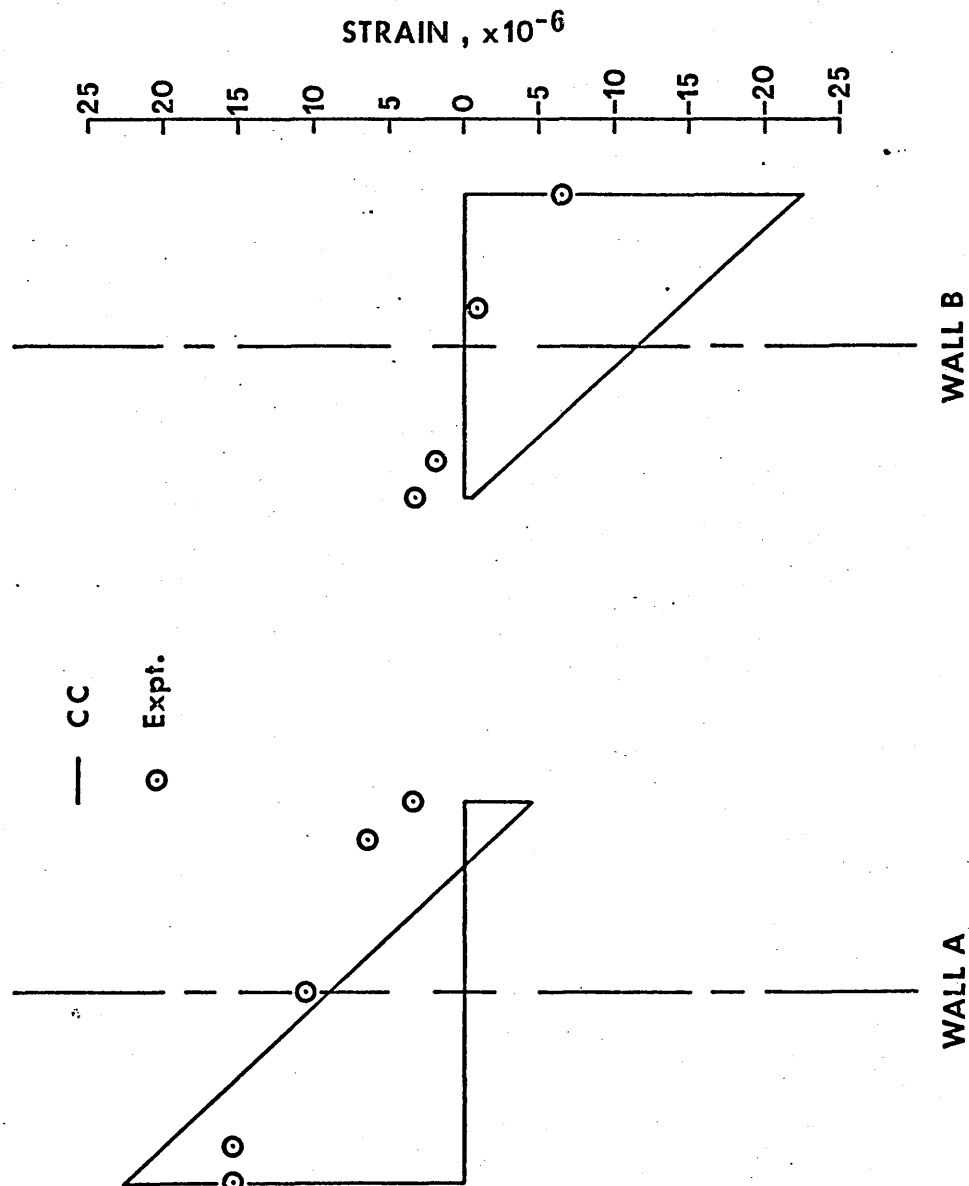


Figure 6.25 Strain distribution across Model 3 at a height of 12.375 in. due to a U.D.L. of 1 lbf/in.

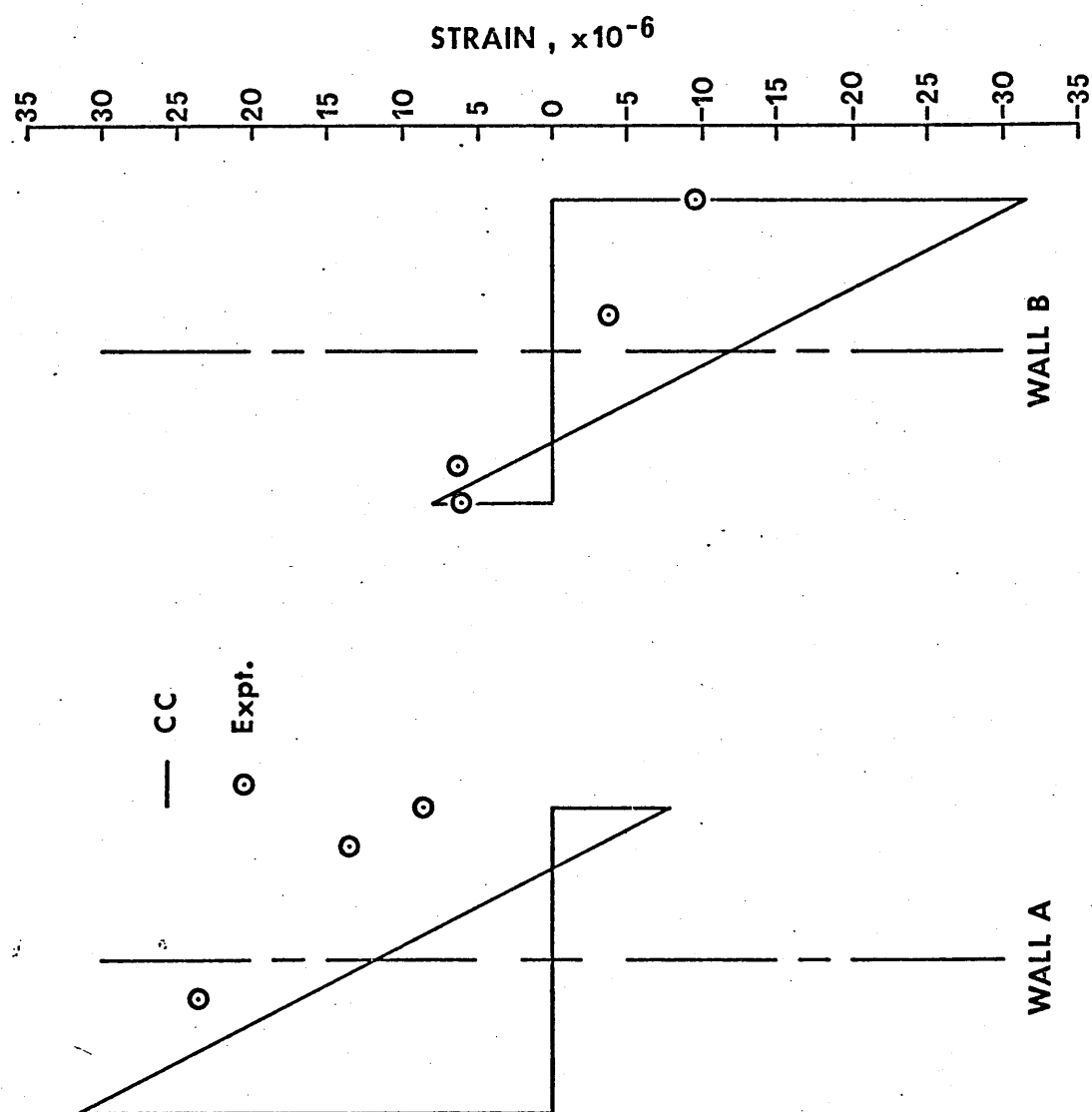


Figure 6.26 Strain distribution across Model 4 at a height of 12.375 in. due to a U.D.L. of 1.1bf/in.

6.4 Results for Uniform Walls Supported on Columns

Typical structures covered in this section are shown in Figure 6.27.

In the range of structures analysed, the following parameters have been varied:-

- (a) The stiffness of the connecting beams.

This has an important effect on the degree of interaction between the two wall sections. The parameter αH is a measure of this interaction, and the two values $\alpha H = 4$ and $\alpha H = 16$ have been used as they represent extremes of the range over which coupling action is considered important.

The basic wall geometry of both wall systems has been taken to be the same, as in Figure 6.28, and the αH value has been artificially varied by assuming the appropriate value of the moment of inertia of the connecting beam.

- (b) The position of the support columns.

Both central and offset columns have been considered, as shown in Figure 6.27.

- (c) The stiffness of the support beam.

Two values have been used, the first in which the depth of the beam is the same as the depth of the wall connecting beams, and the second in which the depth of

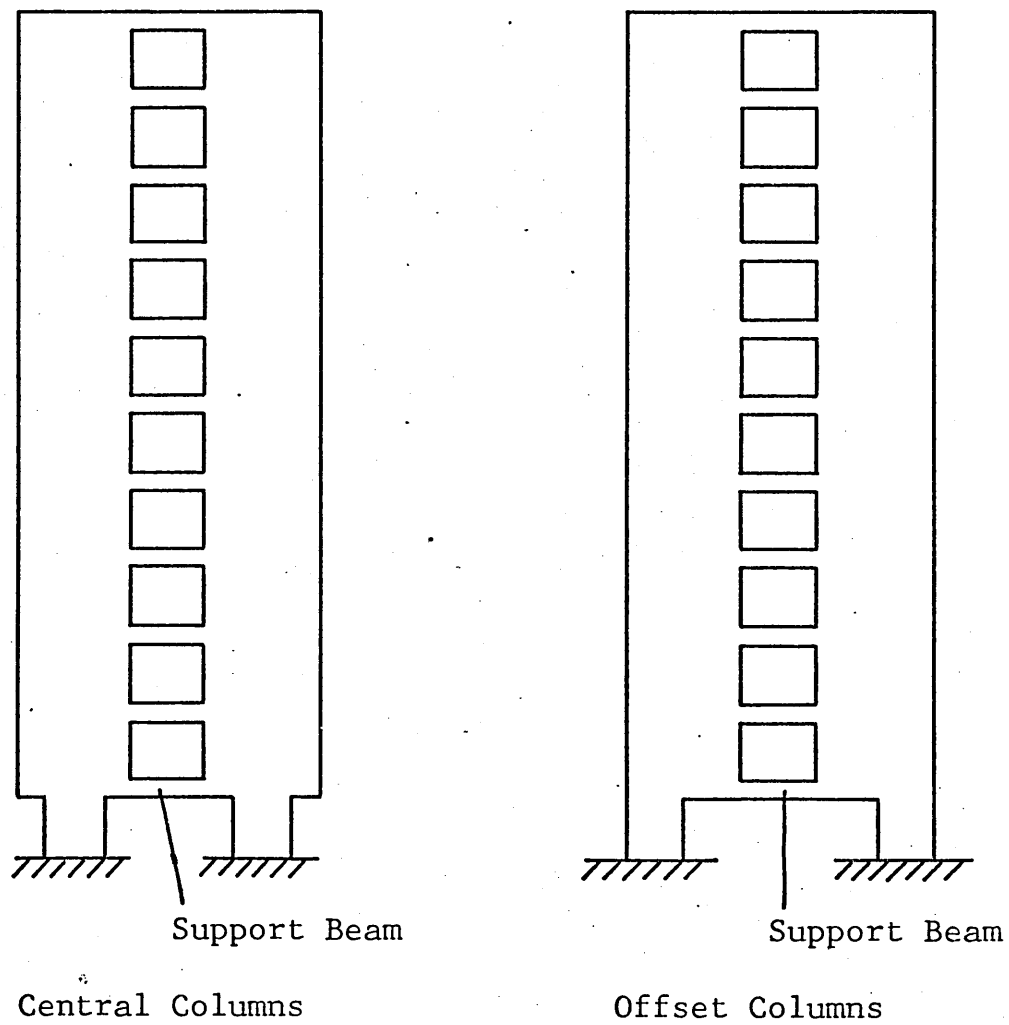
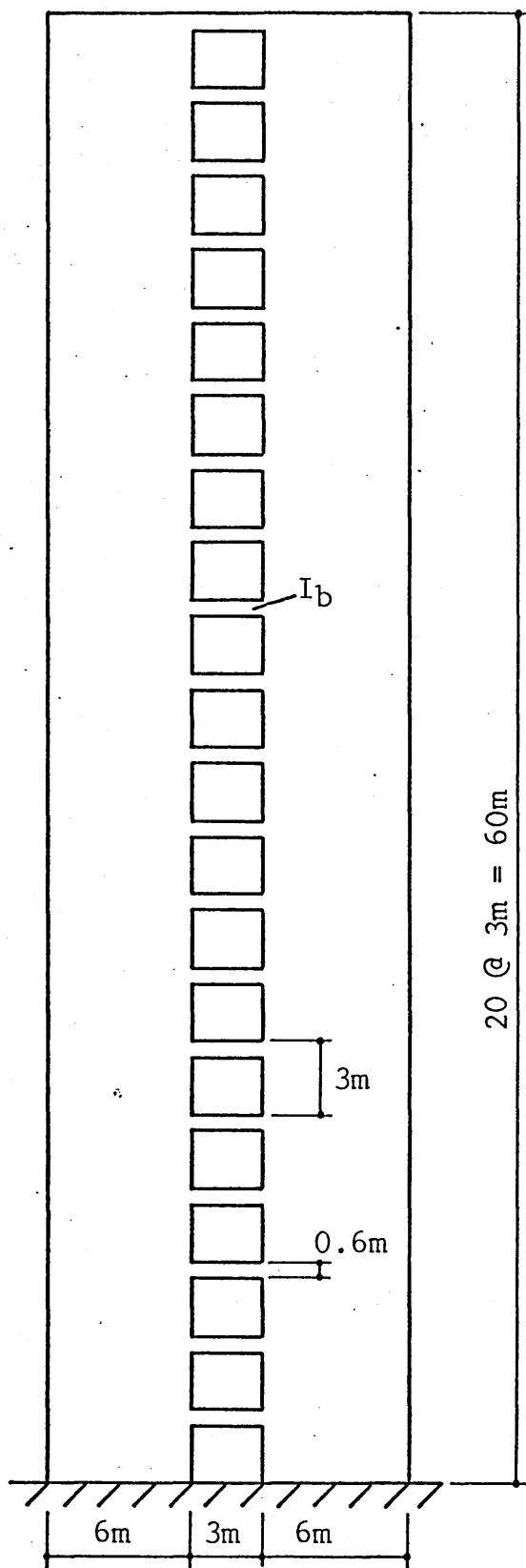


Figure 6.27 Uniform Coupled Shear Walls Supported on Columns

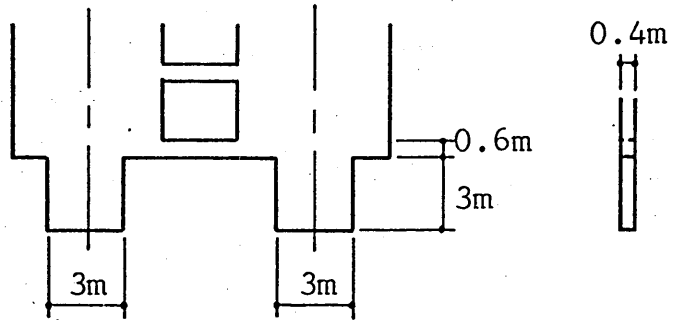


wall thickness = 0.4 m

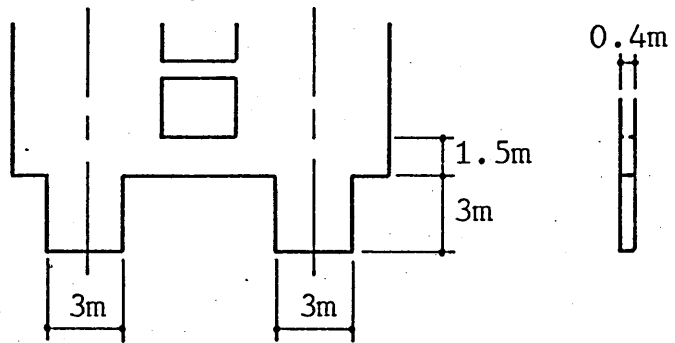
αH	$I_b (m^4)$
4	0.004165
16	0.06664

Figure 6.28 Dimensions of Walls with $\alpha H=4$ and $\alpha H=16$

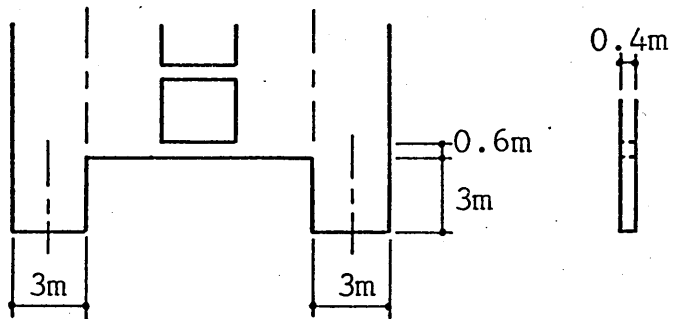
Column
Type 1



Column
Type 2



Column
Type 3



Column
Type 4

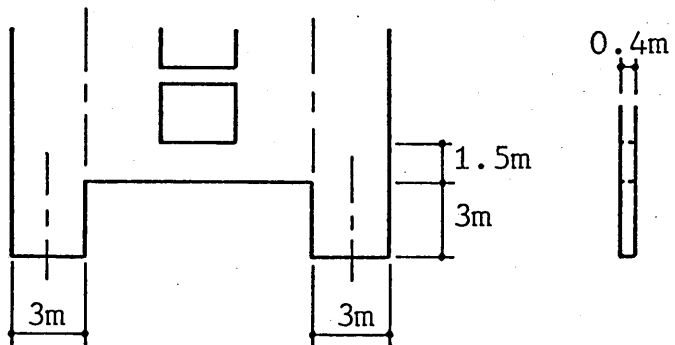


Figure 6.29 Dimensions of Column Systems 1 to 4

the beam is equal to half the storey height.

Items (b) and (c) above have been combined in the four column support systems shown in Figure 6.29.

Both types of wall, supported on each of the four column systems, have been analysed under the action of a uniformly distributed load of 1kN/m .

When obtaining a matrix progression solution, the column system has been treated as a uniform zone with the support beam providing the equivalent continuous connection, and the actual wall has been treated as a second uniform zone.

The results have been compared with those obtained from a wide column frame solution, which is assumed to define the correct behaviour.

Figures 6.32 to 6.39 show the distributions of total wall bending moment M , the distributed vertical shear force v and the deflection y . Zero wall height as shown on the diagrams represents the top of the column system and the base of the wall.

From the bending moment distributions, together with the relevant values of axial force in the walls, stress profiles have been calculated at a height of 6m above the column system/wall base junction. These stress distributions are given in Figures 6.42 to 6.49.

In order to have a basis for comparing the above results, solutions have also been obtained for two walls with rigid bases and relative stiffness values of $\alpha H = 4$ and $\alpha H = 16$.

Distributions of M, N, v and y for these two sets of results are shown in Figures 6.30 and 6.31 and stress distributions at a height of 6m above the base are given in Figures 6.40 and 6.41.

Values of maximum bending moment, maximum distributed shear force and maximum lateral deflection obtained using a wide column frame solution, an analytical solution and a matrix progression solution are compared in Table 6.3.

	αH	W.C.F.	Analytical Solution	C.C.
M at base kN.m.	4	848.0	826.6	850.6
	16	434.8	415.8	425.6
v max kN/m	4	2.33*	2.436	2.35*
	16	4.36*	4.435	4.40*
y at top m	4	1.12×10^{-3}	1.061×10^{-3}	1.109×10^{-3}
	16	5.7×10^{-4}	5.661×10^{-4}	5.719×10^{-4}

* Value obtained from graph (Figures 6.30 and 6.31)

Table 6.3 Values of M_{\max} , v_{\max} and y_{\max} in Walls with Rigid Bases and with $\alpha H=4$ and $\alpha H=16$

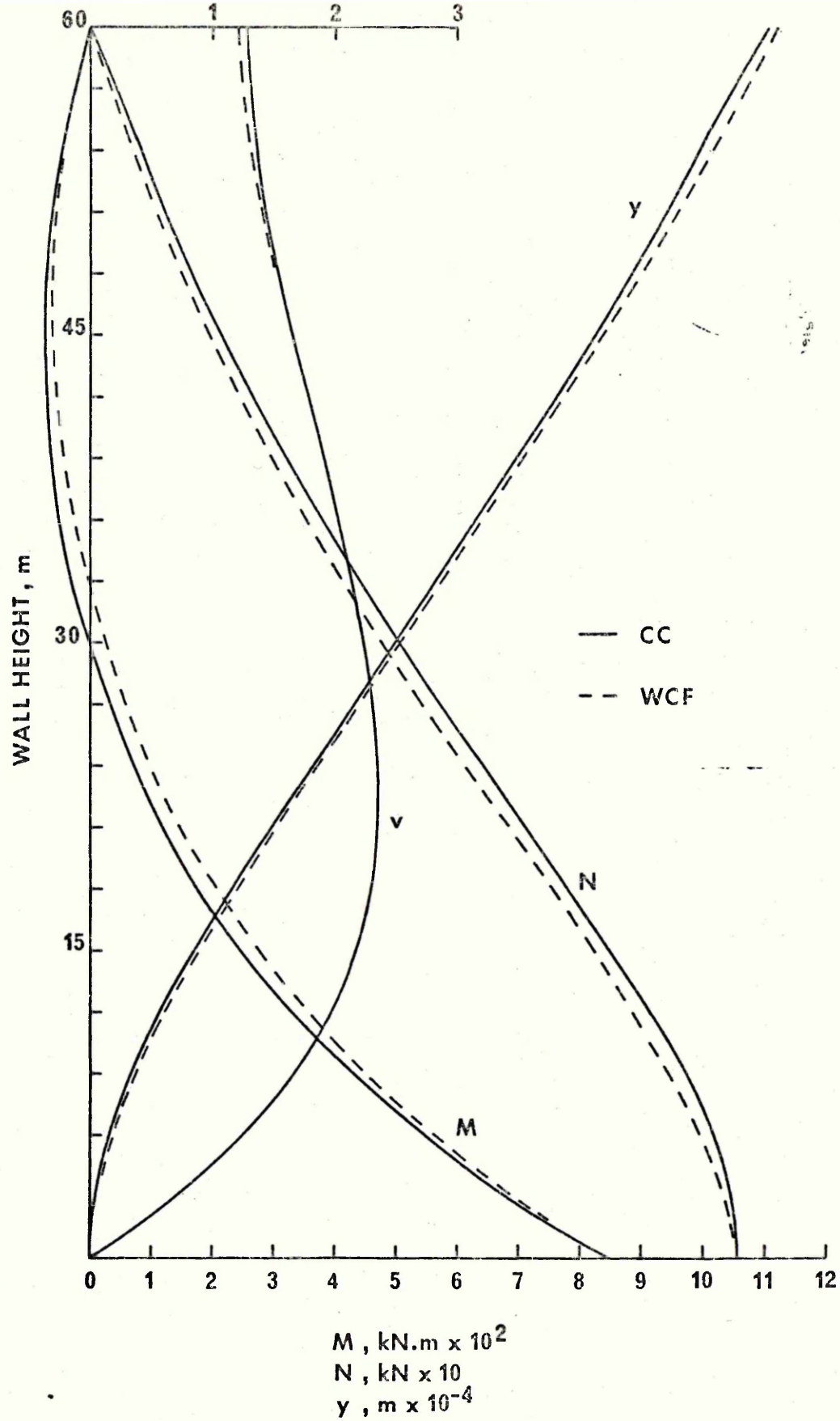


Figure 6.30 Distribution of M , N , v and y in wall with rigid base and with $\alpha H=4$

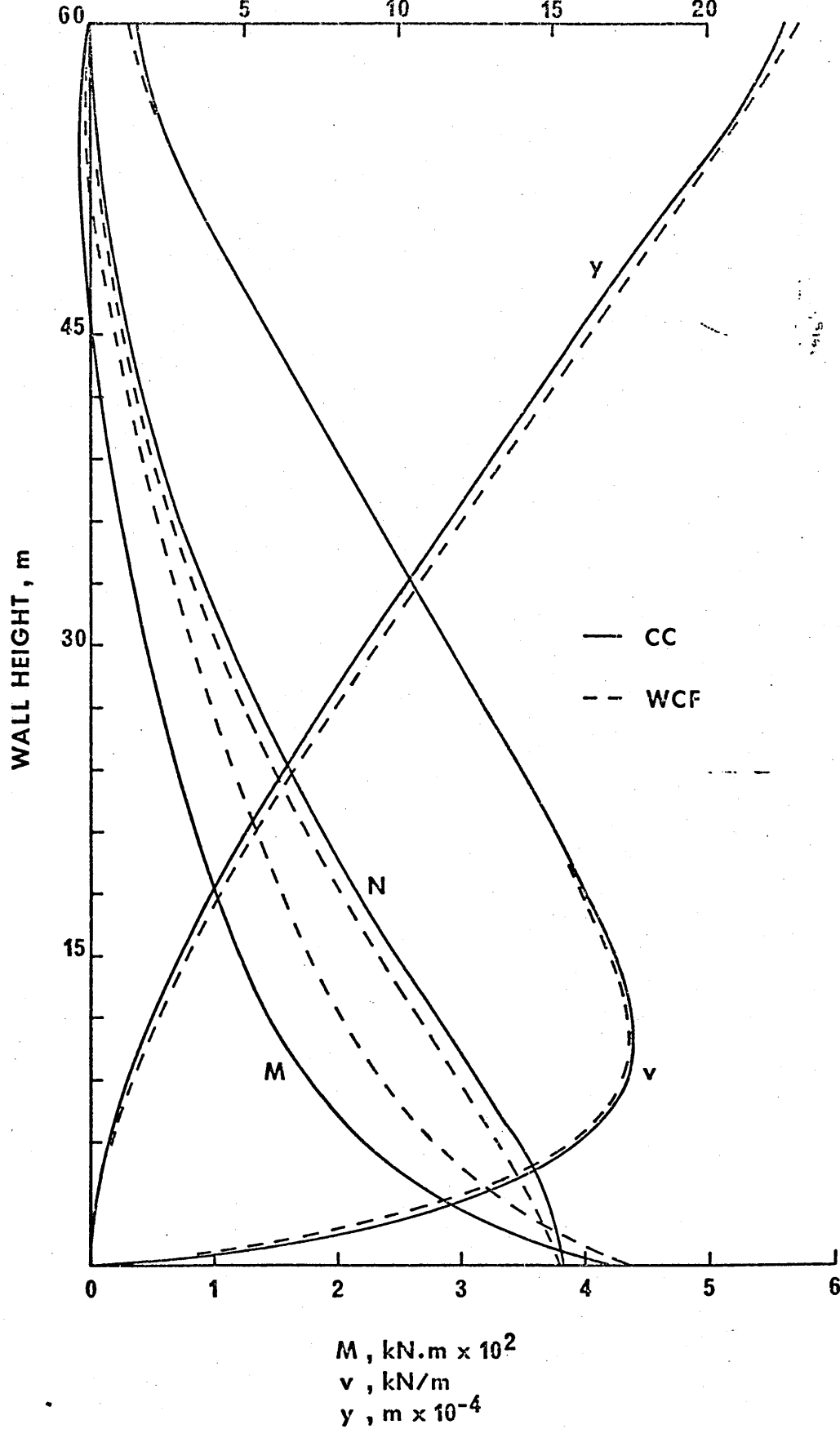


Figure 6.31 Distribution of M, N, v and y in wall with rigid base and with $\alpha H=16$

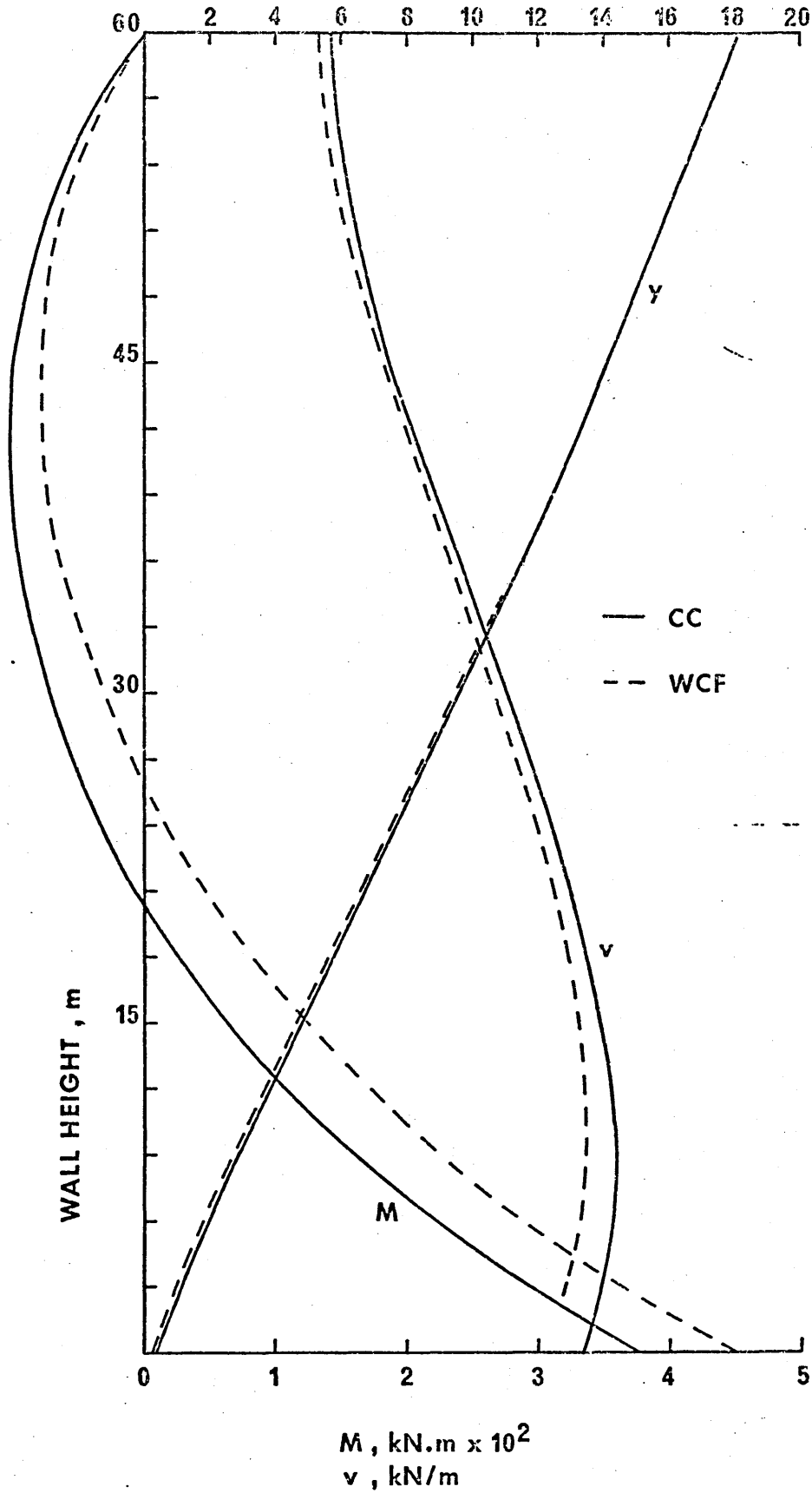


Figure 6.32 Distribution of M, v and y in wall with $\alpha H=4$ supported on Column Type 1

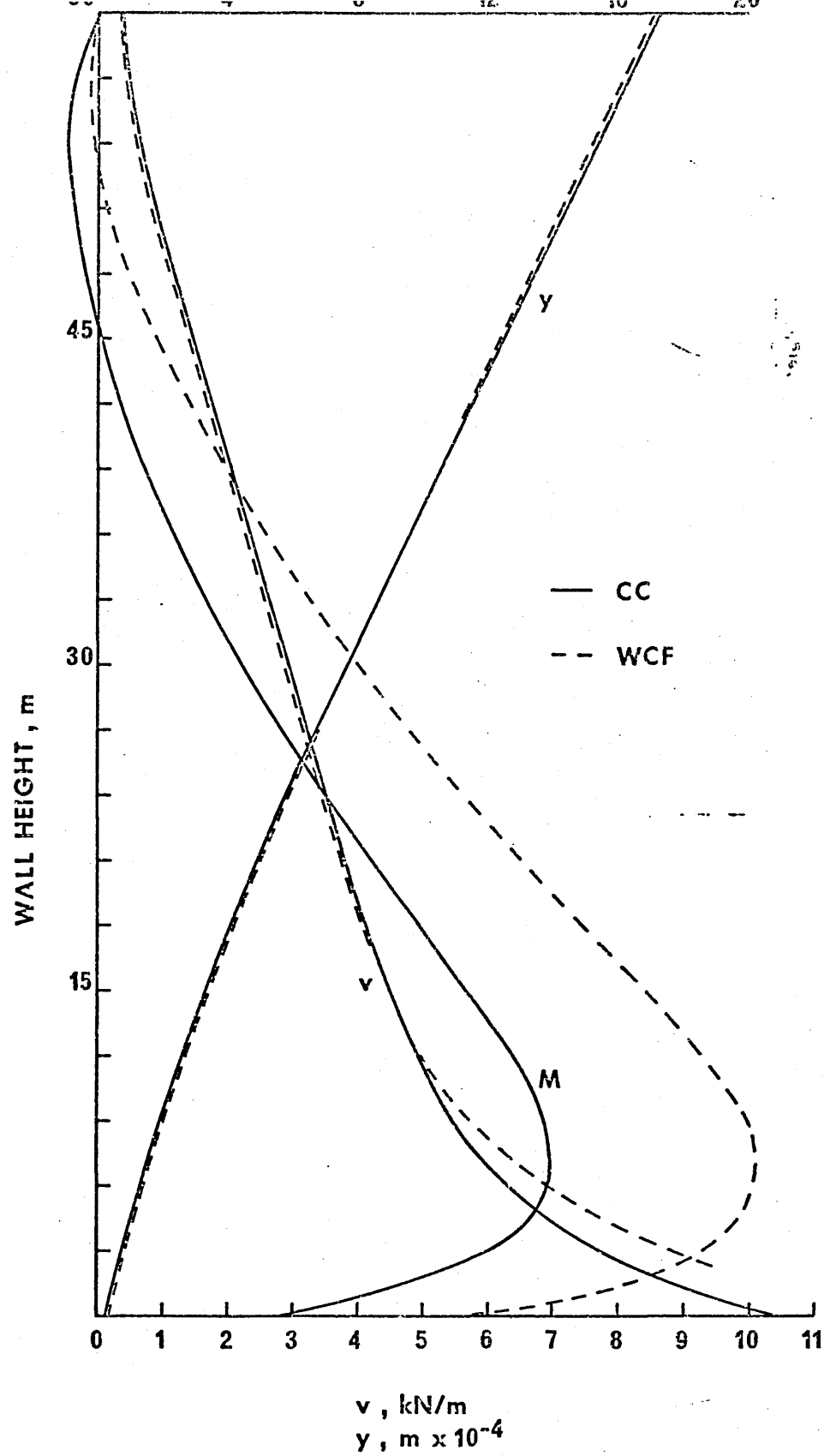


Figure 6.33 Distribution of M, v and y in wall with $\alpha H=16$ supported on Column Type 1

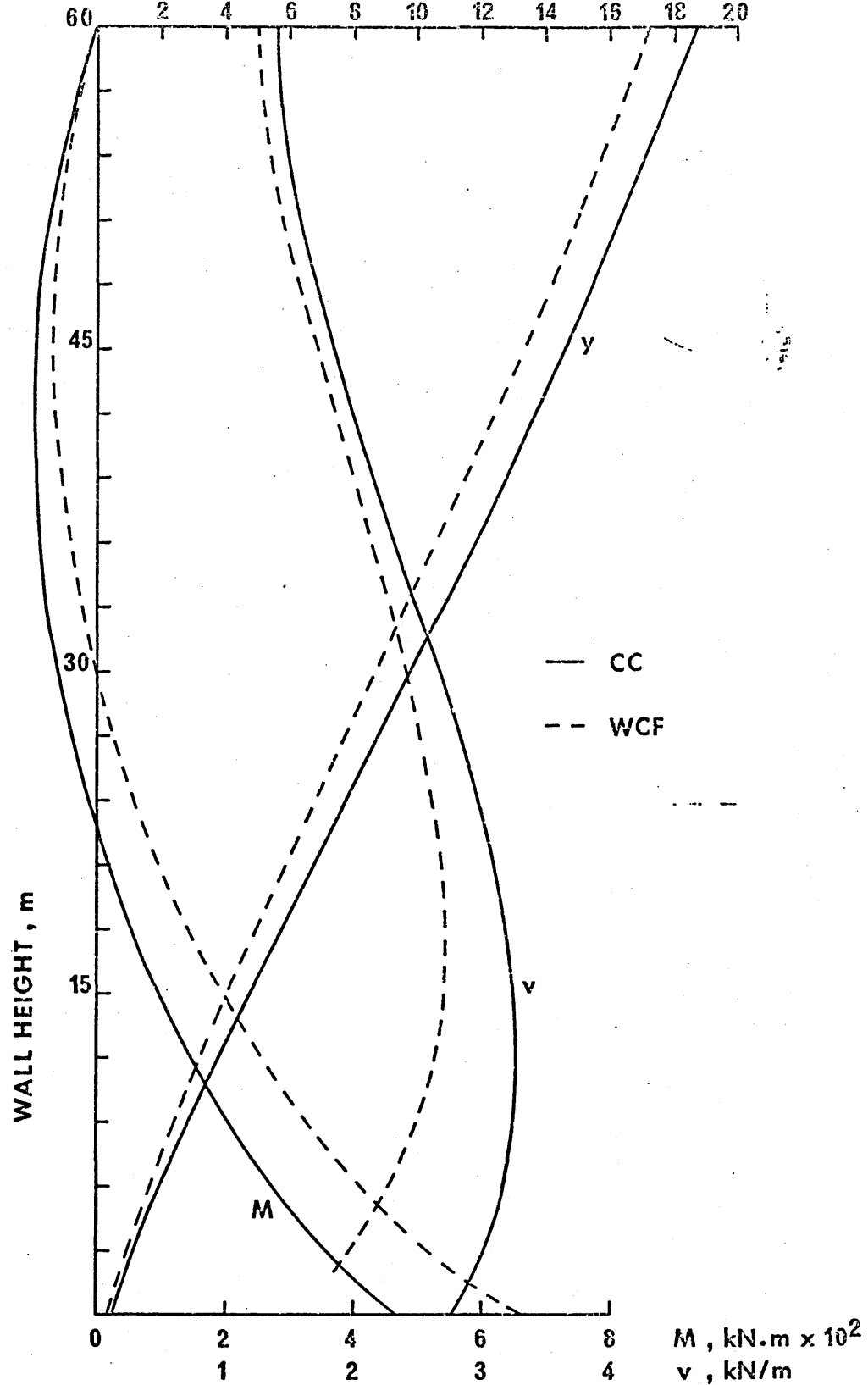


Figure 6.34 Distribution of M, v and y in wall with $\alpha H=4$ supported on Column Type 2

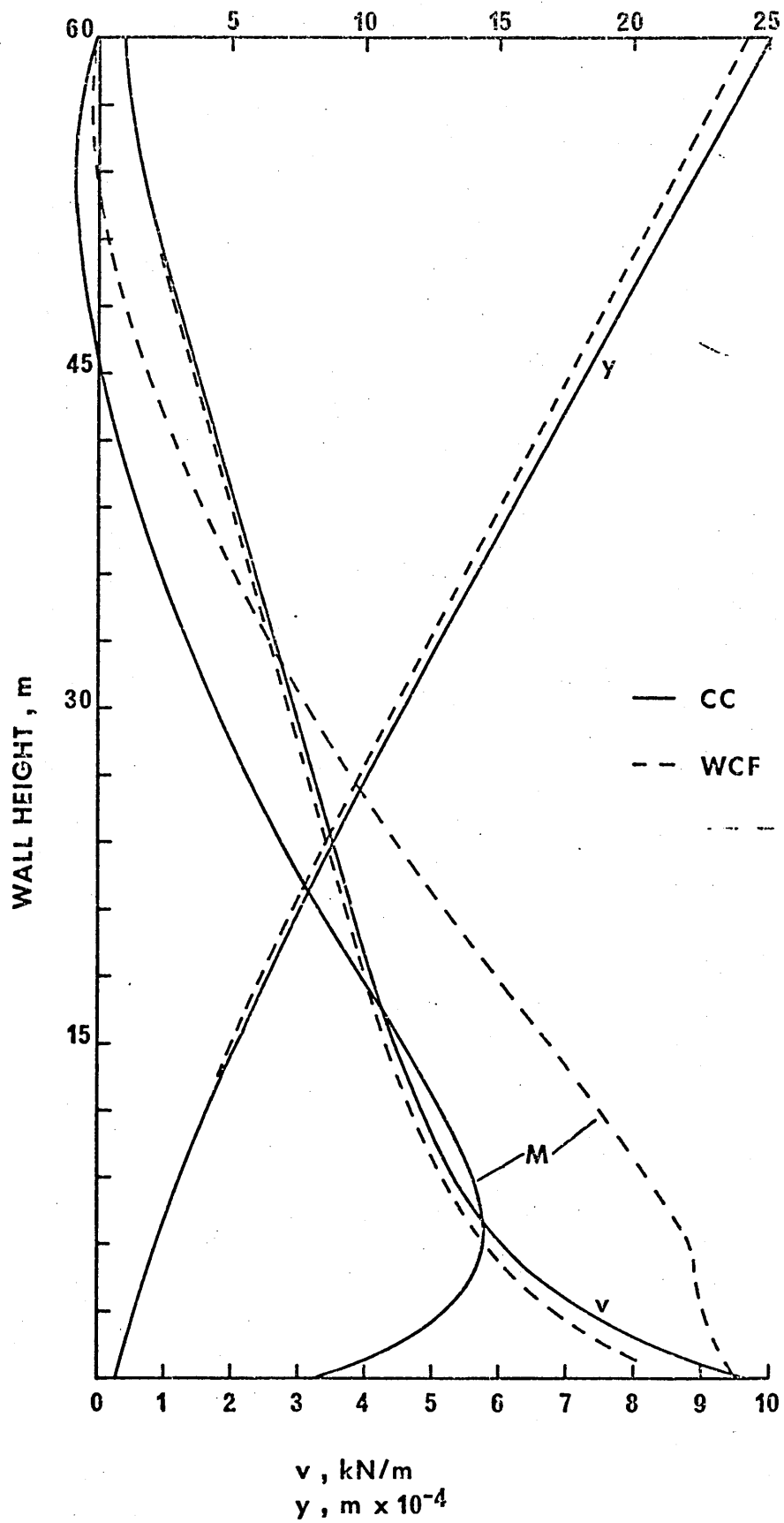


Figure 6.35 Distribution of M , v and y in wall with $\alpha H=16$ supported on Column Type 2

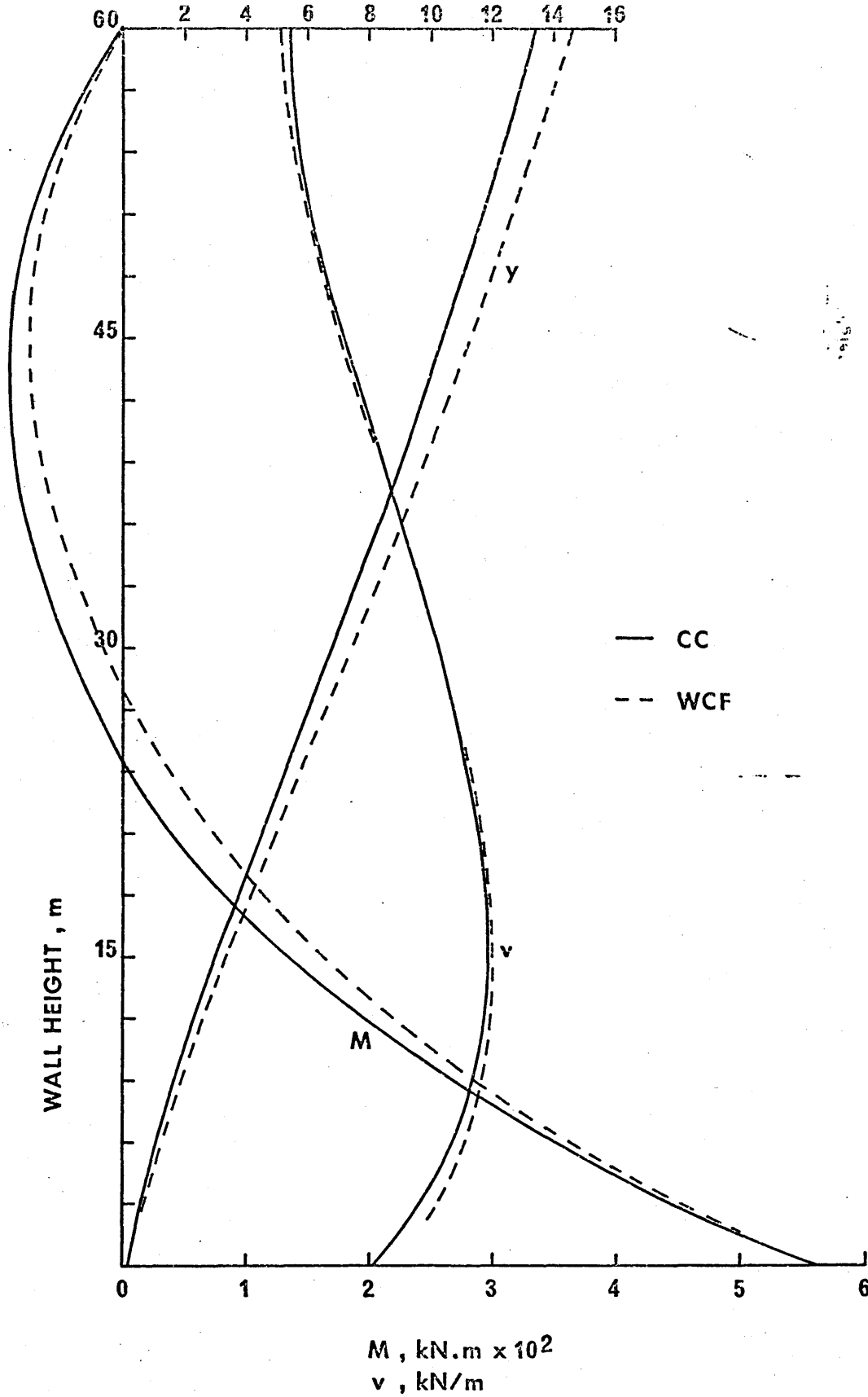


Figure 6.36 Distribution of M, v and y in wall with $\alpha H=4$ supported on Column Type 3

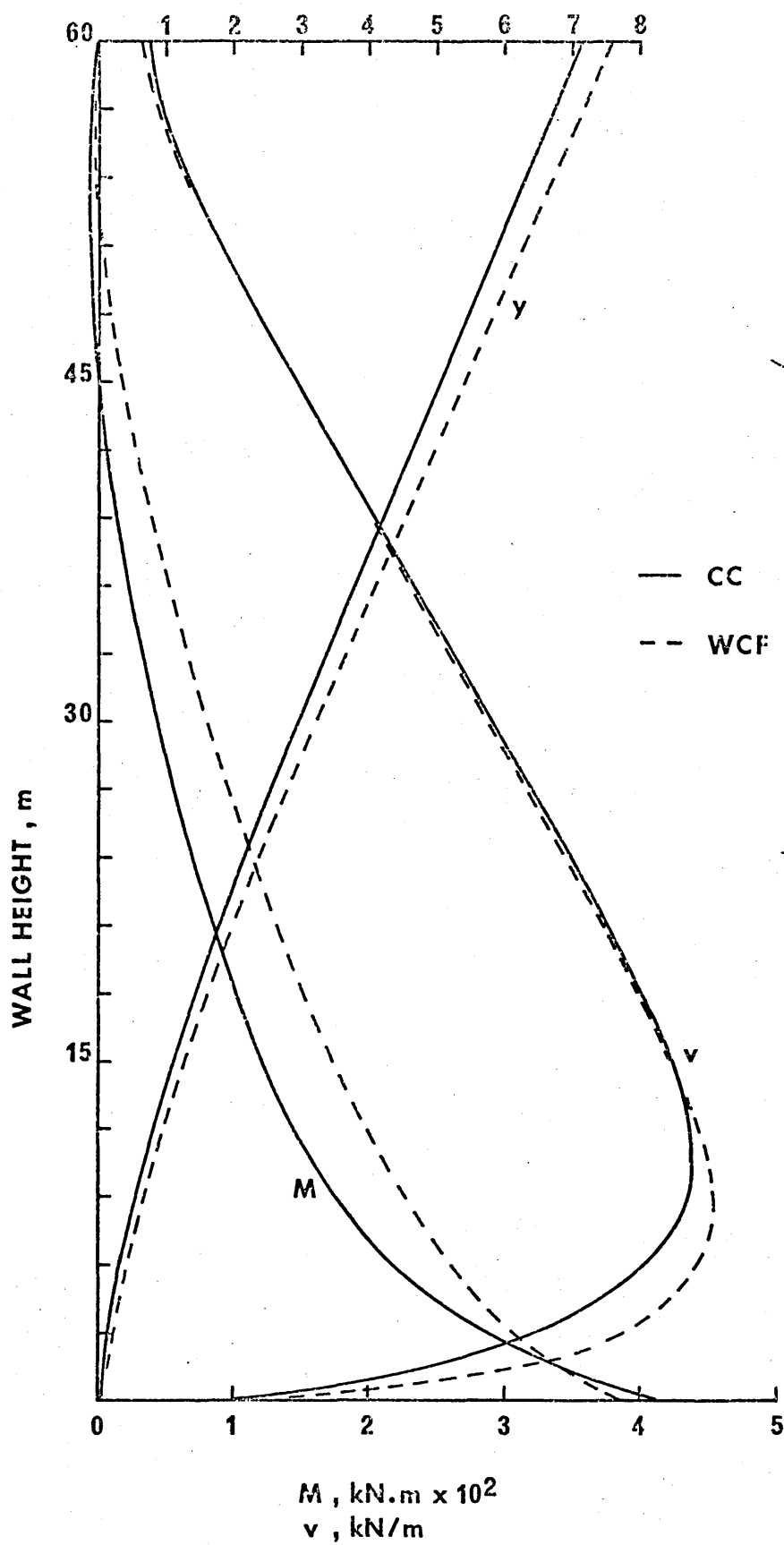


Figure 6.37 Distribution of M, v and y in wall with $\alpha H=16$ supported on Column Type 3

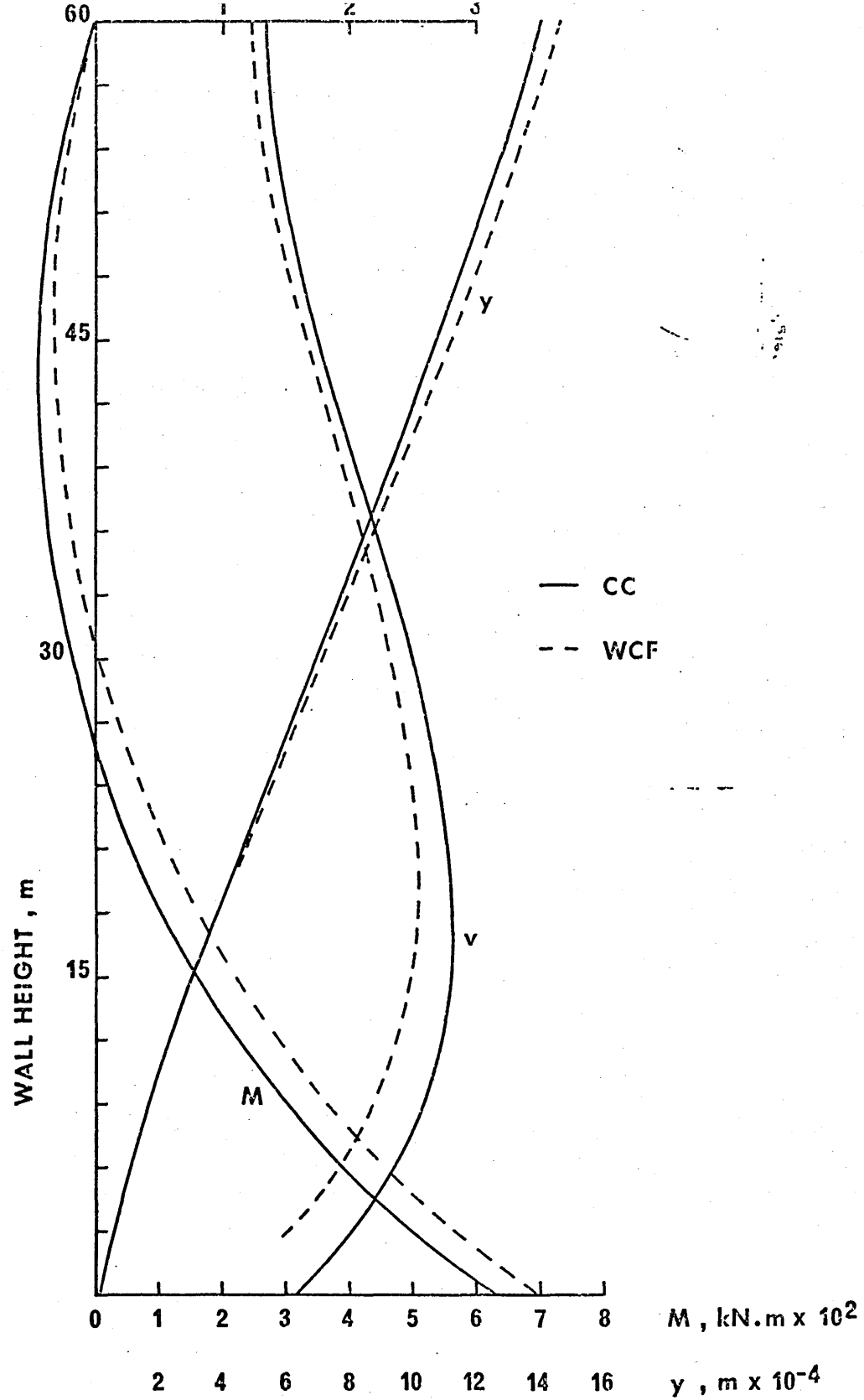


Figure 6.38 Distribution of M, v and y in wall with $\alpha H=4$ supported on Column Type 4

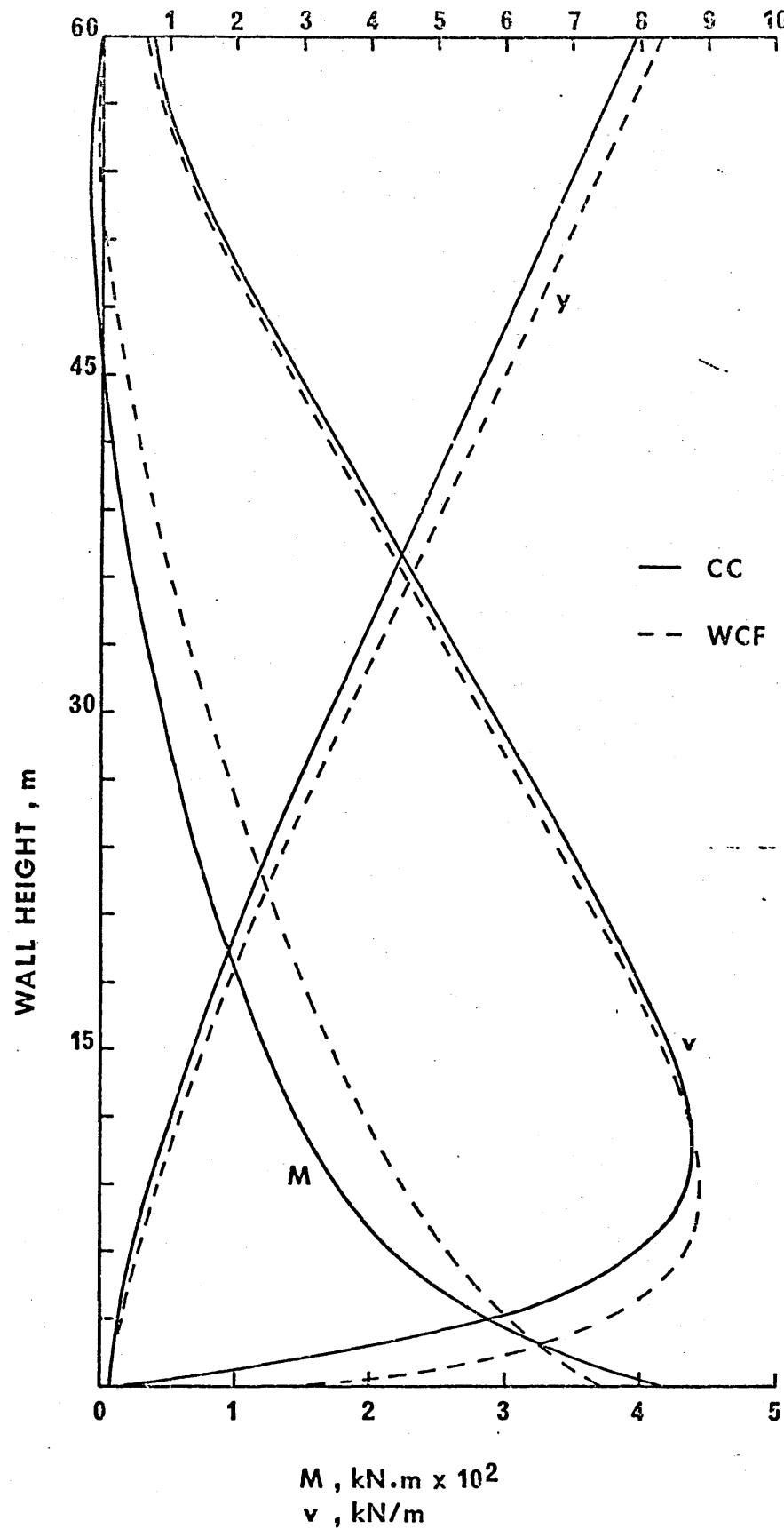


Figure 6.39 Distribution of M , v and y in wall with $\alpha H=16$ supported on Column Type 4

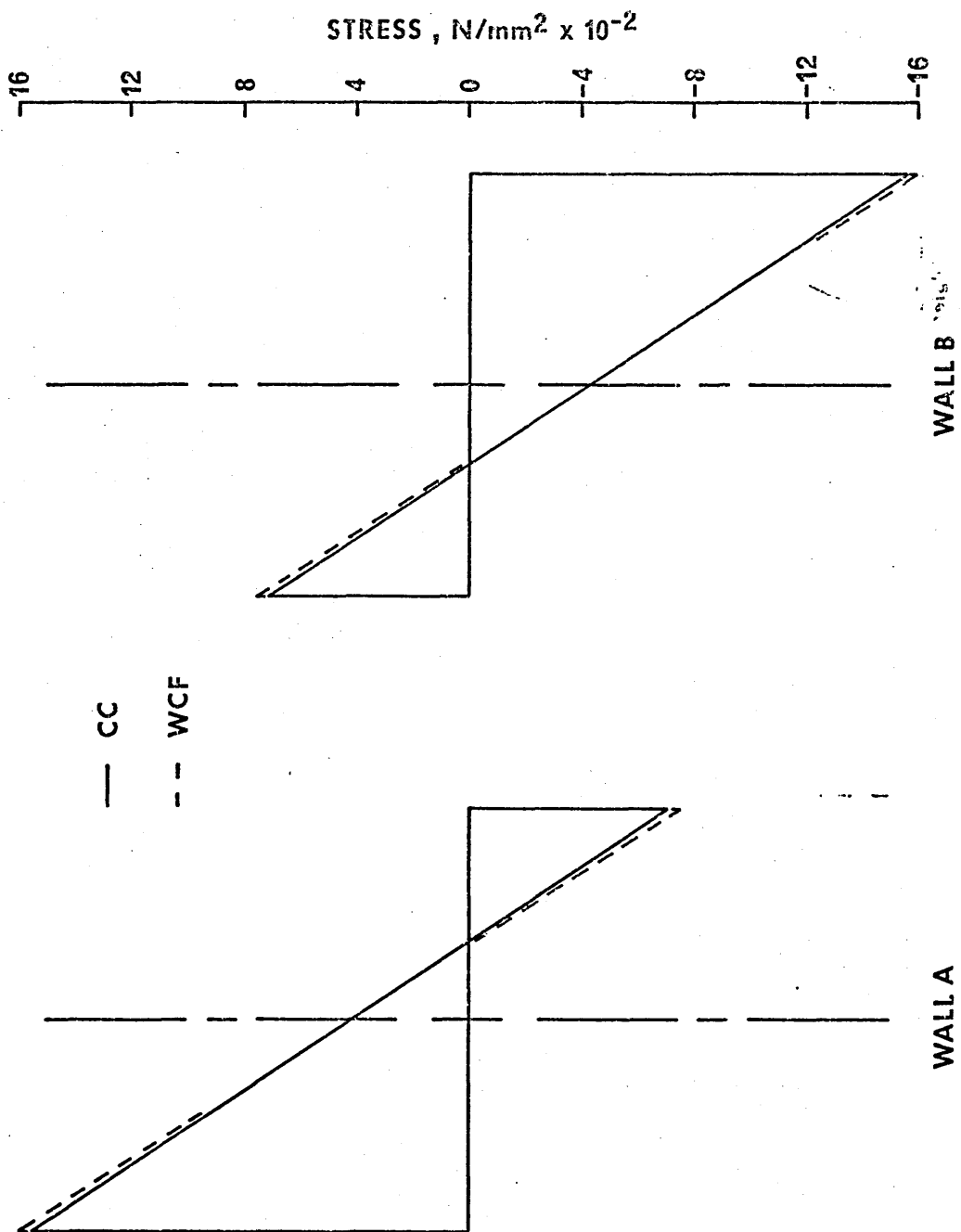


Figure 6.40 Stress distribution at a height of 6m across wall with rigid base and with $\alpha H=4$

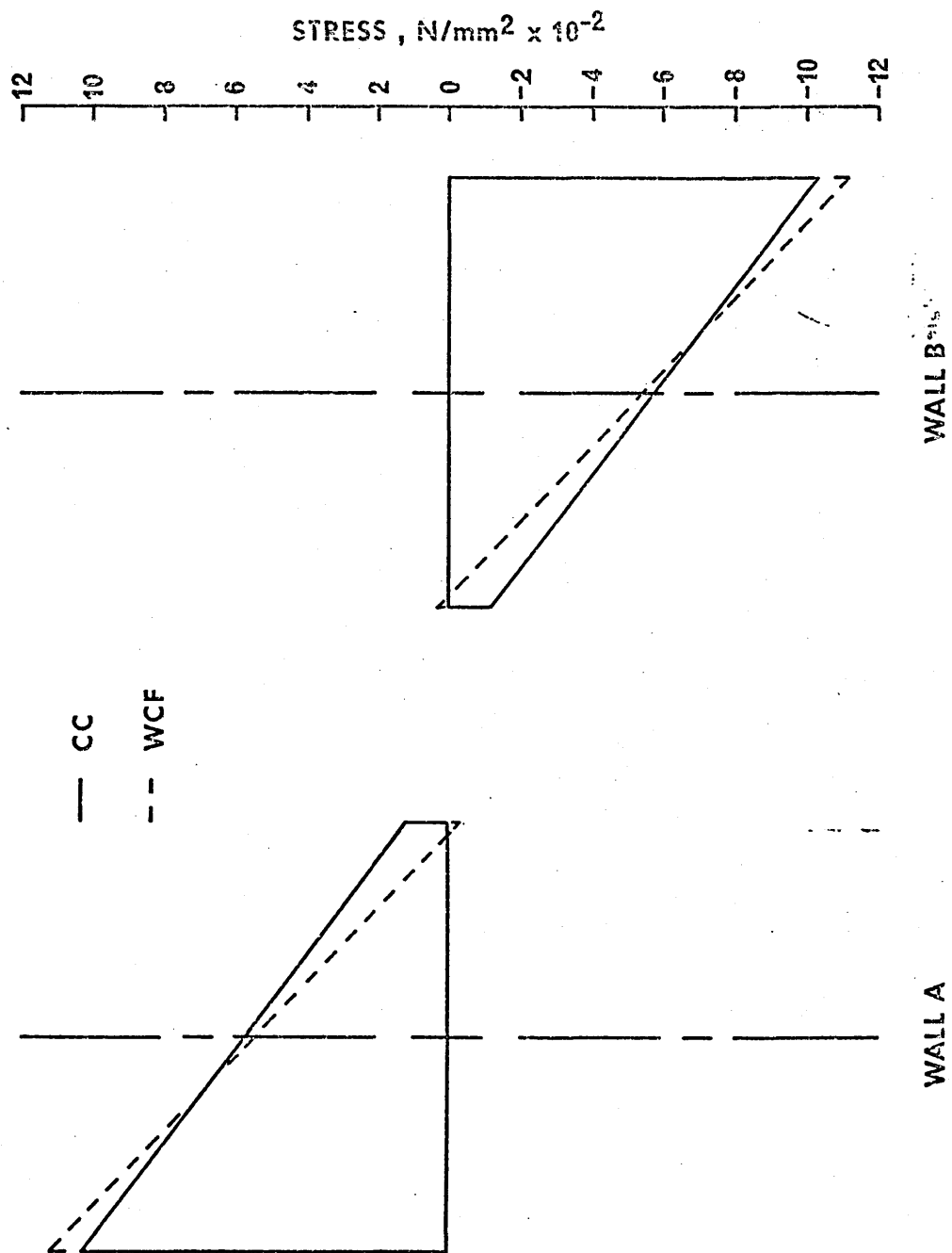


Figure 6.41 Stress distribution at a height of 6m across wall with rigid base and with $\alpha H=16$

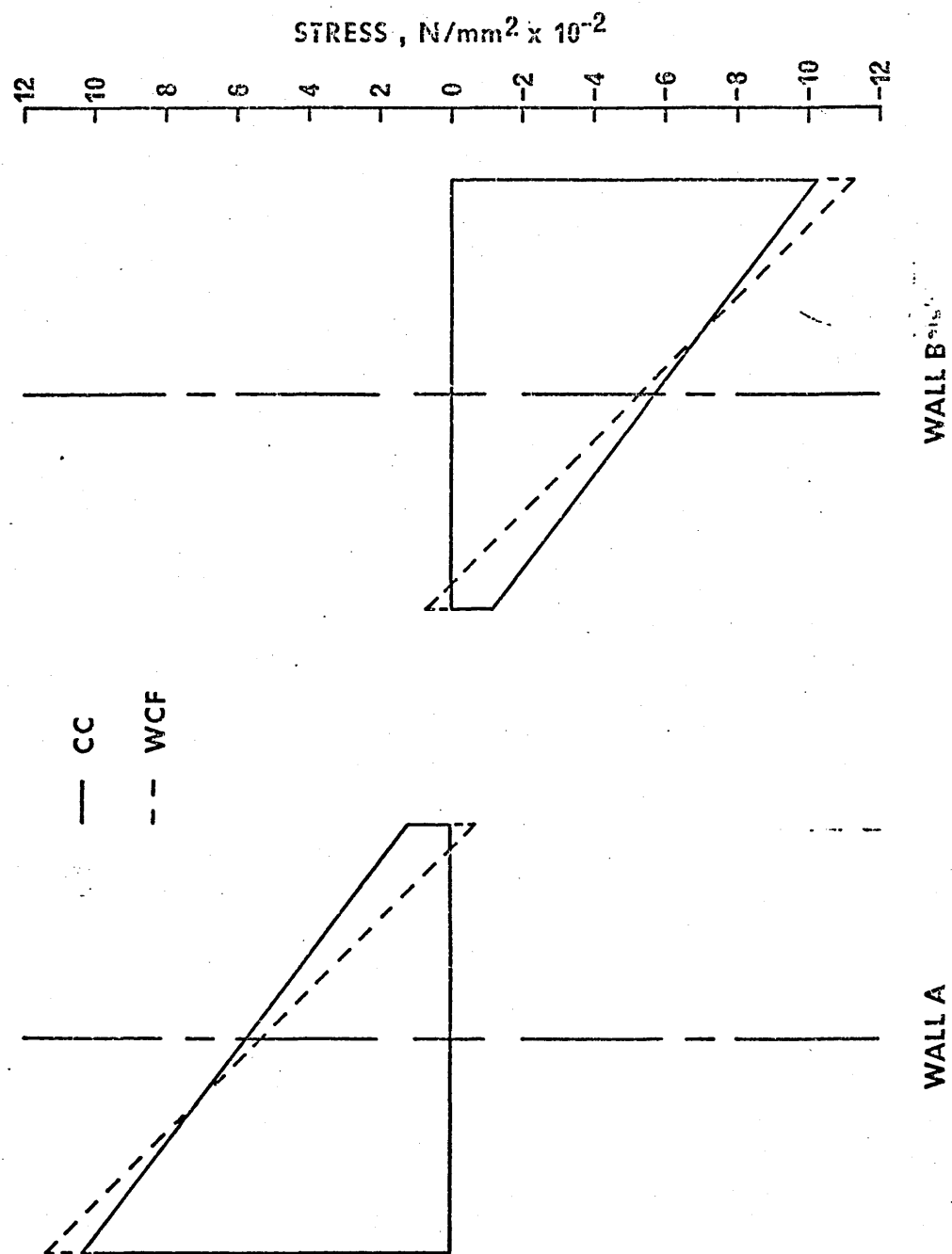


Figure 6.42 Stress distribution at a height of 6m across
wall with $\alpha H=4$ supported on Column Type 1

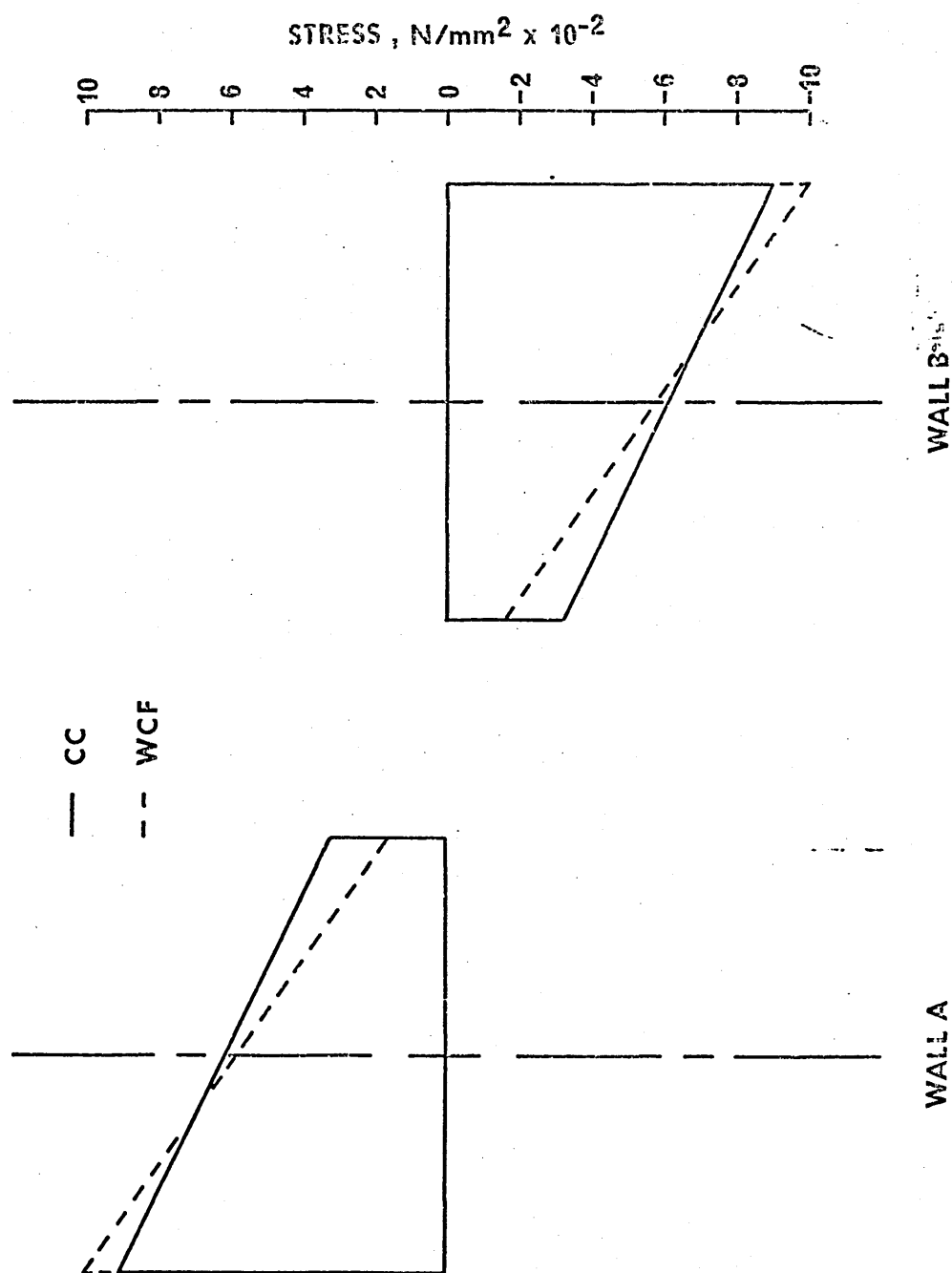


Figure 6.43 Stress distribution at a height of 6m across
wall with $\alpha H=16$ supported on Column Type 1

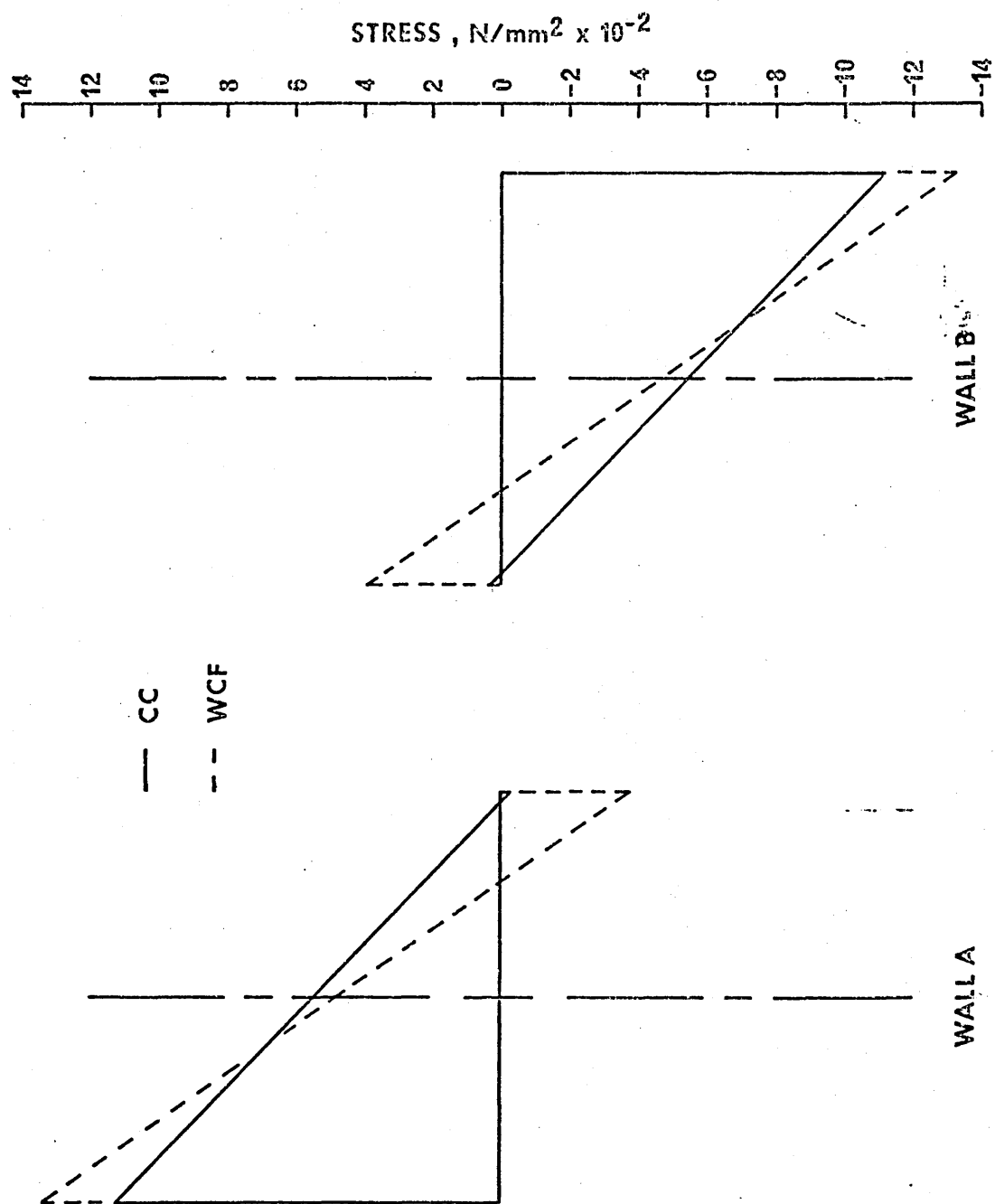


Figure 6.44 Stress distribution at a height of 6m across wall with $\alpha H=4$ supported on Column Type 2

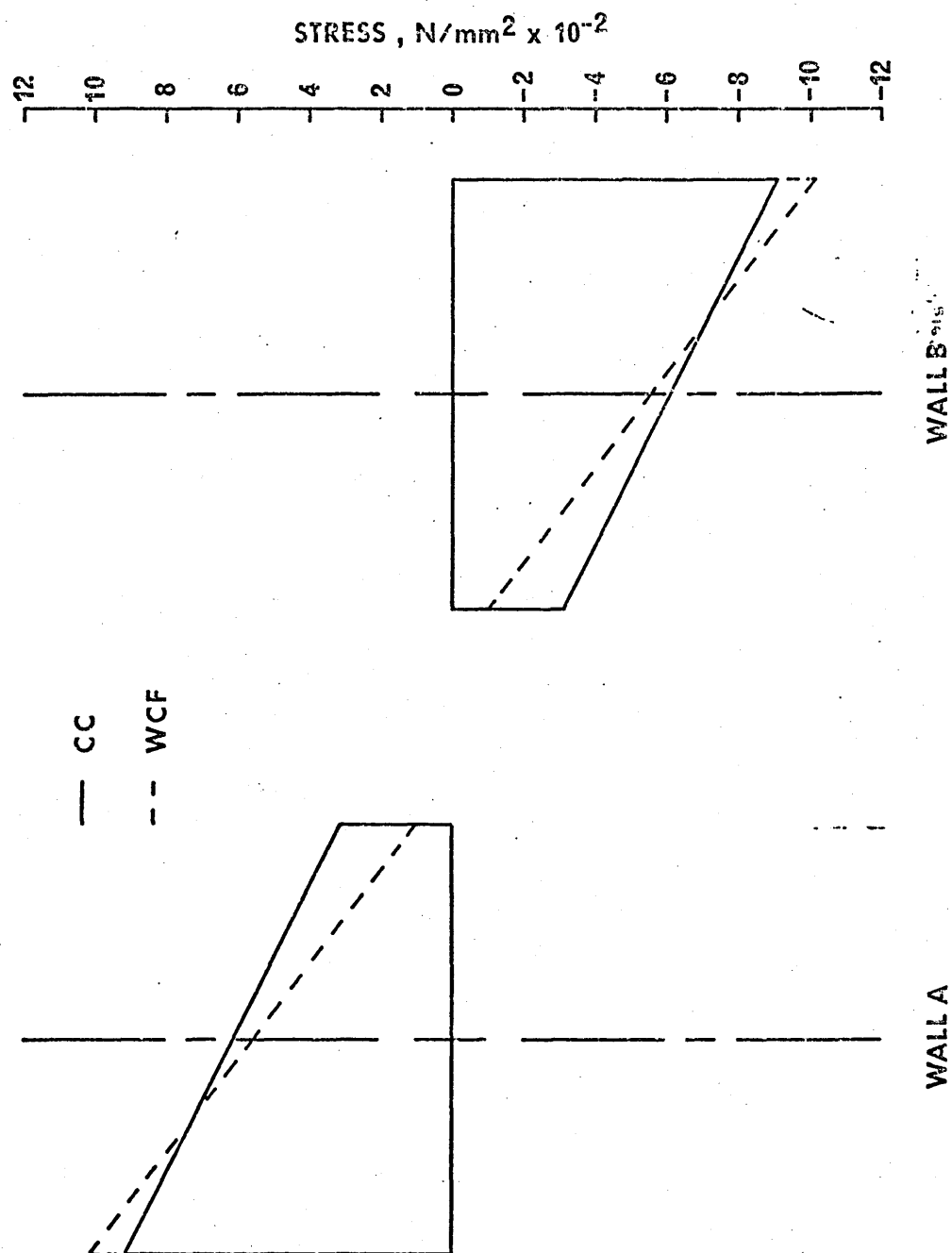


Figure 6.45 Stress distribution at a height of 6m across wall with $\alpha H=16$ supported on Column Type 2

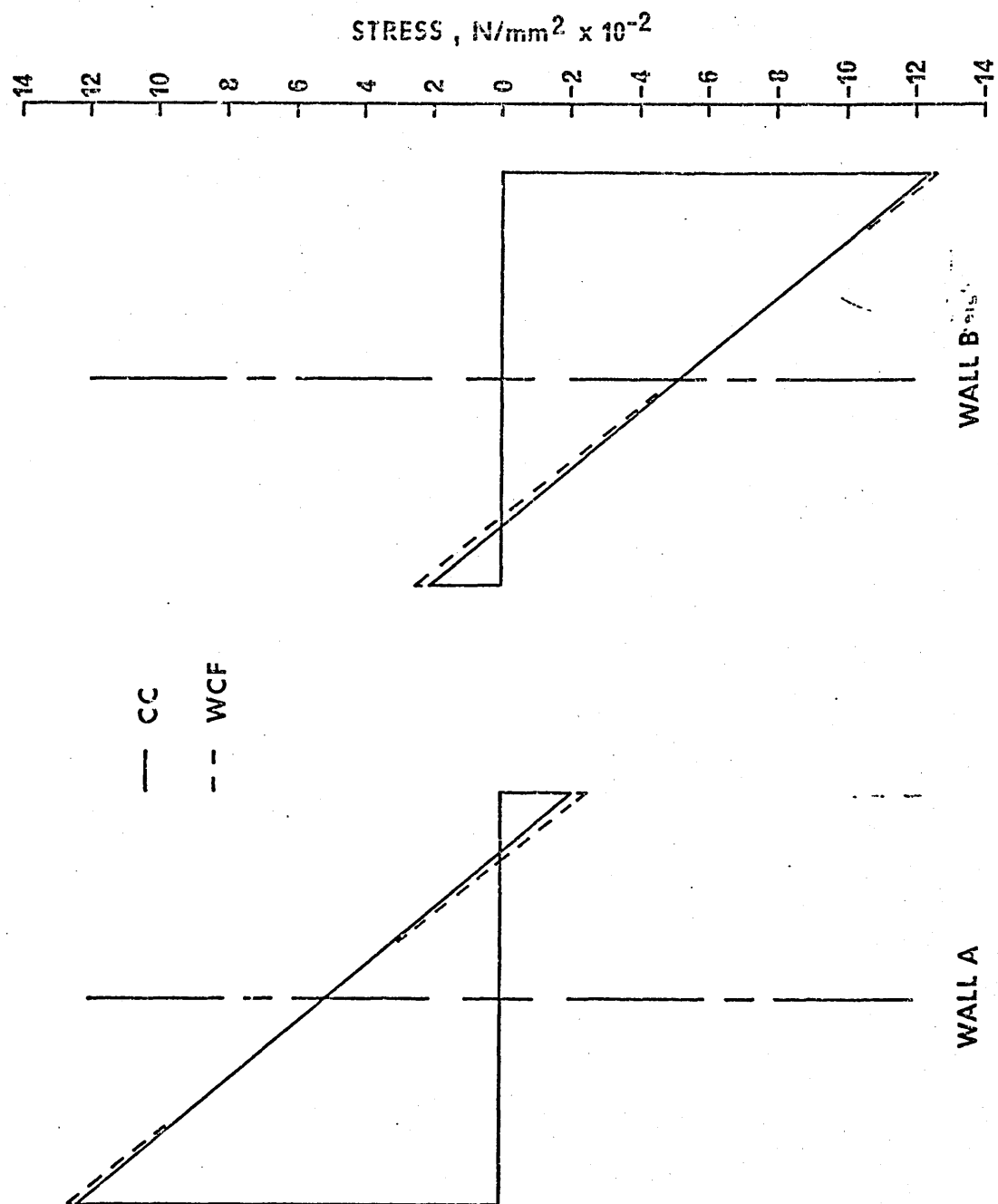


Figure 6.46 Stress distribution at a height of 6m across wall with $\alpha H=4$ supported on Column Type 3

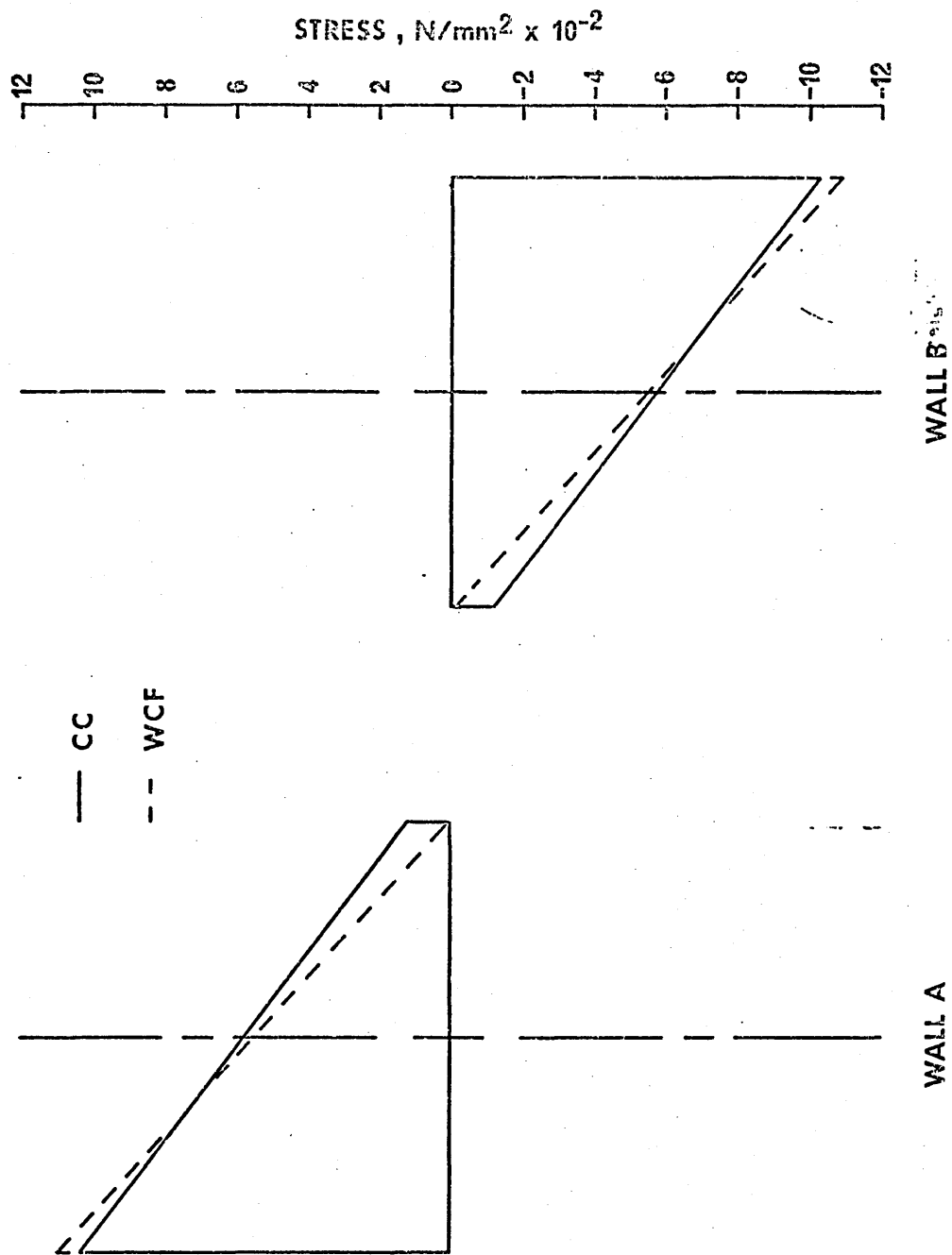


Figure 6.47 Stress distribution at a height of 6m across wall with $\alpha H=16$ supported on Column Type 3

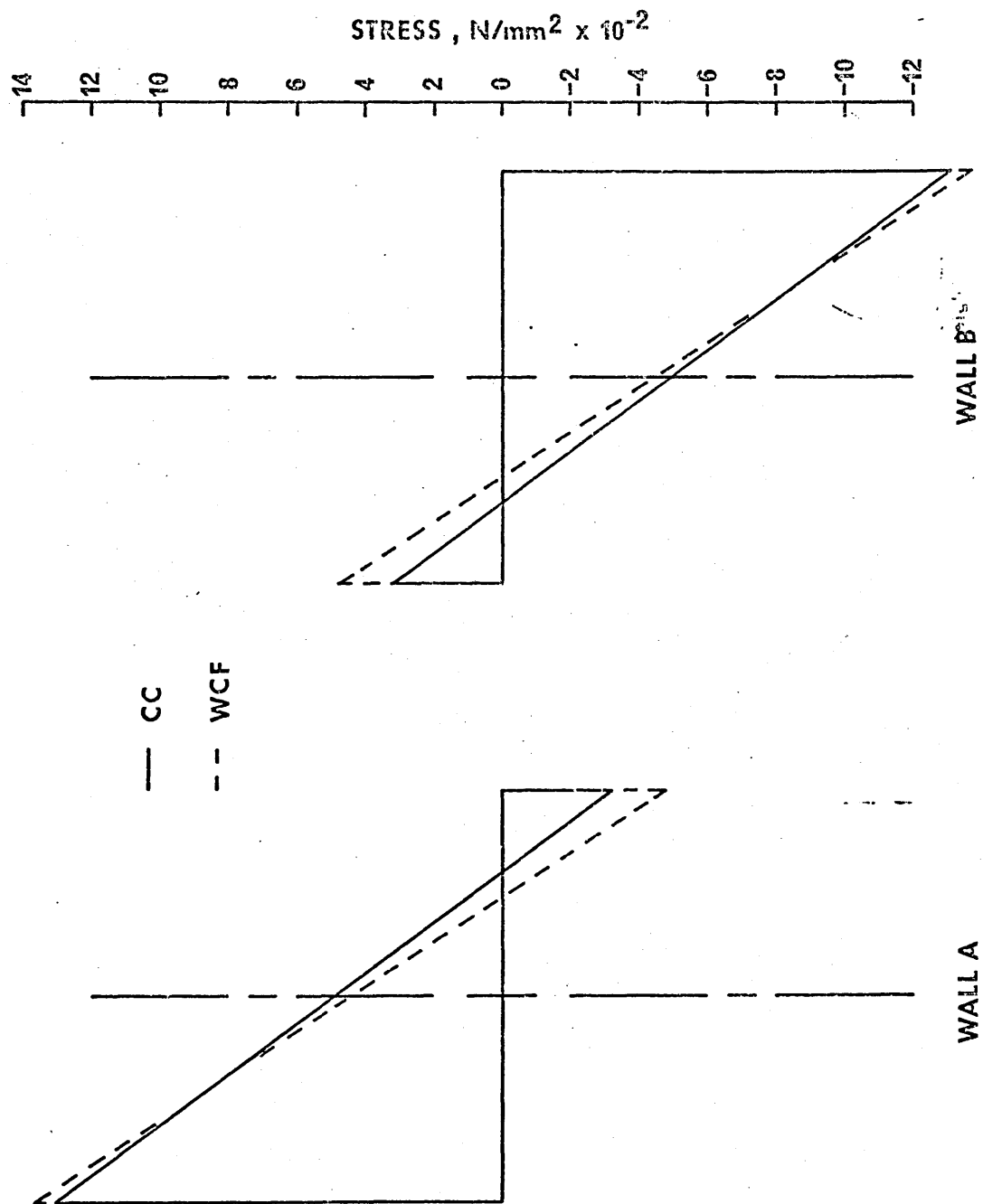


Figure 6.48 Stress distribution at a height of 6m across wall with $\alpha H=4$ supported on Column Type 4

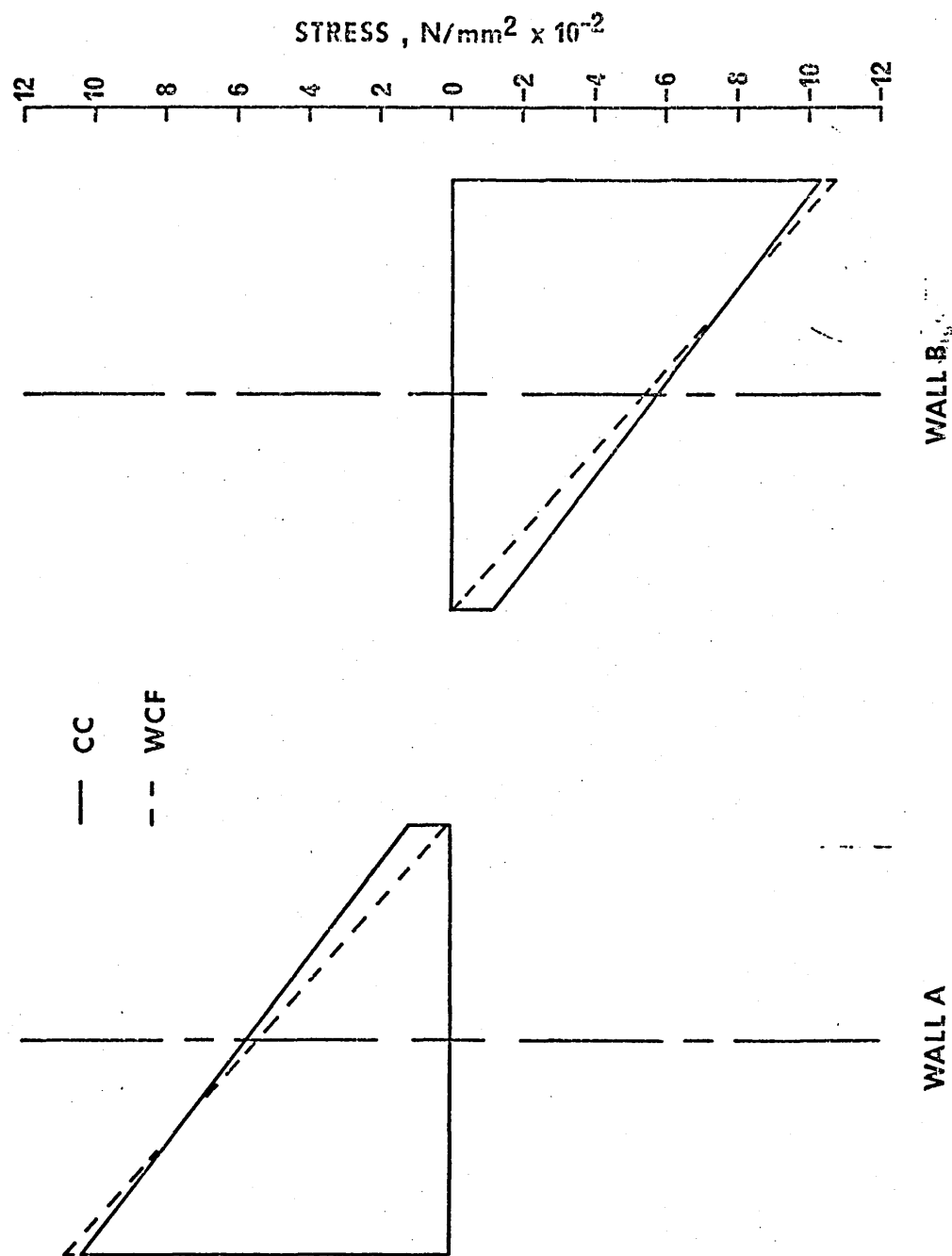


Figure 6.49 Stress distribution at a height of 6m across wall with $\alpha H=16$ supported on Column Type 4

6.5 Results for Walls Containing Two Bands of Staggered Openings

The wall system analysed in this section is shown in Figure 6.50(b), and it was subjected to a uniformly distributed lateral load of 1kN/m .

The results obtained from the matrix progression solution have been compared with those obtained from a wide column frame solution.

Figure 6.52 shows the distributions of total wall bending moment M , the axial force in each end wall N , the vertical shear force in each connecting medium v , and the deflection y .

In order to have a basis for comparing the above- results, solutions have also been obtained for a wall containing two bands of openings as shown in Figure 6.50(a) and the various action distributions are shown in Figure 6.51.

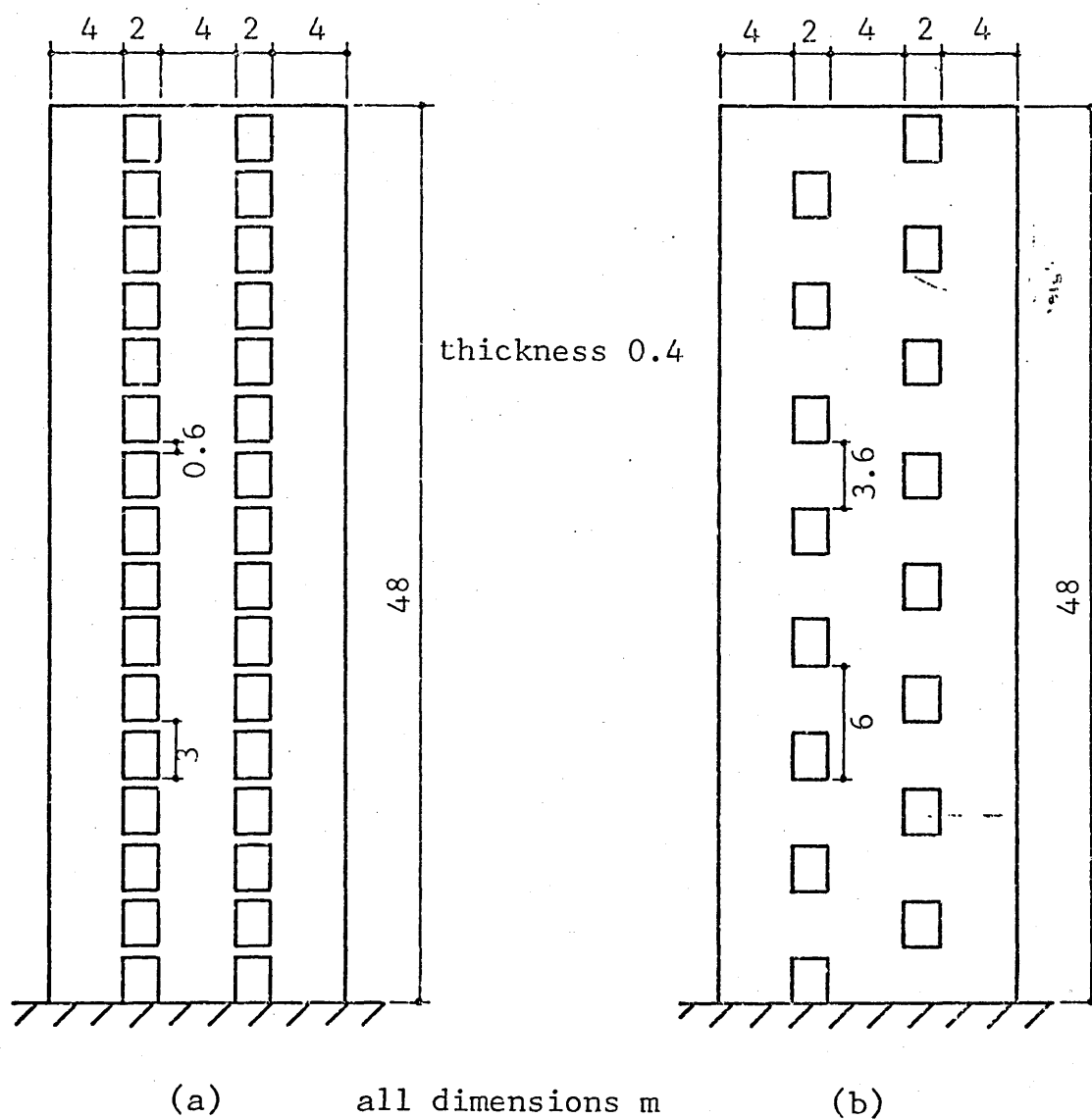


Figure 6.50 Dimensions of 'Three Walls' and 'Staggered Openings'

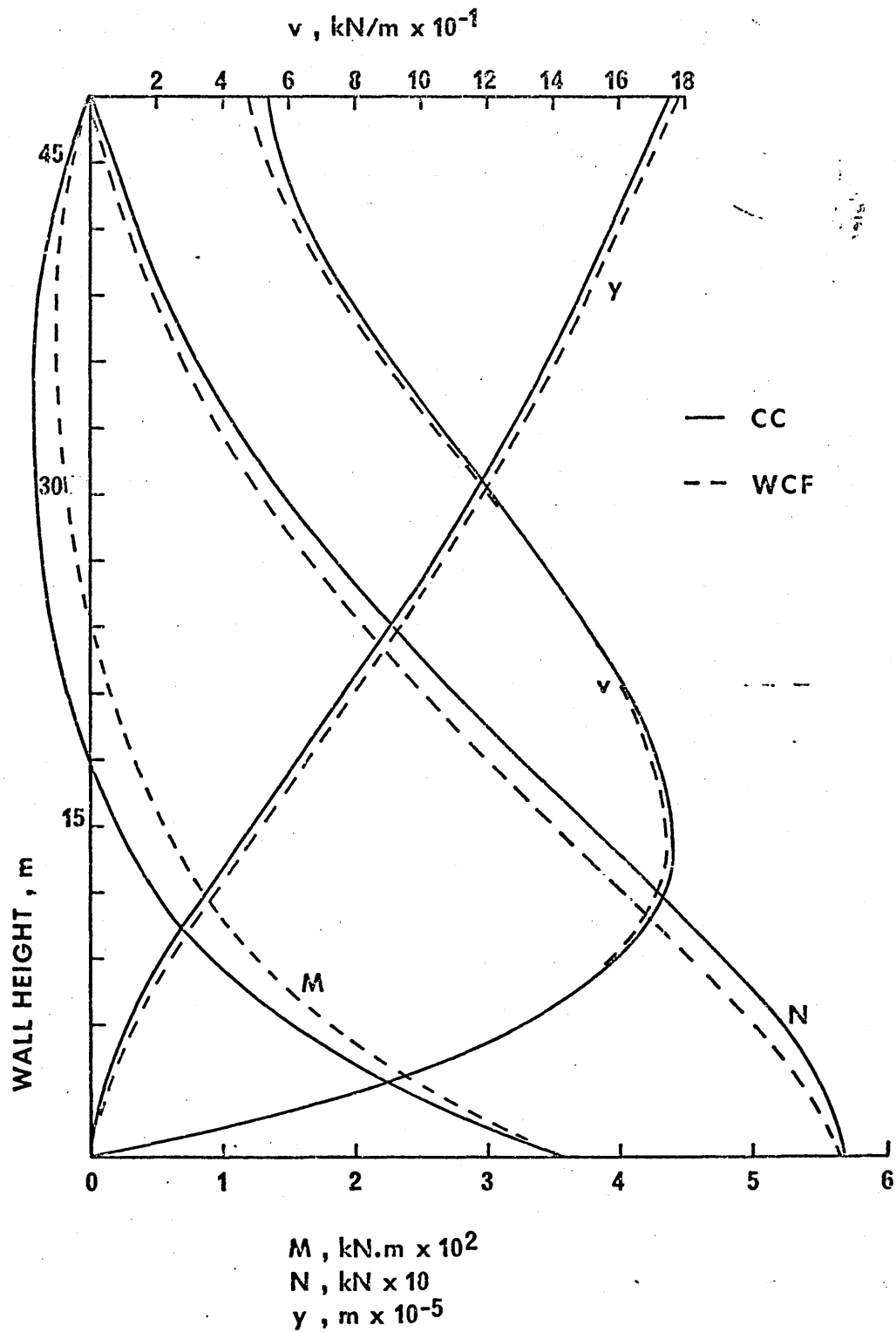


Figure 6.51 Distribution of M, N, v and y in wall containing two bands of openings

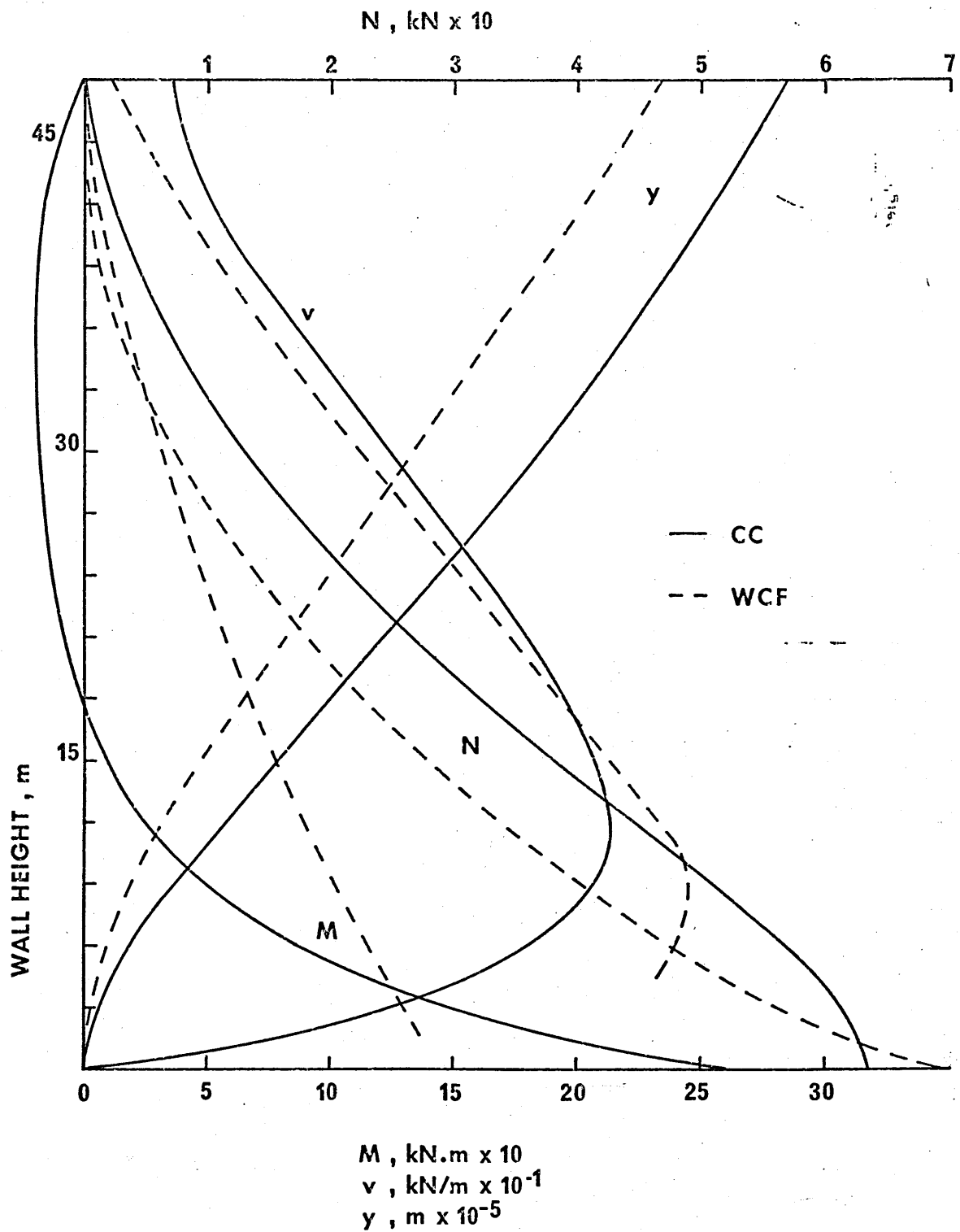


Figure 6.52 Distribution of M , N , v and y in wall containing two bands of staggered openings

DISCUSSION OF RESULTS7.1 Introduction

In order to determine the accuracy of the matrix progression results, it is necessary to have corresponding 'exact' values for comparison. In the present work these values are assumed to be obtained from experimental work and from wide column frame solutions.

With the experimntal work, as described in Chapter 5, there are several possible sources of errors. The first of these is the applied loadings. Point loads were applied by means of a proving ring and apart from any dial gauge calibration errors, they can be assumed to be accurate. Uniform loads, however, were simulated by a series of point loads applied at each storey height. Because of difficulties in ensuring that these loads were truly lateral and that they were applied in the corner of each opening, slight errors may have been introduced.

Dial gauge errors may be assumed negligible and, therefore, the measured deflections can be taken as accurate. Errors in the strain gauge readings are an unknown quantity but an overall check on the accuracy of the results can be made by comparing the measured internal moments with the

known applied external moments, and also by comparing the axial force in each wall. During the uniform loading tests a few load points were in close proximity to some gauges and thus certain readings may have been adversely affected by local stresses. Errors are also likely to be caused by local stiffening effects of the gauges and their adhesive. Tests by earlier researchers on Araldite beams showed this stiffening effect to be responsible for recorded strains being in the order of 10% less than theoretical values. That the effect occurred in the walls being tested is borne out by the results in Table 6.2 which show the measured internal moments at least 10% less than the applied moments.

From the above, it is very difficult to estimate a value for possible percentage errors, but all errors involved were minimised, for both point load and uniform load conditions, by calculating deflections and strains per unit load from the slopes of load-deflection and load-strain curves.

Although the wide column frame method is an idealization of the true structure, it has been shown by past research workers to give a good indication of the real behaviour of different types of coupled shear wall systems, and it is the one most commonly used in practice. For these reasons, the results obtained from the method can be assumed to be a good

basis for comparison of different solutions.

7.2 Walls Containing One Band of Openings and with One Abrupt Variation in Cross-Section

Figures 6.2 to 6.8 show comparisons between the two sets of theoretical results and the experimental values of deflections for Models 1 to 4. It can be seen that close agreement is obtained between the matrix progression method and both the assumed 'exact' solutions. For the point load condition, the experimental values generally lie between the two theoretical curves, with the wide column frame giving maximum values. For the uniform loading condition, however, both the theoretical curves underestimate the deflections with respect to the experimental values.

Table 6.1 compares values of maximum deflections in the models and it can be seen that the matrix progression results agree with the wide column frame results and the experimental values to within 7% and that the two latter sets of values agree within 4% of each other.

When obtaining both the theoretical solutions, the beam wall flexibility was taken into account. If this had not been done there would have been greater disagreement between the matrix progression results and the experimental values but it would have had no relative effect on the two sets of theoretical values.

Figures 6.11 to 6.26 show experimental and theoretical strain distributions across the walls at two particular heights. The theoretical lines are only shown for the matrix progression solution, it being seen from Figures 6.9 and 6.10 that the variations of forces throughout the height of the wall, obtained from both the matrix progression and wide column frame methods are in very close agreement.

When comparing the strain distributions it is seen that the maximum experimental strains are in the order of 7 to 15% less than the corresponding theoretical ones for the point loading condition and up to 30% less than the corresponding theoretical ones for the uniform loading condition. However, it can also be seen from the figures given in Table 6.2 that the internal moments are in the order of 9 to 12% lower than the known applied moments for the point loading condition and up to 38% lower for the uniform loading condition. Bearing this in mind, it is seen that good agreement is reached between the theoretical and experimental results.

The discrepancies in the internal and external moments for the point loading cases are in agreement with the assumed 10% local stiffening effect of the strain gauges, but even allowing for this in the uniform loading cases there are still substantial reductions in the measured

internal moments. Why this should be so cannot readily be explained. Errors in the actual loading, as mentioned in the introduction to this chapter, cannot have been excessive, and this is borne out by reasonable agreement between the deflection results. Local stresses would affect only certain strain gauge readings and although these effects can be noticed on certain strain profiles, they do not affect the overall distributions.

7.3 Uniform Walls Supported on Columns

For walls with rigid bases, Figures 6.30 and 6.31 show that irrespective of the degree of interaction between the two walls there is very good agreement between the deflection profiles obtained using the matrix progression and wide column frame solutions. The matrix progression method gives less deflection throughout the height of the walls but the difference in maximum values is only about 2%.

When the walls are supported on columns, the differences between the two sets of deflection are once again not greatly affected by the value of αH , and are generally in good agreement as is seen from Figures 6.32 to 6.39. However, when the walls are supported on central columns the matrix progression method generally overestimates the deflections whereas with offset columns the method underestimates the deflections. The range of differences is

about +9% to -8%.

The differences in force actions obtained from the two theoretical solutions for the walls with rigid bases and with $\alpha H=4$ and $\alpha H=16$ are shown in Figures 6.30 to 6.31. When the relevant values of M and N are used to plot stress distributions at a height of 6m, as shown in Figures 6.40 and 6.41, the matrix progression method is found to underestimate the maximum stress by 2% for the wall with $\alpha H=4$ and by 8% for the wall with $\alpha H=16$. When looking at the curves for force actions in the walls supported on columns, Figures 6.32 to 6.39, it can be seen that generally the results do not compare as favourably as the rigid base values. The reason for this is that the theoretical model for the column system is quite different from that of the remainder of the structure. This is because the continuous connection over the column height is assumed to come partly from the foundation and partly from the single support beam, whereas the connecting beams for the rest of the structure are at regular intervals for a much greater height and therefore justify being replaced by a continuous system. However, when stress distributions are drawn at a height of 6m, the matrix progression method is found to only underestimate the maximum stress by about 9 to 16% for the central column cases and by about 2 to 6% for the offset column

cases. Thus even when there is a large difference between the moments obtained from the two methods, for example the wall with $\alpha H=16$ supported on column type 1, there is good agreement between stress values. For any given column system, the value of αH does not seem to affect greatly the accuracy of the results.

Generally the value of the moment is a maximum at the base of the wall but for the walls with $\alpha H=16$ supported on central columns, the bending moment 'falls away' near the base. This isolated non-standard behaviour is emphasised by the wall with $\alpha H=16$ supported on column type 2 where the wide column frame results show the moment start to reduce but then increase again.

Overall, the results obtained for the offset columns give closer agreement than the results for the central columns. The matrix progression results for the central column cases indicate behaviour of the walls as if they were supported on more flexible support beams than they actually are. Thus the moments in the walls could be increased, to obtain closer values to the wide column frame by assuming an artificially increased stiffness for the support beam. This increase would be best obtained by considering a decrease in length rather than an increase in the second moment of area. Unfortunately no simple rule for altering

the stiffness seems possible. In general, better results were obtained, for different structures, by reducing the beam length by a factor of between 0.5 and 0.7. However, any such variation in the beam stiffness only affects forces in the lower regions of the wall.

7.4 Wall Containing Two Bands of Staggered Openings

From Figure 6.52 it can be seen that the agreement between the two sets of theoretical results is not very good. The matrix progression method overestimates the wall bending moment at the base but this is not typical of results for most of the height. The matrix progression solution shows a reversal of the bending moment about a third of the way up the wall, but the wide column frame shows no reversal at all. Even the deflection values do not give close agreement, unlike all the other wall systems analysed, with the matrix progression method overestimating the maximum value by about 21%. It is very difficult to explain the difference in behaviour suggested by the two methods but presumably it is due to the connecting stiffness used. The matrix progression results suggest much more flexible connecting beams than the wide column frame results and yet the same reduced stiffness was used in both analyses.

That the method can be adopted for wall systems containing two full bands of openings is shown by Figure 6.51

where close agreement is obtained between all the various actions.

7.5 Conclusions and Suggestions for Future Work

Matrix progression solutions of the continuous connection method have been presented and compared with experimental results and wide column frame solutions for a variety of non-uniform coupled shear walls.

The numerical method has been shown to give good results, in general, for both stresses and deflections of walls with one abrupt change in cross-section and of walls supported on both central and offset columns. The results for walls containing two bands of staggered openings do not agree favourably with the wide column frame solution, but in this case there must be some doubt as to how closely either of the solutions resemble the true behaviour of the structure.

Based on the experimental results obtained, it is suggested that whereas the point loading results are perfectly satisfactory, any results obtained for a uniform loading condition applied as in the present work should be treated with caution.

The matrix progression method has been shown to be capable of dealing with fairly complex shear wall systems and thus overcomes some of the past criticisms levelled at

the continuous connection method. The method has definite advantages over the wide column frame approach in that any solution requires far less data preparation and far less computer processing time. For example, the STRESS program could take up to 10 minutes central processing time for a single solution, whereas the same results were obtained in about 8 seconds central processing time using the matrix progression solution. However, it must be admitted that even in its numerical form, the continuous connection technique does not possess the full flexibility of the frame analogies.

Shear wall research has been continuing for many years now and it would seem that elastic analysis has just about exhausted itself, the only scope being in the solution of individual problems such as the axis of the openings moving laterally at an arbitrary height. The logical movement of research in the future would therefore be to ultimate load analysis and design, and this is one area where the matrix progression method could quite easily be adopted.

REFERENCES

1. Coull A
Stafford Smith B "Analysis of Coupled Shear Walls
(A Review of Previous Research)"
Tall Buildings, pp 139-155
Pergamon Press 1967
2. Coull A
Stafford Smith B "Structural Analysis of Tall Concrete
Buildings"
Proc. Inst. Civ. Engrs. Part 2, V55
March 1973, pp 151-166
3. Fintel M
et al "Response of Buildings to Lateral
Forces"
J. Am. Conc. Inst. V68, Feb 1971,
pp 81-106
4. Green NB "Bracing Walls for Multistorey
Buildings"
J. Am. Conc. Inst. V49, 1952,
pp 233-248
5. Tezcan S "Computer Analysis of Plane and
Space Structures"
J. Struc. Div. Am. Soc. Civ. Engrs.
V92, ST2, April 1966, pp 143-173
6. Jenkins WM "Matrix and Digital Computer Methods
in Structural Analysis"
McGraw-Hill, 1969
7. STRESS - A User's Manual
M.I.T. Press, 1964
8. ICES - STRUDL - II Engineering
User's Manual Vols 1, 2 and 3
M.I.T. Press, 1967-1970
9. Frischmann WW
Prabhu SS
Toppler JF "Multistorey Frames and Inter-
connected Shear Walls Subjected to
Lateral Loads - II"
Conc. and Constr. Engrg, V58,
July 1963, pp 283-292

10. MacLeod IA "Lateral Stiffness of Shear Walls with Openings"
Tall Buildings, pp 223-244
Pergamon Press, 1967
11. Schwaighofer J "Analysis of Shear Walls Using
Microys HF Standard Computer Programs"
J.Am. Conc. Inst., V66, Dec 1969,
pp 1005-1007
12. Stafford Smith B "Modified Beam Method for Analysing
Symmetrical Interconnected Shear
Walls"
J.Am. Conc. Inst., V67, Dec 1970,
pp 977-980
13. Zienkiewicz OC "The Finite Element Method in
Engineering Science"
McGraw-Hill, 1971
14. Rockey KC "The Finite Element Method - A Basic
Evans HR Introduction"
Griffiths DW Crosby-Lockwood-Staples, 1975
Nethercot DA
15. Choudhury JR "Analysis of Plane and Spatial
Systems of Interconnected Shear
Walls"
Ph.D. Thesis, Dept of Civ. Eng.,
University of Southampton, 1968
16. MacLeod IA "New Rectangular Finite Element
for Shear Wall Analysis"
J. Struc. Div. Am. Soc. Civ. Engrs.,
V95, ST3, March 1969, pp 399-409
17. Chitty L "On the Cantilever Composed of a
Number of Parallel Beams Inter-
connected by Cross Bars"
The Philosophical Magazine, V38,
1947, pp 685-699
18. Beck H "Contribution to the Analysis of
Coupled Shear Walls"
J. Am. Conc. Inst., V59, August 1962,
pp 1055-1069

19. Rosman R
"Approximate Analysis of Shear Walls Subject to Lateral Loads"
J. Am. Conc. Inst., V61, June 1964
pp 717-732
20. Coull A
Puri RD
"Analysis of Pierced Shear Walls"
J. Struc. Div. Am. Soc. Civ. Engrs.,
V94, ST1, Jan 1968, pp 71-82
21. Pearce DJ
Mathews DD
"An Appraisal of the Design of Shear Walls in Box Frame Structures"
Property Services Agency Report,
Department of the Environment, 1973
22.
CP3, Chapter V, Part 2 - Wind Loading
Brit. Stand. Inst., 1970
23. Coull A
Choudhury JR
"Stresses and Deflections in Coupled Shear Walls"
J. Am. Conc. Inst., V64, Feb 1967,
pp 65-72
24. Coull A
Choudhury JR
"Analysis of Coupled Shear Walls"
J. Am. Conc. Inst., V64, Sept 1967
pp 587-593
25. Rosman R
"Tables for the Internal Forces of Pierced Shear Walls Subject to Lateral Loads"
Bauingenieur Praxis No.66
Wihelm Ernst and Son (Berlin), 1966
(In German and English)
26. Michael D
"The Effect of Local Wall Deformations on the Elastic Interaction of Cross Walls Coupled by Beams"
Tall Buildings, pp 253-270
Pergamon Press, 1967
27. Bhatt P
"Effect of Beam-Shear Wall Junction Deformations on the Flexibility of the Connecting Beams"
Build. Sci., V8, June 1973, pp 149-151

28. Marshall MG "The Analysis of Shear Wall Structures"
M.Sc. Thesis, University of Waterloo,
Ontario, Sept 1968
29. Traum EE "Multistorey Pierced Shear Walls
of Variable Cross-Section"
Tall Buildings, pp 181-204
Pergamon Press, 1967
30. Coull A "Analysis of Coupled Shear Walls of
Puri RD Variable Cross-Section"
Build. Sci., V2, 1968, pp 313-320
31. Pisanty A "Simplified Analysis of Coupled
Traum EE Shear Walls of Variable Cross-Section"
Build. Sci., V5, July 1970, pp 11-20
32. Coull A "Analysis of Coupled Shear Walls of
Puri RD Variable Thickness"
Build. Sci., V2, 1967, pp 181-188
33. Puri RD "A Study of the Continuous
Connection Method of Analysis of
Coupled Shear Walls"
Ph.D. Thesis, Dept of Civ. Eng.,
University of Southampton, Sept 1967
34. Tottenham H "The Matrix Progression Method in
Structural Analysis"
Introduction to Structural Problems
in Nuclear Reactor Engineering
(Ed. Rydzewski, JR), pp 189-210
Pergamon Press, 1962
35. Coull A "Numerical Elastic Analysis of
Puri RD Coupled Shear Walls"
Tottenham H Proc. Inst. Civ. Engrs., Part 2, V55,
March 1973, pp 109-128
36. Tso WK "Static Analysis of Stepped Coupled
Chan PCK Walls by Transfer Matrix Method"
Build. Sci., V8, June 1973, pp 167-177
37. MacLeod IA "Frame Idealization of Shear Wall
Green DR Support Systems"
Struc. Engr., V51, Feb 1973, pp 71-74

38. Coull A
Chantaksinopas B "Design Curves for Coupled Shear
Walls on Flexible Bases"
Proc. Inst. Civ. Engrs., Part 2,
V57, Dec 1974, pp 595-618
39. Coull A
Mukherjee PR "Coupled Shear Walls with General
Support Conditions"
Conf. on Tall Buildings, Kualar
Lumpar, Dec 1974
40. Arvidsson K "Elastically Founded Shear Walls
with Two Rows of Openings"
J. Am. Conc. Inst., V37, March 1976
pp 151-154